Reliability of mercury and arsenic sampling and analysis in the petrochemical and oil industry

Aurore Méré

▶ **To cite this version:**

Aurore Méré. Reliability of mercury and arsenic sampling and analysis in the petrochemical and oil industry. Analytical chemistry. Université de Pau et des Pays de l'Adour, 2022. English. NNT : 2022PAUU3024 . tel-04085642

HAL Id: tel-04085642

https://theses.hal.science/tel-04085642v1

Submitted on 29 Apr 2023

HAL is a multi-disciplinary open access archive for the deposit and dissemination of scientific research documents, whether they are published or not. The documents may come from teaching and research institutions in France or abroad, or from public or private research centers.

L'archive ouverte pluridisciplinaire **HAL**, est destinée au dépôt et à la diffusion de documents scientifiques de niveau recherche, publiés ou non, émanant des établissements d'enseignement et de recherche français ou étrangers, des laboratoires publics ou privés.

THESE

présentée à

L'Université de Pau et des Pays de l'Adour
Ecole Doctorale des Sciences Exactes et de leurs Applications

par

Aurore MERE

pour l'obtention du grade de

DOCTEUR

Spécialité :

Chimie Analytique

La fiabilité de l'échantillonnage et de l'analyse du mercure et de l'arsenic dans l'industrie pétrochimique et pétrolière

Date de soutenance : 04 juillet 2022

Composition du jury :

Charles-Philippe Lienemann	Rapporteur	Ingénieur de recherche, IFPEN-Lyon
José-Luis Todoli	Rapporteur	
Florence Pannier	Présidente du jury	Professeur, Université de Pau et des Pays de l'Adour
Stuart Baker	Examinateur	
Jorg Feldmann	Examinateur	
Brice Bouyssiere	Directeur de thèse	Professeur, Univ. de Pau et des Pays de l'Adour
Honggang Zhou	Responsable industriel	Référent Thermodynamique, TOTALEnergies
Emmanuel Tessier	Co-directeur de thèse	Ingénieur de recherches, IPREM
Maxime Enrico		

Remerciements

Table des matières

Table des figures

Table des tableaux

Table des abréviations

AAS	Spectromètre d'absorption atomique
AFS	Spectromètre de fluorescence atomique
$AgNO_3$	Nitrate d'argent
As	Arsenic
AsH_3	Arsine
AsO_4^{3-}	Arséniate
Au	Or
BIC	Bordeaux Imaging Center
BrCl	Monochorure de brome
BuMgCl	Chlorure de butylmagnésium
$(C_2H_5)_3As$	Triéthylarsine
$(C_6H_5)_3As$	Triphénylarsine
$(CH_3)As$	Monométhylarsine
$(CH_3)_2As$	Diméthylarsine
$(CH_3)_3As$	Triméthylarsine
CH_3Hg^+	Methymercure
Cl^-	Chlorure
Cryo	Cryogénie
CSTJF	Centre Scientifique et Technique Jean Féger
CV	Vapeur froide
DDP	Polarographie différentielle par implusions
DLs	Limites de détection
DMHg	Diméthylmercure
EDX	Spectroscopie de rayons X énergétiques
ETAAS	Spectrométrie d'absorption atomique électrothermique
EtHg	Ethylmercure
ETV	Vaporisation électrothermique
FAAS	Spectrométrie d'absorption atomique à flamme
FD	Facteur de dilution
FeO	Oxyde ferreux
Fe_2O_3	Oxyde ferrique

FeS_2	Pyrite
FIA	Analyse par injection en flux continu
Ge	Germanium
GFAAS	Spectrométrie d'absorption atomique à four graphite
GPC	Chromatographie par perméation de gel
HCl	Acide chlorhydrique
$HClO_4$	Acide perchlorique
H_2O_2	Peroxyde d'hydrogène
H_2S	Sulfure d'hydrogène
H_2SO_4	Acide sulfurique
HG	Génération d'hydrures
Hg	Mercure
Hg^0	Mercure élémentaire
$HgCl_2$	Dichlorure de mercure
Hg_2Cl_2	Calomel
HgS	Cinnabre
HNO_3	Acide nitrique
HPLC	Chromatographie en phase liquide à haute performance
HR	Haute résolution
HS	Espace de tête
HTL	Hydroliquéfaction
I_2	Diiode
ICP-MS	Spectrométrie de masse à plasma à couplage inductif
ID	Dilution isotopique
$KMnO_4$	Permanganate de potassium
LA	Ablation laser
LA_2O_3	Oxide de lanthane
LNG	Gaz naturel liquéfié
MDLs	Limites de détection de méthodes
MeHg	Méthylmercure
$MgNO_3$	Nitrate de magnésium
MIP-AES	Spectrométrie d'émission atomique à plasma induit par micro-ondes
MMHg	Monométhylmercure

$NaBH_4$	Tétrahydruroborate de sodium
NaCl	Chlorure de sodium
NaOCl	Hypochlorite de sodium
NaOH	Hydroxyde de sodium
NG	Gaz naturel
$(NH_4)_2C_2O_4$	Oxalate d'ammonium
NH_4I	Iodure d'ammonium
$Ni(NO_3)$	Nitrate de nickel
OES	Spectrométrie d'émission optique
Pb	Plomb
Ph_3As	Triphénylarsine
Pt	Platine
PTFE	Polytétrafluoroéthylène
PVG	Génération de vapeur photochimique
PVT	Pression Volume Température
S^0	Sulfate
SEC	Chromatographie d'exclusion stérique
SEM	Microscopie électronique à balayage
$SnCl_2$	Chlorure d'étain
THT	Tétrahydrothiophène
TMA	Triméthylarsine
TMAH	Hydroxyde de tétraméthylammonium
UV	Photooxydation

INTRODUCTION GENERALE

Le mercure (Hg) et l'arsenic (As) sont des éléments naturellement présents dans les produits pétroliers. Le Hg est présent à des concentrations allant de 0,01 à 10 µg.Nm^{-3} dans toutes les fractions pétrolières (Wilhelm and Bloom, 2000). L'As, quant à lui, est présent à des concentrations allant de 10 à 63000 µg.Nm^{-3} dans le gaz naturel (Irgolic et al., 1991). Dans les fluides pétroliers, la présence du mercure pourrait résulter de son existence initiale, avant son enfouissement, dans la matière organique qui deviendra par la suite du pétrole mais également, de sa mobilisation à partir de roches environnantes, vers le pétrole formé (Filby, 1994; Lambertsson et al., 2018). Tandis que pour l'arsenic, sa présence pourrait résulter de la capacité des organismes marins à bioaccumuler cet élément (Liu et al., 2014), leur décomposition ayant conduit à la génèse de pétrole contenant de l'As (Irgolic et al., 1991).

La présence de mercure et d'arsenic dans les matrices pétrolières est à l'origine de divers problèmes pour les compagnies pétrolières. Ces éléments, à des concentrations importantes, représentent un risque pour la santé du personnel en contact avec ces matrices, en raison de leur toxicité pouvant provoquer, à long terme, différents cancers (Boffetta et al., 1993; Yeh et al., 1968). Ceux-ci peuvent aussi poser des problèmes environnementaux, notamment par le rejet du Hg et de l'As dans l'atmosphère, lors de la combustion de gaz naturel par exemple (Krupp et al., 2007). D'un point de vue industriel, le Hg a la faculté de catalyser la corrosion de composants en aluminium : ce qui a des conséquences économiques (remplacements des tubes et autres pièces plus fréquemment qu'à l'ordinaire) mais surtout potentiellement dramatiques du point de vue de la sécurité, dans les usines de traitements des fluides pétroliers (Leeper, 1980). La présence d'As dans les fluides pétroliers pose deux problèmes majeurs d'un point de vue industriel. En effet, la précipitation des composés contenant de l'As conduit à l'obstruction des tuyaux et des vannes dans les « pipes » (Delgado-morales et al., 1994). De plus, la présence d'As dans les fluides pétroliers est à l'origine de l'empoisonnement des catalyseurs pendant le vapocraquage et le traitement du gaz naturel : ce qui représente des coûts financiers élevés (Delgado-morales et al., 1994; Irgolic et al., 1991).

Des systèmes d'élimination du mercure et de l'arsenic efficaces peuvent être mis en place par les compagnies pétrolières afin de traiter les fluides pétroliers. Le développement et le dimensionnement de ces unités de traitements sont basés sur la concentration totale de ces

deux éléments et, si possible, sur la spéciation de ceux-ci dans les fluides pétroliers à traiter. De plus, le gaz d'export est très souvent sujet à spécification en ce qui concerne ce type de composés. Ainsi, un dépassement de spécification peut avoir comme conséquence l'arrêt de l'export. Il est par conséquent indispensable d'évaluer avec fiabilité les concentrations en mercure et en arsenic.

La détermination et la spéciation de ces deux éléments dans les effluents gaziers et pétroliers ont une approche très différente de celle appliquée en salle blanche ou en laboratoire. Le questionnement sur la fiabilité et la représentativité de l'échantillonnage réalisé sur site est prédominant par rapport à l'analyse et la spéciation du mercure et de l'arsenic. L'échantillonnage et l'analyse des éléments traces dans le gaz naturel et le pétrole sont pleins d'artefacts potentiels. Par exemple, la concentration de Hg en phase gazeuse peut parfois être surestimée de plus d'un ordre de grandeur, cela étant dû, notamment, à la présence d'H_2S (Rumayor et al., 2017). De plus, des pertes significatives de mercure et d'arsenic par adsorption sur les parois des « pipes » ou par réaction en présence d'oxygène peuvent être observées et donc fausser les résultats. Pour finir, il existe un risque de faux positifs dus à une contamination ou de faux négatifs dus à l'effet de percée retardée de ces composés lors d'un test de puits.

L'objectif de cette thèse est de traquer des artéfacts potentiels et de proposer des améliorations durant l'échantillonnage du mercure et de l'arsenic afin d'évaluer avec fiabilité et de façon représentative leurs concentrations dans les fluides pétroliers.

Le chapitre 1 de cette thèse est un état de l'art de méthodes d'échantillonnage, de préparations d'échantillons et d'analyses afin de déterminer la concentration et la spéciation du mercure et de l'arsenic dans les flux pétroliers. Les parties 1 et 2 du chapitre 2 présentent ensuite les travaux expérimentaux menés sur la fiabilité de l'échantillonnage à l'aide notamment de cylindres et de sacs Tedlars et de l'analyse du mercure dans le gaz naturel. La partie 3 du chapitre 2 présente les recommandations sur l'échantillonnage et l'analyse du mercure lors d'un essai de puits. Le chapitre 3 présente ensuite les travaux expérimentaux menés sur la fiabilité de l'échantillonnage par cylindres et de l'analyse de l'arsenic dans le gaz naturel. Le chapitre 4 présente les travaux expérimentaux menés sur la compréhension du phénomène d'adsorption du mercure et de l'arsenic à la surface des cylindres d'échantillonnage. Pour finir, ce manuscrit est clôturé par une conclusion générale et des perspectives sur le travail de thèse ainsi que les résultats obtenus.

CHAPITRE I : ETAT DE L'ART

Partie 1 : Total and speciation analyses of mercury in the crude oil industry: a review

***Energy Fuels* 2020, 34, 11, 13307–13320** - https://doi.org/10.1021/acs.energyfuels.0c02730
Received: August 13, 2020; Revised: October 7, 2020; **Publication Date: October 19, 2020**

Maxime Enrico[1,2 II], Aurore Mere[1,2,3 II], Honggang Zhou[3], Hervé Carrier[2,4], Emmanuel Tessier[1,2], Brice Bouyssiere[1,2*]

[1]Institut des Sciences Analytiques et de Physico-Chimie Pour L'environnement et les Matériaux, CNRS/ UNIV PAU & PAYS ADOUR/ E2S UPPA, UMR5254, 64000, Pau, France
[2]Joint Laboratory C2MC: Complex Matrices Molecular Characterization, Total Research & Technology, Gonfreville, BP 27, F-76700 Harfleur, France
[3]TOTAL E&P, CSTJF, Av. Larribau, 64018 Pau, France
[4]CNRS/TOTAL/ UNIV PAU & PAYS ADOUR / E2S UPPA, LFCR-IPRA UMR 5150, 64000, Pau, France
*Corresponding Author: Brice Bouyssiere – brice.bouyssiere@univ-pau.fr

II - M.E. and A.M. contributed equally to this work.

Abstract

Mercury is one of most dangerous contaminants of natural gas and petroleum and petroleum fractions present in the crude oil industry due to its corrosive properties. The determination of Hg levels in petroleum products is a prerequisite for risk evaluation and ensuring an efficient Hg removal. This Review focuses on total and speciation analyses of Hg in the petroleum industry. We describe the constraints related to sampling and analysis for both natural gas and liquid petroleum products and the different methodologies developed over the past decades. Despite the low detection limits reached with various methodologies, the reliability of measurements might strongly depend on sampling and storage practices. The preservation of all Hg species from sampling to analysis might require some further evaluation. We evaluated the speciation methodologies based on reported performances. We however conclude that the lack of reference material for Hg speciation analysis in petroleum hampers a robust evaluation of the methods. Future developments might allow a better characterization of the different Hg species, helpful to understand the partitioning of Hg between the different petroleum phases.

1. Introduction

Mercury is a naturally occurring and problematic component of petroleum products. This heavy metal is present in all petroleum fractions at levels varying by several orders of magnitude ranging from 0.01 ppb to 10 ppm.[1] Its presence in hydrocarbon fluids might result from Hg present in organic matter prior to burial, mantle degassing of gaseous Hg^0 and scavenging by petroleum or mobilization of mineral Hg from surrounding rocks.[9,77] Hg is a toxic and volatile heavy metal. In its metallic form (Hg^0), it is generally found as a gas, although it might also occur as liquid drops when the gas phase is saturated. Upon oxidation, Hg^0 might be converted to salts (such as $HgCl_2$) or complexes (thiolates, amines, etc.). The most toxic forms of Hg are methylated Hg neurotoxins that are soluble (monomethylmercury) or volatile (dimethylmercury, DMHg).

In addition to being problematic for both health and the environment, Hg catalyzes the corrosion of aluminum components, with potentially dramatic consequences in petroleum processing plants.[2] Failures of a liquefied natural gas due to Hg-induced corrosion were responsible for numerous deaths. The implementation of mercury removal units (MRUs) efficiently prevents such failure, yet some maintenance is necessary. In particular, each MRU can remove a given amount of Hg that depends on the amount of hydrocarbons treated and their Hg concentration. Reliable evaluation of Hg concentrations in hydrocarbon streams is therefore necessary to avoid saturation of the MRU, which could lead to inefficient Hg removal.

Hg partitioning between the different phases of petroleum can be estimated by thermodynamics. This, however, generally supposes that Hg is present in its volatile form of Hg^0.[1,3] The partitioning of Hg between these phases is governed by Henry's law. Although this approach sometimes gives satisfactory results, the gas-phase Hg concentration is sometimes overestimated by more than an order of magnitude.[4] It has been noted that this was particularly the case when H_2S was present. The presence of H_2S and other sulfur compounds is known to affect Hg speciation.[5] The initial assumption of Hg^0 being the only species is therefore erroneous when sulfur is present at high concentrations, and the presence of soluble Hg species concentrates Hg in the relatively heavy hydrocarbon fractions. A better understanding of Hg chemistry in petroleum is therefore required to better anticipate Hg partitioning and implement appropriate structures and maintenance procedures.

The assessment of Hg levels in hydrocarbon streams is complicated by several constraints. The exposure of fluids to pipeline inner surfaces allows for some reactions that

might affect Hg chemistry. These different issues presented in the first section of this work need to be taken into account when sampling and analyzing Hg in hydrocarbons streams. Different methods have been developed over the past few decades to reliably determine the Hg concentration in both gas and liquid hydrocarbon samples. We summarize these methods in sections 2 and 3 of this Review.

In addition to Hg concentration, the efficiency of the MRUs depends in part on the Hg species present. The different Hg species that can be found in liquid hydrocarbons (including Hg^0, ionic Hg, organic Hg and particulate Hg) have different chemical properties.[6–8] In natural gas, it is usual to consider Hg^0 to be the only significant species due to its high volatility compared to those of the other, more soluble species. The study of Hg speciation in liquid hydrocarbons is of interest because of the need for sufficient treatment procedures. Although Hg^0 might be the dominant form of Hg in deep reservoirs,[9] the presence of oxidized Hg, particulate Hg and alkylated Hg species was reported.[10,11] For Hg concentration, various techniques are used to evaluate the relative abundance of these species. Section 4 is dedicated to the description of these techniques.

Among the numerous method developments for both Hg concentration and speciation determination in petroleum streams, only few gave rise to standard methods. The present standard methods are also relatively old and were only adapted through minor revisions and did not consider the major recent developments in the field.

2. General Constraints Related to the Sampling and Quantitative Analysis of Mercury

2.1. Natural Gas

The objective of Hg analysis in petroleum products is to assess any risk to downstream operations. Therefore, Hg analysis must be representative for such an assessment. Several constraints need to be considered for reliably estimate Hg levels. We first focus on general issues that apply to any sampling methodology.

2.1.1. Hg Adsorption

2.1.1.1. Current Knowledge

The Hg adsorption process is not yet completely resolved. However, significant losses of Hg are observed for H_2S-containing streams, which probably indicates a reaction involving both H_2S and Hg. Two studies reported the following reactions:[12,13]

$$H_2S + Fe_2O_3 \rightarrow 2FeO + S^0 + H_2O \quad (1a)$$

$$Hg^0 + S^0 \rightarrow HgS \quad (1b)$$

Cinnabar (HgS) is a solid mineral and can therefore accumulate in pipes. These two studies did not show this reaction but cited an earlier study[2] to support this concept.

Larsson et al.[13] observed that a gas containing both H_2S and Hg had no loss of Hg when flowing through PTFE tubes, but significant losses were observed in stainless steel tubes. This suggests that the Hg and H_2S gases do not react directly, which would support the mechanism described by eqs 1a and 1b.

2.1.1.2. Thermodynamic Considerations

The standard free enthalpy of formation of the iron oxide Fe_2O_3 is −825.5 kJ.mol^{-1}, while that of FeO is −272.04 kJ.mol^{-1}. Balancing eq 1a (taking into account H2O, S^0 and H_2S) gives a net enthalpy of +18 kJ.mol^{-1}. A positive net standard reaction enthalpy indicates that the reaction should not take place at room temperature. Adsorption of Hg on stainless steel surfaces in the presence of H_2S was observed at 25°C, so the proposed reaction seems unlikely.

However, from our point of view, another reaction between iron oxide and H_2S is more favorable:

$$4\,H_2S + Fe_2O_3 \rightarrow 2\,FeS_2 + H_2 + 3\,H_2O \quad (2)$$

The net enthalpy for this reaction is −155 kJ.mol^{-1}, which is more likely than reaction 1a. Pyrite (FeS_2) formation could explain the adsorption of Hg. The surface of pyrite contains pyritic groups (S-S) and Fe (hydr)oxides. Sorption of Hg(II) on the pyrite surface occurred at both the oxide and pyritic sites,[14,15] with Hg bound to an additional counterion (as =S-Hg-Cl, =S-Hg-OH, =O-Hg-Cl, and =O-Hg-OH). In natural gas streams, however, Hg is present in its elemental

form (Hg^0) and therefore requires an oxidation step for such surface complexation. In these studies, precipitation of HgS was excluded, but these studies were not conducted on hydrocarbon samples.

2.1.2. Implication of Adsorption Problems for New Pipes

The concentration of Hg in natural gas can vary over time, making it difficult to determine precisely. In particular, the analysis of natural gas from a new well may not be informative of the concentration of Hg in the reservoir. Indeed, Hg adsorption may occur on the inner surfaces of the reservoirs, and the gas is therefore depleted of Hg. Hg analysis could therefore underestimate the Hg content of a gas stream by several orders of magnitude.

In addition, gases that first reach the Earth's surface may be depleted of Hg relative to that in the reservoir because sorption can occur on the well walls. It is therefore important to regularly monitor the Hg concentration in natural gas until a stable value is reached.

In addition, Ryzhov et al.[16] observed an oscillation in Hg concentration during sampling campaigns. A 25-hour cycle was attributed to the lunar tidal cycle, while higher frequency oscillations were observed but not included. These oscillations sometimes do not significantly affect the Hg concentration range. In some cases, however, the fluctuations could lead to an error of more than 20% if a single sample is analyzed. Diurnal and annual cycles can also be anticipated, as temperature affects adsorption/desorption of Hg in pipes and thus increase the Hg concentration during the summer.[17]

2.1.3. Implication of Adsorption Problems for the Sampling System

Natural gas sampling requires a bypass of the main gas stream. This sampling system is not constantly filled with natural gas, so the initial gas stream is not in equilibrium with respect to Hg adsorption. An equilibration time is therefore necessary before sampling with the chosen methodology. This time depends on the total internal surface area of the bypass line. A reduced line is therefore preferable.

Adsorption also depends on temperature. An experimental study on the efficiency of Hg transport in stainless steel tubes showed that heating from 70 to 100°C hinders Hg adsorption.[13] Therefore, a heated bypass line would significantly reduce sampling times.

2.2. Liquid Petroleum Products

Sampling procedures must be appropriate to preserve the stability of Hg in liquid hydrocarbons. The different species of Hg found in liquid hydrocarbons (including Hg^0, ionic Hg, organic Hg, and particulate Hg) have different chemical properties and behaviors.[6–8] To determine the mercury species composition of a hydrocarbon, it is very important that Hg is preserved in the sample during sampling, storage, and sample preparation prior to analysis. Several studies have shown that inappropriate sampling and treatment could lead to an underestimation of the Hg concentration in the condensate.[3,20] The different mechanisms to be avoided are discussed below.

2.2.1. Volatile Hg Loss

Two species of Hg are particularly volatile: Hg^0 and DMHg.[10,18] DMHg is generally very low in concentration and often below the limit of detection.[19] Therefore, the main issue is the loss of Hg^0. In the study of Hg speciation in condensates in Egypt, Ezzeldin et al.[3] found that following a pressure drop between the first and second separators, Hg0 was transferred to the gas phase. A similar process may occur during sampling or sample storage, as condensate samples are taken at atmospheric pressure. In the same study, the authors compared their speciation results to the total Hg measurements. For condensate samples containing mainly Hg^0 (untreated condensate), the summed concentration of the detected Hg species was only half of the total Hg concentration measured independently. This unsatisfactory mass balance was attributed to losses of Hg^0.

Wilhelm et al.[20] observed that the Hg concentration in crude oil samples decreased with the number of bottle openings. During sample storage, dissolved Hg^0 may also volatilize into the free space of a container. These results suggest that sample containers should be filled without free space and that the opening of containers should be avoided to prevent evaporation and/or transformation of Hg species over time. Snell et al.[21] also observed a significant loss of Hg^0 in mixed hydrocarbon solutions over time.

Different sampling procedures can be designed to avoid volatile Hg losses. Pressurized cylinders can be used to preserve the initial sample pressure conditions.[5] The use of a container with a septum cap could be practical, as a syringe could be used to take an aliquot of the sampled gas without opening the container. The ASTM protocol for “Sampling, Storage, and Handling

of Hydrocarbons for Mercury Analysis" [22] recommends the use of glass vials with PTFE-lined septum caps. In this way, it is possible to limit the volatilization of Hg^0 by filling the sample vial with no free space.

2.2.2. Ionic Hg Adsorption on Container Walls

Hg is known to bind to the walls of storage and/or sampling containers/containers. Despite its relative inertness compared to other materials, glass tends to be negatively charged and can attract cationic forms of Hg that will absorb onto the glass surface. Acidification of the glass surface can repel Hg species and stabilize them within the sample, thus preventing further Hg loss.[3]

The adsorption of Hg depends on the nature of the material but also on the chemical species of Hg contained in the matrix. Bloom et al.[23] showed that Hg^0 and DMHg diffuse through the walls of plastic containers.

The composition of the sample matrix may play a role in this adsorption effect. Bloom[10] tested the stability over time of Hg^0, inorganic Hg, and dimethyl- and methylmercury chloride species contained in doped paraffin oil and in composite oil in different containers (borosilicate glass containers with Teflon-lined caps, Teflon FEP bottles, polyethylene bottles, stainless steel bottles (No. 316) and glass bottles lined with aluminum). A significant loss of inorganic Hg was observed in doped paraffin oil in a glass container, whereas no loss of inorganic Hg was observed in composite oil contained in the same glass container. This shows that the composition of the matrix, especially its polarity, can influence this adsorption phenomenon.

This adsorption induces an underestimation of the measured Hg concentration. Various studies have shown that this problem can be solved by using appropriate sample containers. The ASTM D7482-17 protocol suggests the use of glass vessels with a PTFE-lined cap.[22] Recently, Gaulier et al.[5] showed that the use of a Swagelok cylinder lined internally with PTFE could preserve anoxic conditions for Hg(II) preservation.

2.2.3. Precipitation of Hg-Containing Minerals

Particulate Hg is potentially naturally present in condensates. However, no studies have actually identified this. Only one study showed the existence of metacinnabar (β-HgS, black

cinnabar) in crude oil residues.[24] However, it has been shown that Hg can precipitate with S to form HgS minerals when the sample is exposed to ambient air.[5] This is particularly true when H_2S is present in the sample. While Hg does not react directly with H_2S,[19] contact with air can promote the oxidation of H_2S, leading to the generation of elemental sulfur. HgS minerals can then precipitate from Hg and elemental sulfur. This is an additional reason why contact with ambient air should be avoided prior to Hg analysis.

Another potential precipitation process may occur. Snell et al.[21] observed that when the two Hg species Hg^0 and Hg(II) are present in a condensate sample, they can react and form a metallic bond, giving rise to insoluble Hg(I) species:

$$Hg^0 + HgCl_2 \rightarrow Hg_2Cl_2 \quad (3)$$

The factors that might affect this precipitation reaction are poorly understood (pressure, temperature, chemical characteristics of the sample, etc.), so it may be advisable to remove Hg0 from the condensate sample after sampling. Such a procedure exists and is part of a speciation procedure.[25]

2.2.4. Sample Homogeneity

Any analysis performed on a sample aliquot assumes that the Hg is homogeneously distributed in the sample. Heterogeneous samples can lead to a poor estimate of Hg concentration and inconsistent repeat analyses.[26] Depending on the Hg species present, the different mechanisms described above (adsorption on container walls, volatilization of Hg^0, as well as sedimentation of particles) need to be taken into account.

Wilhelm et al.[20] tested different homogenization procedures and found that ultrasonic treatment at 30°C gave Hg recoveries >80%, while the heating and stirring procedure exhibited only a 30% recovery. Ultrasonic treatment is therefore recommended prior to aliquoting for total mercury and speciation analysis

3. Mercury Analysis in Natural Gas

3.1. Sampling method

3.1.1. Bubbling System

This sampling procedure involves bubbling natural gas into a trapping solution. This solution is a mixture of potassium permanganate and sulfuric acid.[27] Usually, three bubblers are used in series to monitor the potential inefficiency of Hg trapping in the first bubbler. This mixture oxidizes the Hg^0 contained in the gas into soluble ionic Hg(II). This soluble ionic Hg(II) is retained in the trapping solution and can then be analyzed. The sampling time must be long enough to reach a mercury concentrate that is sufficient for quantification. The amount of Hg recovered in solution (sum of three trapping solutions) divided by the volume of gas bubbled into the solution gives the Hg concentration in natural gas. This method was recently adapted to allow for sampling at pressures up to 100 bar with direct connection to distribution and transportation networks.[41] The results showed that more than 90% of Hg was trapped in the solution of the first bubbler with insignificant Hg breakthrough, showing the efficiency and reliability of this sampling system.

Table 1. Commercial Instruments Dedicated to Hg Analysis in Gases

Brand	Name	Detector	Analysis	DL (ng/m^3)	Accuracy (%)	Weight (kg)	Flow rate (L/min)
Brooks Rand	Model III	AFS	lab, gold traps (requires amalgamation)	0.1			
Nippon Instrument Corp.	WA-5A	AAS	Au traps, Tedlar bags, gas cylinders	1 pg		13	0.1 – 1
	WA-5F	AFS	Au traps, Tedlar bags, gas cylinders	<0.1 pg		13	0.1 – 1
	EMP (3 different instruments)	AAS	in situ	100 – 50000	10		0.3 – 1
	AM-4	AAS	Air Monitoring	0.01	2		0.1 – 0.5
LUMEX	RA-915+	AAS	Direct gas analysis	2		7.5	
	RA-915M	AAS	Direct gas analysis	2		7	
	Light 915	AAS	Direct gas analysis	100		3.3	
	RA-915M + RP-91NG	AAS	in situ (special NG)	10			
	AMNG	AAS	Monitoring for NG	1 - 1000			
	Jerome 431-X	gold film	in situ	3000	5	3.2	0.75

Arizona Instruments	Jerome J405	gold film	in situ	500	5 - 10	2.4	0.75
	Jerome 451	gold film	in situ, monitoring	3000	8	24	0.75
	Jerome J505	AFS	in situ	50	10 - 15	3	1
PSA	PSA 10.54X Sampling System + PSA 10.670 Process Analyzer	AFS	in situ, monitoring (special NG)				
	10.525 Sir Galahad	AFS	lab, gold traps	<0.1 pg			
Ion Science	MVI mercury vapor detector	UV absorption	in situ	100	10		
Mercury Instruments	VM-3000	AAS	in situ, monitoring	100		7	
	3000-IP		in situ	100		5	
	UT-3000	AAS	in situ, monitoring	0.1		9	
	UT-3000 + NG-sampling system 3000	AAS	in situ, for NG	0.1		50	
	MMS	AAS	in situ, monitoring	100		35-175	
	MMS-NG	AAS	in situ, monitoring, for NG	1			
TEKRAN	2600 NG	AFS	in situ, monitoring, for NG	1			
	2537A and 2537B	AFS	in situ, monitoring, ambient air	0.1			
	2500	AFS	lab				

Hg recovery is, however, significantly reduced in the presence of high H2S concentrations. Brombach and Pichler[28] observed that in the presence of H_2S, the recovery of Hg in potassium permanganate dropped by nearly 50% due to the formation of mercury sulfide (HgS). This issue was overcome by bubbling the gas in a solution of sodium borohydride upstream of the Hg trapping solutions to trap H_2S and avoid any interference in Hg oxidation.

3.1.2. Hg-Selective Sorption

For this sampling method, a stream of natural gas is carried through a glass tube containing iodine-impregnated silica gel. The Hg is trapped by chemisorption inside this tube. The adsorbed Hg is then extracted from this tube by dissolving it in an ammonium iodide/iodine (NH_4I/I_2) solution.[29] This solution is then analyzed to determine the total Hg content of a natural gas, taking into account the volume of gas sampled. Quantitative recovery of Hg (91−109%) was achieved using this methodology in gas wells from China.[30] However, the existence of a liquid extraction stage hinders in situ analysis. In addition, the simplest procedures are always preferred, as the addition of several processing steps can lead to higher background signals and possibly more potential for contamination.

3.1.3. Gold Amalgamation

The system is based on trapping Hg from natural gas by directing the flow through a tube of a solid sorbent containing gold.[31] However, this process has a major advantage over the use of iodine impregnated sorbents. Gold amalgamators can indeed be analyzed without any digestion steps.[3] After sampling, the amalgamator is heated, and Hg is released in an atomic absorbance spectroscopy (AAS) or atomic fluorescence spectroscopy (AFS) detector. The most widely used metal for trapping Hg is gold, but Hg can form amalgams with the most noble metals. Different studies have investigated the use of metal alloys and their efficiency for Hg trapping.[13,32] Silver, gold and platinum−gold alloys allow for quantitative Hg retention.

By using the thermal release procedure, the analysis can be performed on the site if a detector is available (Table 1). This allows a direct evaluation of the sampling efficiency, and the sampling time and volume can be directly adjusted. A reduction in pressure is necessary, however, as the amalgamators operate at ambient pressure.

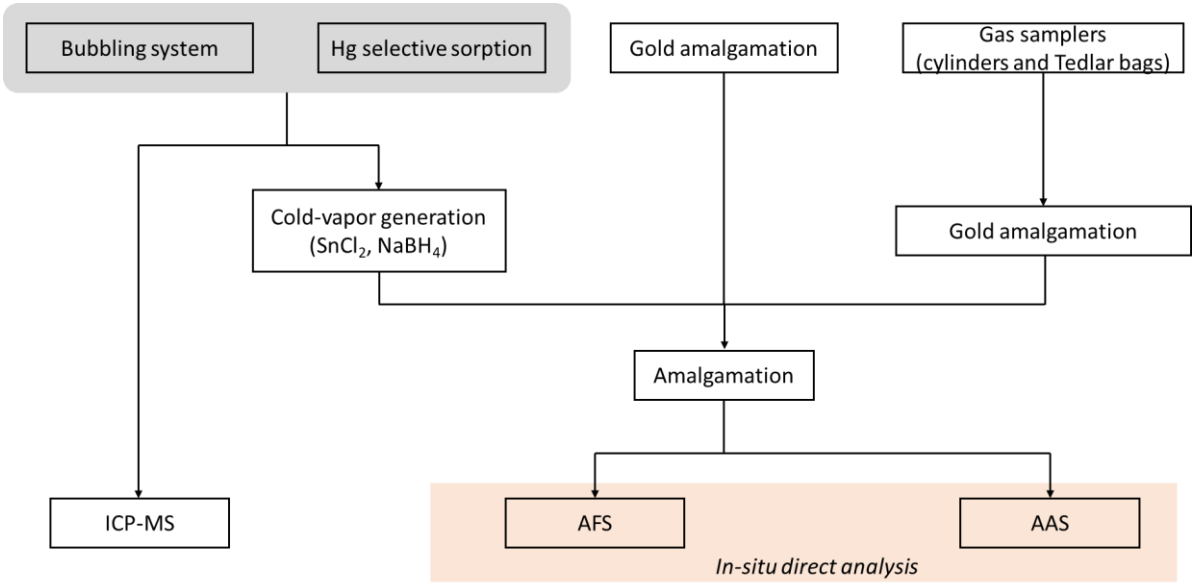

Figure 1. Schematic presenting the different methodologies for Hg quantification in natural gas, from sampling (top boxes) to sample processing (middle boxes) and detection (right boxes)

This method can be used to determine the total Hg content ranging from 0.01 to 100 $\mu g.m^3$ in natural gas samples.[31] Adapted sampling flow rates are also required to avoid Hg breakthrough. Frech et al.[33,34] suggested that the maximum natural gas flow rate should be 2 $L.min^{-1}$, and the maximum sample volume should be 10 L when using a Pt−Au amalgamator. Despite these results, Larsson et al.[13] obtained Hg recoveries greater than 90% with amalgamators similar to Frech et al.,[34] with higher flow rates (up to 10 $L.min^{-1}$) and higher sampling volumes (up to 100 L). This difference can be explained by the different compositions of natural gas that could influence the transport efficiency of Hg on these traps, although this has not been proven.[13] Despite this, a recent study has shown that the efficiency of Hg trapping on gold traps is much lower or almost nil when the natural gas sample contains H_2S.[28]

Heating the amalgamator during sampling generally increases Hg recovery. The aim is to avoid condensation of liquids that could poison the amalgamator and thus reduce the trapping efficiency. The temperature to which the amalgamator can be heated depends on the alloy used. Frech et al.[34] showed that Pt−Au amalgamators could be heated up to 200°C without any loss in trapping efficiency, whereas gold amalgamators were ineffective at over 170°C.

3.1.4. Gas Samplers: Cylinders and Tedlar Bags

The use of pressurized cylinders is generally very convenient for sampling natural gas. Because pressurized cylinders can handle high pressures, sampling is fast. Hg measurements can be made once back in the laboratory by releasing some or all of the sampled gases through a gold amalgamator, which is then analyzed by AAS or AFS.[31] Although sampling is made easier with such a system, its reliability is of great concern. Hg is known to adsorb to most surface materials, including the inner walls of most cylinders.[2,12,35] Measuring the concentration of Hg would therefore underestimate the true concentration of natural gas. Solutions have been developed to overcome this problem. The application of a silicon coating on the walls inside the cylinders to make it inert to Hg adsorption. A silicon coating (SilcoNert 2000, Siltek, or Sulfinert) was specifically designed for this purpose. Its effectiveness has been tested by the manufacturer and has shown stable Hg concentrations for a period of at least 2 months.[36] Other tests showed that the inertness of the coating is compromised by repeated sampling of natural gas samples.[35]

Alternatively, natural gas can also be sampled using inert plastic bags (Tedlar bags).[37−39] Despite its ease of use, this sampling technique does not allow for natural gas to be sampled under pressure, and the conservation of compounds in the gas samples over time is not assured within these bags.[40,41] Although the onsite sampling portion can be simplified by the use of cylinders, the processing of samples in the laboratory may require more time. All disadvantages associated with the use of amalgamators (discussed in the gold amalgamation section) remain, as an amalgamation is required prior to analysis. Despite this constraint, the use of such samplers allows for a reduction in sampling time in the field, which can be advantageous.

3.2. Hg Analysis

In natural gas, mercury exists almost exclusively as Hg^0. [1,3] Therefore, the analyses performed provide only the total amount of Hg in natural gas, i.e., Hg^0.

The trapping solutions ($KMNO_4/H_2SO_4$ solution) obtained after bubbling the gas sample as well as the ammonium iodide/ iodine (NH_4I/I_2) solutions obtained after extraction of the Hg contained in the iodine-impregnated silica gel can be analyzed by cold vapor generation (CV)-AFS, CV-AAS, and inductively coupled plasma mass spectrometry (ICP-MS).[27,29] For the first

two analytical techniques, the detector is based on AAS or AFS, respectively (Figure 1). During analysis, a reducing agent ($SnCl_2$, $NaBH_4$) must be added to the solution to convert Hg^{2+} to Hg^0 [42] during CV.

For gold traps (direct sampling and/or after release of natural gas sampled in Tedlar cylinders/bags), the usual method for Hg quantification is based on thermal desorption. The sampled gold trap is heated to ~500°C under an inert gas stream carrying Hg to another gold trap. This other trap is heated again to ~500°C, and the released gases are directed to the detector. The detector can be either an AAS[43] or an AFS.44 The AFS typically has a detection limit (DL) 10 times lower than that of the AAS with the ability to detect up to a few picograms of Hg (Table 1). For a robust measurement, the Hg trapped in the amalgamator must be above the quantitation limit of the device because gold amalgamators may contain small amounts of Hg even after a cleaning procedure.

Table 2. Summary of Sample Preparation Methods Used for Total Hg Concentration Analysis

Reference	Sample type	Sample processing	Analysis	MDL	Sample size
		By Liquid – Liquid Extraction			
Schickling and Broekaert[34]	Gas condensates	Aqua regia extraction	CV-AAS	0.01 ng/g	NR
Liang et al.,[45]	Gasoline, kerosene diesel, heating oil	BrCl extraction	CV-AFS	0.01 ng/g	5 mL
Zettlitzer et al.,[30]	Gas condensates and brines	Aqua regia extraction	CV-AAS	100 ng/mL	NR
Bloom,[10]	Crude oil, condensates, light distillates, fuel oil, asphalt	BrCl extraction	CV-AFS	0.17 ng/g	0.5 – 1.5 g
Liang et al.,[51]	Crude oil and related products	BrCl extraction	CV-AFS	0.05-0.12 ng/g	1
Brandão et al.,[54]	Gasoline	BrCl extraction	CV-AAS	0.14 µg/L (BrCl extraction)	5 mL
Conaway et al.,[55]	Gasoline and diesel	BrCl extraction	CV-AFS	NR	NR
Uddin et al.,[56]	Crude oil and petroleum products	Dilution in toluene, extraction with BrCl/HCl	CV-AFS	0.38 ng/g	5 g
Vicentino et al.,[46]	Oil products (diesel, biodiesel mineral oil°	Emulsion (Triton X-100 + HNO_3)	CV-AAS	0.6 ng/mL	20 mL
		By Sample Digestion			
Knauer and Milliman,[50]	Crude, fuel and light oil	HNO3/H2SO4 digestion, distillation	CV-AAS	10 ng/g	5 g

Kelly et al.,[52]	Crude oil and diesel fuel SRMs	Digestion by closed system combustion with HNO3 + isotope dilution	ID-CV-ICP-MS	0.01 ng/g	0.25-.5 g
Liang et al.,[51]	Coke (solid)	HNO3/H2SO4 digestion at 95°C	CV-AFS	0.15 ng/g	1 g
Munoz et al.,[49]	Crude oil and diesel fuel	Microwave digestion	Stripping voltammetry	194 ng/g	0.1 g
			Stripping chronopotentiometry	104 ng/g	0.1 g
Wilhelm et al.,[26]	Oil	Autoclave HNO3 digestion (300°C, 130 bar)	CV-AFS		
Yun et al.,[57]	Crude oil and gasoline	Microwave digestion with HNO3/H202	CV-AFS	< 0.26 ng/g	0.1 – 0.2 g
Pontes et al.,[47]	Crude oil, oil sludge	HNO3 digestion in closed pressurized system	CV-AAS	1.3 ng/g	0.25 g
		Aqua regia digestion in cold-finger system		8.6 ng/g	0.5 g
		Alumina digestion in thermal decomposition technique		3.3 ng/g	0.0253 g
Ezzeldin et al.,[3]	Gas condensates	Autoclave HNO3 digestion (90°C)	CV-AFS	0.01 to 0.08 ng/g	~ 1 mL
Gajdosechova et al.,[11]	Petroleum hydrocarbon	Microwaves digestion (90°C) with HNO3	CV-AFS		0.3 g
			ICP-MS		0.3 g
Pereira et al.,[48]	oily sludge	Microwaves digestion with HN03, HCl and H2O2	CV-AFS	0.07 ng/g	0.1 g
			HPLC-ICP-MS	0.01 ng/g	
By Thermal Decomposition					
Knauer and Milliman,[50]	Crude, fuel and light oil	Combustion	CV-AAS	5 ng/g	20 g

Osborne,[58]	C5 to C14	Electrothermal vaporization (graphite furnace, GF)	ETV-ICP-MS	3 ng/g	
Tao et al.,[59]	Crude oil, naphta and condendates	Thermal decomposition	AAS	< 1.5 ng/g	
Shafawi et al.,[60]	Gas condensates	Combustion and amalgamation	AFS	0.7 to 2.5 ng/mL	0.25 mL
Ceccarelli et al.,[61]	Naphtas	Thermal decomposition	AFS	32 ng/g	
		ETV (GF)	AAS		
Liang et al.,[62]	Crude oil	Combustion and amalgamation	AFS	0.2 ng/g	0.04 g
Liang et al.,[51]	Crude oil and related products	Combustion and amalgamation	AFS	0.05 – 0.12 ng/g	0.04 g
Bouyssiere et al.,[63]	Gas condensates	Combustion and amalgamation	AAS	0.3 ng/mL	0.1 mL
Wilhelm et al.,[26]	Oil	Combustion and amalgamation	AFS	0.5 ng/g	
Torres et al.,[64]	Gasoline	Dilution by ethanol, CV generation and transfer in an oven graphite furnace	AAS	0.14 ng/mL	1.5 g
		Dilution by ethanol, CV generation, amalgamation and transfer in an oven graphite furnace		0.08 ng/mL	1.5 g
Pontes et al.,[47]	Crude oil, oil sludge	pyrolysis	AAS	3.3 ng/g	<0.0253 g
Gaulier et al.,[5]	Crude oil, condensates	Adsorption of 20 µL in a pellet, combustion	AAS		0.02 mL
Lambertsson et al.,[9]	Crude oil	Thermal decomposition	AAS	0.03 ng/g	
Other Methods					
Olsen et al.,[65]	Condensates and naphtas	Dilution in xylene	ICP-MS	0.13 ng/g	2 g

Kumar and Gangadharan,[66]	Naphtas	Emulsion with Triton X-100 aqueous solution	ICP-MS	0.12 ng/mL	2 mL
Bouyssiere et al.,[67]	Gas condensate	Dilution in 2-propanol	ICP-MS (HR)	< 9 ng/mL	
Brandão et al.,[54]	Gasoline	Microemulsion with 2-propanol + HNO_3	CV-AAS	0.10 µg/L	20 mL
Bouyssiere et al.,[63]	Gas condensate	Microflow injection	ICP-MS	0.5 ng/mL	0.0025 mL
Vorapalawut et al.,[68]	Crude oil and asphaltene	silica gel plate impregnation	LA-ICP-MS	11 ng/g	
da Silva et al.,[69]	Bio ethanol	Addition of formic or acetic acid, dilution	PVG-AAS	0.05 to 0.09 ng/g	> 50 mL
de Jesus et al.,[70]	Naphta and condensates	Microemulsion (sample + propan-1-ol + water 25:24:1)	PVG-AAS	0.6 ng/mL	1 mL
Lambertsson et al.,[9]	Crude oil	Isotope spike, heating at 200°C	ID-HS-GC-ICP-MS	0.03 ng/g	

3.3. Direct In Situ Analysis

A few companies offer instruments for the determination of Hg gas in the field (Table 1). Among them, some are dedicated to natural gas. Ryzhov et al.[16] used a system based on AAS with Zeeman correction for direct monitoring of Hg concentration in natural gas. The analysis is fast and can be used to monitor the evolution of Hg concentration over time. This method is very convenient because sampling and analysis are performed simultaneously. Such a tool would be very effective for natural gas with high Hg concentrations (a few $\mu g.m^{-3}$), although it may also be useless if there are only a few $ng.m^{-3}$ of Hg in the natural gas. Ryzhov et al.[16] reported DLs of approximately 10 $ng.m^{-3}$. This instrument (LUMEX RA915M coupled to RP-91NG) can be easily transported and is a good alternative to other quantification methods because no sampling steps are required.

Other automated instruments based on amalgamation and AAS or AFS also exist and are suitable for natural gas (Table 1). These automated instruments are, however, more expensive, require some maintenance and cannot be easily moved. Such an instrument could be recommended for sites where variable Hg concentrations have been detected to monitor any changes over time and to avoid any downstream problems.

Direct in situ analysis via direct AAS analysis can monitor the concentration of Hg in the gas over time, even during the equilibration time. This can provide additional information on the adsorption process of Hg, especially in natural gases containing H_2S.[12,13]

4. Mercury Analysis in Hydrocarbon Liquids

4.1. Total Hg Analysis

4.1.1. Preparation

4.1.1.1. Liquid-liquid Extraction

Mercury can be extracted from liquid hydrocarbons by liquid−liquid extraction. The oxidant solution of BrCl seems to be the most used (Table 2). This technique is simple and rapid because the oxidation and recovery of mercury in the BrCl solution is carried out at the same time.[45] BrCl solution converts the mercury present in the samples to its oxidized ionic form (Hg^{2+}), so a reducer must be used, prior to any analysis, to convert the recovered Hg^{2+} in

Hg^0. It has also been shown that the use of an HCl solution does not allow an optimal recovery of Hg from a $NaBH_4$ solution[45] and more recently from a Triton X-100 + HNO_3 solution.[46]

4.1.1.2. Sample Digestion

Unlike the liquid−liquid extraction mentioned above, here, the organic matrix remains in the sample. Digestion by heating with the addition of HNO_3 is the most widespread (Table 2). Pontes et al.[47] showed that thermal digestion coupled with this solution made it possible to obtain a very satisfactory recovery rate as well as a method detection limit (MDL) of 1.3 $ng.g^{-1}$ and 8.6 $ng.g^{-1}$, respectively, which were much lower than those obtained with digestion by a cold system and the addition of aqua regia. This technique is simple, fast and inexpensive.[48] Munoz et al.[49] showed that when using a closed-tank microwave oven, they did not observe any loss of Hg, including volatile Hg. Despite this, several studies have shown that wet digestion by heating is highly vulnerable to contamination and Hg loss.[11,50,51] Isotopic dilution, as mentioned by Kelly et al.,[52] corrects for Hg losses by assuming they are the same for the spike and the hydrocarbon liquid sample. This digestion therefore seems to be the most advantageous for Hg analysis, and Kelly et al. also noted that isotopic dilution allows for correction of potential losses (with the addition of a Hg spike) during digestion.[52] Digestion combined with isotope dilution therefore appears to be the most advantageous method for Hg analysis.

4.1.1.3. Thermal Decomposition

The most common method for sample preparation is the use of thermal decomposition of samples, followed by gold amalgamation. In the first step, Hg is thermally released from the sample, and the Hg compounds are decomposed so that only Hg^0 remains. Produced gases are transferred to a gold amalgamator by a carrier gas that is then analyzed.[26,60,63] Other systems use the same principle without any amalgamation step. The sample is thermally decomposed in a graphite furnace (GF), and the gases are analyzed directly in the graphite furnace coupled with AAS.[9,47,64] However, without the fusion stage, the DLs are usually relatively high. In fact, Pontes et al.[47] wanted to compare their method, which did not have an amalgamation stage, with that of Liang et al.[62] who did have an amalgamation stage. Pontes et al.,[47] obtained a DL of 3.3 $ng.g^{-1}$ with GF-AAS, which was higher than the MDL of 0.2 $ng.g^{-1}$ reported by Liang et

al.,[62] when using an amalgamation step (Table 2). Comparisons between thermal decomposition and liquid− liquid extraction or sample digestion procedures generally show a better recovery with thermal decomposition than without this step. Thermal decomposition is therefore preferred for Hg analysis.[26,51]

4.1.1.4. Other Methods

Several methods of sample preparation for the determination of total Hg may also be used (Table 2). Sample injection into a carrier solvent was shown to be a practical method that does not require sample treatment and fast analysis.[63,65,67]

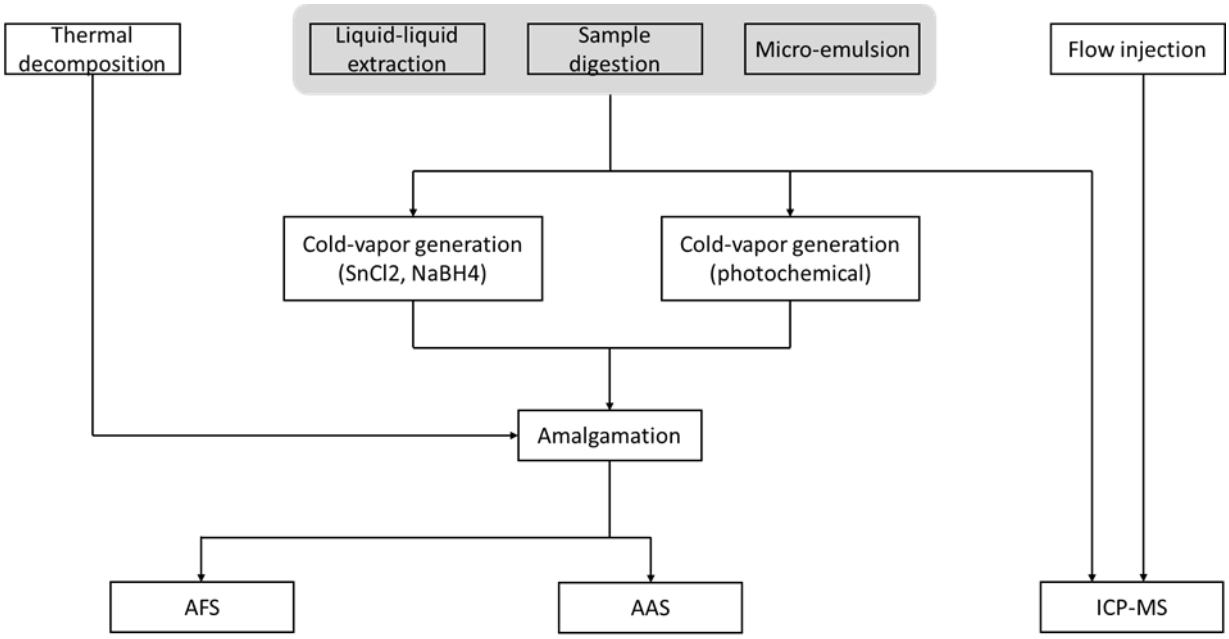

Figure 2. Summary of the different methodologies for total Hg analysis in liquid petroleum, from sample treatment (left boxes) to processing

This technique makes it possible to use very small quantities of samples, with a DL comparable to those of thermal desorption-AAS or AFS.[9,63]

Several authors investigated the possibility of analyzing microemulsions by CV-AAS or photochemical vapor generation (PVG)-AAS. This technique uses a very small sample and reagent volume,[70] and the DLs are comparable to those obtained by extraction with a solution of BrCl: 0.10 $ng.g^{-1}$ for a microemulsion and 0.14 $ng.g^{-1}$ for extraction.[54]

Lambertsson et al.[9] recently developed a new method for determining Hg in liquid oil samples: ID-HS-GC-ICP-MS, which is based on the concentration of Hg in the head space (HS) of a sample vial combined with isotope dilution (ID), GC separation, and ICP-MS detection. An isotopic compound ($^{198}HgCl_2$) is added to the sample to accurately trace the Hg concentration in the samples. The procedure includes one heating step that allows for the complete conversion of all Hg species to Hg^0. Hg^0 then balances between the gas and the dissolved phase. An aliquot of the headspace gas is injected into a gas chromatography (GC)-ICP-MS system. Both ^{202}Hg and ^{198}Hg are monitored to allow for isotope addition correction. This method provides a DL similar to that of thermal desorption coupled to AAS (0.3 $ng.g^{-1}$). Dilution of the condensate may sometimes be necessary to reduce its viscosity or to provide a reasonably stable background for mercury signals. Benzene, toluene, and xylene are universal solvents, but some condensates may be dissolved in hexane, isooctane, or isopropanol, which may be useful in some cases.[56,71]

4.1.2. Analysis

The detection limit of a method depends on the detector used, the dilution factors, the sample matrix after processing and the sample size (Table 2). Analyses by AAS, AFS, and ICP-MS are the most widely used and produce very low MDLs of approximately 0.1 $ng.g^{-1}$ (Table 1). Several studies have shown that these three analytical systems provide similar MDL, accuracy and repeatability values.[11,52,54,61,63]

For liquid−liquid extraction and digestion methods coupled with CV-AAS and CV-AFS (Figure 2), a reducer must be added to the solution prior to analysis to convert Hg^{2+} to Hg^0. [42] A $SnCl_2$ solution can be used,[10,53] but Brandao et al.[54] demonstrated that $NaBH_4$ provides better repeatability and sensitivity and a lower DL than those achieved when using $SnCl_2$. In addition, Gajdosechova et al.[11] reported an underestimation of the Hg concentration when using SnCl2 because of the consumption of $SnCl_2$ for reducing sulfates to sulfides. In addition, Da Silva et al.[69] noted that the reducing agents are often unstable and costly. We concluded that sample preparations avoiding the use of reducing agents should be favored for Hg analysis. Cold vapor generation can also be achieved through the photochemical reduction of Hg. The DLs reported for PVG-AAS are relatively high (1.1 $ng.g^{-1}$).[69,70]

Gajdosechova et al.[11] found that CV-AFS should be used with alkaline samples, i.e., the use of a 2% $SnCl_2$ solution prepared in NaOH (5 M), to avoid underestimating the amount of Hg.

Analysis of hydrocarbon samples by ICP-MS after dilution or emulsification was also found to yield an acceptable MDL (0.2 $ng.mL^{-1}$).

ICP-MS analysis has advantages over the AAS or AFS analyses because the samples can be analyzed directly without pretreatment, and the analysis is faster than the other methods mentioned above.[63,65] However, the DL of ICP-MS (0.5 $ng.mL^{-1}$) is slightly higher than those of the other analytical procedures, which could interfere with the analysis of very low Hg concentrations.[63]

Laser ablation coupled to ICP-MS enables a relatively fast and accurate analysis of petroleum samples. This procedure eliminates the typical drawbacks of ICP-MS analysis of organic solutions, such as matrix signal suppression, carbon deposition, and the formation of interfering ions in plasma.[68] However, the DL of this method is too high (11 $ng.g^{-1}$) for application to liquid hydrocarbons.

4.2. Hg Speciation

Speciation analysis of Hg in liquid hydrocarbons can be performed by different methods. At present, there is no method capable of simultaneously detecting all species contained in liquid hydrocarbon samples because of the different properties of Hg species.[1]

Different methods have been tested for the determination of Hg speciation in liquid hydrocarbons. We can categorize Hg separation methods into two classes: chromatographic techniques and sequential extractions. Since a review published in 2000,[71] few studies have attempted new methodologies for the speciation of Hg in liquid hydrocarbons. Table 3 shows the commercial analytical devices dedicated to the analysis of Hg speciation without the use of liquid samples.

Table 3. Commercial Instruments Dedicated to Hg Analysis in Liquid and Solid Samples and to Hg Speciation in Liquid Samples

Brand	Name	Determined Hg species	Detector	Analysis	Samples	DL	Weight (kg)
Leco	AMA-254	Total Hg	AAS	Direct analysis (thermal decomposition), Lab	Solid/liquids		46 kg
Milestone	DMA-80	Total Hg	AAS	Direct analysis (thermal decomposition + amalgamation), Lab	Solid/liquids	0.001 ng	56 kg
	DMA-1	Total Hg	AAS		Solid/liquids	0.001 ng	
	FMA	Total Hg	AFS and AAS		Lab, liquids	0.01 ng/g	
Nippon instruments Corp.	MA-3000	Total Hg	AAS	Direct analysis (thermal decomposition), Lab	Lab		55 kg
	PE-1000	Total Hg	AFS	Direct analysis (Petro-pyrolysis), Lab	Specific liquid hydrocarbons		40 kg
Perkin Elmer	SMS 100	Total Hg	AAS	Direct analysis (thermal decomposition + amalgamation), Lab	Solid/liquids	0.005 ng	20 kg
Brooks Rand	Model III + MERX Total Hg Purge & Trap Module	Total Hg	AFS	Direct analysis (thermal decomposition + amalgamation), Lab	Solid/liquids	< 0.03 ng/L	
PSA	10.025 Millenium Merlin	Total Hg	AFS or AAS	Direct analysis (thermal decomposition + amalgamation), Lab	Solid/liquids		
LUMEX	RA-915 M + PYRO-915	Total Hg	AAS	Direct analysis (Pyrolyse), Lab	Liquid	0.01 ng/g	

Buck Scientific	410 cold vapor mercury analyzer	Total Hg	AAS	Lab	Solid/liquids	0.0005 ng/g	20 kg
HIRANUMA	HG-400	Total Hg	AAS	Lab	Solid/liquids	0.01-10 ng/g	4 kg
Mercury instruments	LabAnalyzer LA 254	Total Hg	AAS	Lab	Only liquids	5 pg ng/g	10 kg
	AULA-254 Gold	Total Hg	AAS	Direct analysis, Lab	Only liquids	5 ng/L	18.6 kg
Teledyne	Hydra IIAA	Total Hg	AAS	Direct analysis, Lab	Liquids	0.001 g	
	Hydra IIC	Total Hg	AAS	Direct analysis (thermal decomposition + amalgamation), Lab	Solid and semisolid	0.05 ng/L	
	M-8000	Total Hg	AFS	Lab	Liquids	0.5 ng/L	
	M-7600	Total Hg	AAS	Lab		Sub-pg	
TEKRAN	2600	Total Hg	AFS	Lab			
PSA	10.725 GC	Speciation	GC-AFS	Lab	Liquids		
	10.820	Speciation	HPLC-AFS	Direct analysis (Online UV digestion), Lab	Liquids		
Brooks Rand	MERX-M	Speciation	GC-AFS	Direct analysis (Online ethylation), Lab	Liquids	0.002 ng/L	
TEKRAN	2700	Speciation	GC-AFS	Lab	Liquids	0.002 ng/L	

4.2.1. Sample Preparation: Operationally Defined Procedures

The UOP938 protocol proposes a methodology for the speciation of Hg in liquid hydrocarbons (UOP Method 938-10, n.d, n.d.). This technique uses three extraction steps, the first of which consists of sample filtration to determine the particulate Hg fraction (Figure 3). The UOP938 method recommends performing pressure filtration with 0.22 μm polyvinylidene fluoride filters. The second step consists of purging and trapping the volatile Hg species (Hg^0 and eventually DMHg) contained in the sample. After this second step, only soluble Hg (oxidized species) remains in the sample. The third step consists of a liquid−liquid extraction step to separate the ionic and organic Hg species before their analysis. The UOP938 method recommends using a 0.01% sodium chloride solution in water with a volume ratio of 1:5 for this liquid−liquid extraction.

The MDL for each species depends, in part, on the sensitivity of the detector. The volatile Hg and particulate Hg concentrations also depend on the size of the sample due to the preconcentration step (if the filters are analyzed after thermal decomposition and amalgamation). This method has both advantages and disadvantages: it allows for onsite sample processing for the first steps of the procedure, which is an important advantage because it prevents Hg losses and species interconversion during storage.[10] The purging step allows for the collection of volatile Hg^0. In the second step volatile Hg^0 can be removed from the sample to avoid its reaction with Hg(II) and, above all, the precipitation of insoluble Hg(I) resulting from this reaction.[21] However, it has been found that when one species dominates a hydrocarbon sample, it can affect the results for other species.[1] In addition, this method does not allow for the identification of organic species of Hg (MMHg, EtHg, etc.), and MMHg is generally the dominant species.[1] Recently, Gaulier et al.[5] optimized the three steps of the UOP938 method to make it more robust and accurate. They showed that the technique could be more robust by measuring the Hg recovered from the filter instead of quantifying the difference between the unfiltered and filtered solutions, as suggested in the UOP938 method.

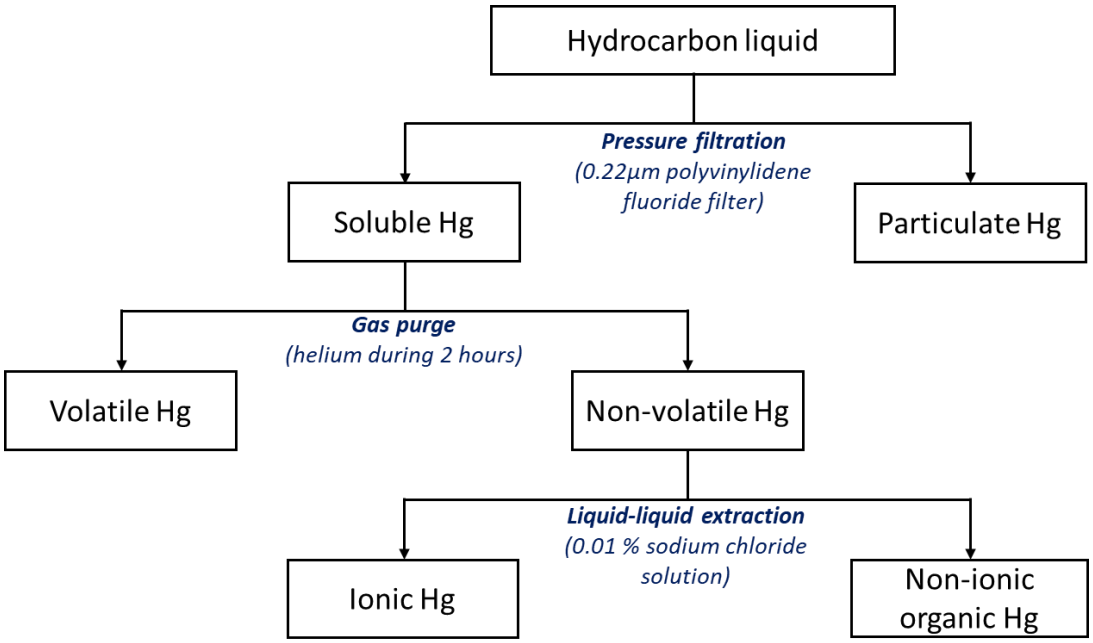

Figure 3. Diagram of mercury speciation analysis in liquid hydrocarbon by UOP Method 938-10 (adapted with permission from ref 5).

Similarly, recovering the Hg^0 purged using a gold amalgamator with subsequent analysis provides a better estimate of its concentration. Sodium chloride used for successive liquid−liquid extraction can damage some analyzers, and an alternative L-cysteine solution was reported to give similar extraction yields (95%) with fewer analytical issues than those occurring with the use of sodium chloride.[5]

Recently, Gajdosechova et al.[72] developed a method based on headspace gas sampling. Hg compounds present in the organic matrix were first extracted by chelation with dithizone (diphenylthiocarbazone), and then sodium tetrapropyl borate was added to volatilize the mercury species. These species were then collected and preconcentrated on ITEX tubes (online preconcentration using in-tube extraction). This sample preparation resulted in a very low DL for MeHg (0.06 $ng.g^{-1}$). Nevertheless, these preparation techniques are specific and generally allow for only certain Hg species to be extracted, contrary to the UOP938 protocol.

4.2.2. Gas Chromatography

GC is a widely used technique for the analysis of Hg speciation in petroleum.[3,11,59,67,72–75] Coupled with suitable detection instruments such as AFS, ICP-MS, or MIP-AES, this technique is capable of separating all volatile Hg species. Only Hg^0 and dialkyl-

Hg species are volatile,[10,18] while monoalkyl-Hg and ionic Hg remain in solution.[3] A derivatization step is necessary to convert Hg(II) to dibutyl-Hg and methyl-Hg to methylbutyl-Hg. A Grignard reagent, generally butylmagnesium chloride (BuMgCl), must be used to carry out this derivatization step.[11,74]

$$2\,BuMgCl + Hg^{2+} = Bu_2Hg + \quad (3)$$

$$BuMgCl + CH_3Hg^{+} = BuCH_3Hg + \quad (4)$$

Analysis of the samples before and after derivatization theoretically allows for complete speciation of Hg in a condensate sample.

Despite the robustness and sensitivity of this technique, some Hg compounds present in the samples may interfere with the analysis. Gajdosechova et al.[11] showed that the GC input temperature can affect the Hg^0 signal during analysis if particulate HgS is present in the sample. They hypothesized that particulate Hg could release Hg^0 when it underwent thermal decomposition when samples were introduced into the GC instrument. Gajdosechova et al.[11] therefore recommends that these HgS particles be removed from the sample prior to speciation analysis of the sample.

Although no speciation method can allow for the direct and complete speciation of Hg, GC coupled to ICP-MS is capable of quantifying all Hg species (except for particulate Hg). Presently, there is no other method capable of such achievement. GC has been coupled to different detectors, but to date, the most robust and the most sensitive is ICP-MS.[67,74] The use of MIP-AES was found to be impractical because of background interferences due to organic compounds; its use is, however, possible if the eluted Hg is first preconcentrated in a gold amalgamator.[75]

4.2.3. HPLC Separation

HPLC is less commonly used than GC for the separation of Hg species. Bouyssiere et al.[71] considered HPLC to be less effective than GC for the separation of Hg species. This method does not require a derivatization step, which allows for a shorter analysis time than that of GC.[59] Schickling and Broekaert[53] coupled HPLC separation with CV-AAS detection. Detection limits of approximately 10 ng.mL^{-1} were achieved for Hg species, which were well

above those found using the GC-ICP-MS methods (<1 $ng.mL^{-1}$). In addition, transient signals and baseline instability were observed.

More recent studies have used HPLC for the separation of Hg species.[57,76] Both of these studies must have used a digestion or extraction step before HPLC-ICP-MS detection. Yun et al.[57] tested different extraction/digestion procedures and found the best recovery rates by microwave-assisted extraction with the addition of tetramethylammonium hydroxide (TMAH). Despite this, the recovery rates were only 87% and 71% for MeHg and EtHg, respectively. The addition of an extraction or digestion step before determining the speciation of Hg is impractical since the initial advantage of HPLC-based systems is to avoid treatment steps and promote the precision of the method.[53] HPLC-ICP-MS analysis might be combined with an isotope addition procedure to take into account Hg species conversions and losses.[76]

4.2.4. Gel Permeation Chromatography

Size-exclusion chromatography (SEC) and gel permeation chromatography (GPC) are not yet widely used for the separation of Hg species. Until now, only one study has investigated the potential of this chromatographic technique for Hg speciation in liquid hydrocarbons.[5] This method allows for the separation of species by hydrodynamic volume.

This method may have significant advantages over other Hg speciation procedures,[71] such as the GC-ICP-MS technique, as it requires no chemicals and does not affect the association of Hg with functional groups until they reach the plasma. Separation by GPC is carried out according to the hydrodynamic volume, and the large molecules elute earlier than small molecules, which can take a longer path in the porous GPC column.

This technique allows for the co-monitoring of various elements, particularly sulfur, which can provide crucial information on Hg-binding molecules. Indeed, some sulfur compounds interact with mercury in liquid hydrocarbon samples.[9,24] The use of this technique, coupled with an ICP-MS detector, makes it possible to simultaneously monitor various elements, including Hg and sulfur, and potentially to identify the important blinding ligands for oxidized Hg.

However, this method was not evaluated quantitatively. Although very good trends were observed for Hg^0 species, no linear relationship was found between the Hg concentration and the detection signal for other Hg species, presumably because of interactions of oxidized Hg

with the column. Further method developments might make GPC-ICP-MS a quantitative and powerful speciation technique for Hg analysis in the future.

5. Challenges and Perspectives

Total Hg analysis itself in both natural gas and liquid petroleum products can be efficiently evaluated using the above-described methods. However, the reliability of Hg measurements is debatable, with the under-evaluated interspecies conversion and losses by volatilization during sampling and sample storage prior to analysis. More investigations on the evolution of Hg species concentrations after sampling are required to assess the reliability of laboratory measurements. The development of robust storage procedure stabilizing Hg species is one of the potential next important steps. Alternatively, onsite procedures might be better representative of Hg concentration and speciation in streams. In particular, the volatile Hg species were shown to be critical.

Many studies reported a dominance of HgII species in petroleum products, yet identifying Hg as HgII is not precise enough to anticipate its properties and behavior during petroleum processing and in MRUs. A better characterization of HgII (Hg salts, Hg thiolates, etc.) might lead to a better understanding of Hg partitioning between the different petroleum phases and help the development of more efficient treatment units. We admit that combining such precise characterization to the onsite analysis we previously recommended might be challenging, which further reinforces the need for more investigations relative to Hg species conversion following sampling.

Our effort in reviewing all developed methodologies revealed a clear gap. The assessment of techniques, in particular for Hg speciation, is often based on Hg species spiking and detection. Although this can be considered as a good proof of concept, the development of an oil reference material with known Hg speciation seems to be necessary to evaluate speciation methods. Presently, we could only compare the methods based on the number of Hg species detected and DLs, which is clearly insufficient for choosing the appropriate technique. In addition, the different laboratories involved in developing Hg (and especially speciation) research in the field also have the responsibility to provide additional evidence for the reliability of their measurements. For this purpose, we suggest the implementation of laboratory inter-

comparison campaigns, consisting in the parallel analysis of several samples. Such campaigns conducted with seawater samples during the past decade notoriously harmonized the results from different laboratories.[77,78]

Another difficulty for upstream sector is to obtain reliable estimation of the mercury content of the gas from new fields during short well tests. As explained above, due to possible chemical reactions and adsorption−desorption equilibrium, mercury can be retained on all kind of surface, including on the surface of the well tubing and of the testing equipment. For this reason, mercury will take some time before its arrival at the separator gas outlet. The lower the mercury content of the gas, the higher the amount of the gas to be produced before being able to measure the actual mercury content.

Sampling or measuring mercury downhole during a well test can be a solution to significantly increase the sensitivity and reduce the duration of the test. However, unlike surface sampling, corrective action becomes nearly impossible in this case. Thus, traceability of the operation and consistency check will be the key challenge in this case.

6. Conclusion

We compiled different sampling constraints and analytical methods for the determination of Hg concentration and speciation in petroleum hydrocarbons. Generally, almost all methods developed for the quantification of Hg have sufficiently low detection limits. Hg speciation methods give variable information depending on the technique used. The presence of different Hg species in petroleum might require further investigations using novel methodologies. Generally, abundant oxidized Hg is only quantified as the sum of Hg species in the +2 oxidation state. Recent developments, such as SEC separation or X-ray absorption fine structure spectroscopy, might better identify the different salts and/or complexes within a single oxidation state. Such information might be critical for a better understanding of Hg partitioning in the different hydrocarbon phases.

Overall, Hg concentration and speciation measurements are no longer a challenge, although some future developments might provide more detailed information on Hg behavior from extraction to processing. The main concern in Hg analysis remains in sampling and storage procedures. Because sampling induces a modification of the conditions (pressure, temperature), the partitioning coefficient between different Hg species might be affected and might ultimately

cause volatilization, oxidation, methylation or precipitation of Hg; thus, rapid onsite analysis is recommended

References

(1) Wilhelm, S. M.; Bloom, N. Mercury in Petroleum. *Fuel Process. Technol.* **2000**, 63, 1−27.

(2) Leeper, J. Mercury-LNG's Problem. *Hydrocarbon Process.* **1980**, *59*, 237−240.

(3) Ezzeldin, M. F.; Gajdosechova, Z.; Masod, M. B.; Zaki, T.; Feldmann, J.; Krupp, E. M. Mercury Speciation and Distribution in an Egyptian Natural Gas Processing Plant. *Energy Fuels* **2016**, *30*, 10236−10243.

(4) Rumayor, M.; Gallego, J. R.; Rodríguez-Valdes, E.; Díaz-́ Somoano, M. An Assessment of the Environmental Fate of Mercury Species in Highly Polluted Brownfields by Means of Thermal Desorption. *J. Hazard. Mater.* **2017**, *325*, 1−7.

(5) Gaulier, F.; Gibert, A.; Walls, D.; Langford, M.; Baker, S.; Baudot, A.; Porcheron, F.; Lienemann, C. P. Mercury Speciation in Liquid Petroleum Products: Comparison between on-Site Approach and Lab Measurement Using Size Exclusion Chromatography with High Resolution Inductively Coupled Plasma Mass Spectrometric Detection (SEC-ICP-HR MS). *Fuel Process. Technol.* **2015**, *131*, 254− 261.

(6) INRS. *Fiche D'information à L'intention Des Medecins: Fiche No. 1: Cannabis;* Institut National de Recherche et de Securite: France, **2014**.

(7) Lide, D. R. *Handbook of Chemistry and Physics*, 79th ed; CRC Press: Boca Raton, FL, **1999**.

(8) Strem. *Chemicals for Research Metals, Inorganics and Organo-metallic*, **2001**.

(9) Lambertsson, L.; Lord, C. J.; Frech, W.; Björn, E. Rapid Dissolution of Cinnabar in Crude Oils at Reservoir Temperatures Facilitated by Reduced Sulfur Ligands. *ACS Earth Space Chem.* **2018**, *2*, 1022−1028.

(10) Bloom, N. S. Analysis and Stability of Mercury Speciation in Petroleum Hydrocarbons. *Fresenius' J. Anal. Chem*. **2000**, *366*, 438− 443.

(11) Gajdosechova, Z.; Boskamp, M. S.; Lopez-Linares, F.; Feldmann, J.; Krupp, E. M. Hg Speciation in Petroleum Hydrocarbons with Emphasis on the Reactivity of Hg Particles. *Energy Fuels* **2016**, *30*, 130−137.

(12) Harfoushian, J. H. Quantification of Low Levels of Mercury in Gas Reservoirs Using Advanced Sampling and Analysis Techniques. *Proceedings of SPE Annual Technical Conference and Exhibition*; Society of Petroleum Engineers, **1995**.

(13) Larsson, T.; Frech, W.; Björn, E.; Dybdahl, B. Studies of Transport and Collection Characteristics of Gaseous Mercury in Natural Gases Using Amalgamation and Isotope Dilution Analysis. *Analyst* **2007**, *132*, 579−586.

(14) Behra, P.; Bonnissel-Gissinger, P.; Alnot, M.; Revel, R.; Ehrhardt, J. J. XPS and XAS Study of the Sorption of Hg(II) onto Pyrite. *Langmuir* **2001**, *17*, 3970−3979.

(15) Ehrhardt, J. J.; Behra, P.; Bonnissel-Gissinger, P.; Alnot, M. XPS Study of the Sorption of Hg(II) onto Pyrite Fes2. *Surf. Interface Anal.* **2000**, *30*, 269−272.

(16) Ryzhov, V. V.; Mashyanov, N. R.; Ozerova, N. A.; Pogarev, S. E. Regular Variations of the Mercury Concentration in Natural Gas. *Sci. Total Environ.* **2003**, *304*, 145−152.

(17) Klusman, R. W.; Jaacks, J. A. Environmental Influences Upon Mercury, Radon and Helium Concentrations in Soil Gases at a Site near Denver, Colorado. J. *Geochem. Explor.* **1987**, *27*, 259−280.

(18) Cameron, C. J.; Didilion, B.; Benayoun, D.; Dorbon, M. Mercury: A Trace Contaminant in Natural Gas and Natural Gas Liquids. *Proceedings Eurogas* 96, June **1996**.

(19) Wilhelm, S. M.; Liang, L.; Kirchgessner, D. Identification and Properties of Mercury Species in Crude Oil. *Energy Fuels* **2006**, *20*, 180−186.

(20) Wilhelm, S. M.; Kirchgessner, D. A.; Liang, L.; Kariher, P. H. Sampling and Analysis of Mercury in Crude Oil. *J. ASTM Int.* **2005**, *2*, 12985.

(21) Snell, J.; Qian, J.; Johansson, M.; Smit, K. Stability and Reactions of Mercury Species in Organic Solution. *Analyst* **1998**, *123*, 905−909.

(22) ASTM D7482-17. *Standard Practice for Sampling, Storage, and Handling of Hydrocarbons for Mercury Analysis*; ASTM International: West Conshohocken, PA, **2017**.

(23) Bloom, N. S.; Horvat, M.; Watras, C. J. Results of the International Aqueous Mercury Speciation Intercomparison Exercise. In *Mercury as a Global Pollutant: Proceedings of the Third International Conference Held in Whistler, British Columbia;* Porcella, D. B., Huckabee, J. W., Wheatley, B., Eds.; Springer Netherlands: Dordrecht, **1995**; pp 1257−1268.

(24) Avellan, A.; Stegemeier, J. P.; Gai, K.; Dale, J.; Hsu-Kim, H.; Levard, C.; O'Rear, D.; Hoelen, T. P.; Lowry, G. V. Speciation of Mercury in Selected Areas of the Petroleum Value Chain. *Environ. Sci. Technol.* **2018**, *52*, 1655−1664.

(25) UOP Method 938-10. *Total Mercury and Mercury Species in Liquids Hydrocarbon, Mercury (Element), Solubility;* ASTM International: West Conshohocken, PA, 2018.

(26) Wilhelm, S. M.; Liang, L.; Cussen, D.; Kirchgessner, D. A. Mercury in Crude Oil Processed in the United States (2004). *Environ. Sci. Technol.* **2007**, *41*, 4509−4514.

(27) Norme NF EN 13211. *Qualité De L'air - Emissions De Sources Fixes - Methode Manuelle De Determination De La Concentration En Mercure Total (Air Quality - Fixed Source Emissions - Manual Method for Total Mercury Determination);* Association Francaise De Normalisation (AFNOR): Paris, France, **2001**.

(28) Brombach, C. C.; Pichler, T. Determination of Ultra-Low Volatile Mercury Concentrations in Sulfur-Rich Gases and Liquids. *Talanta* **2019**, *199*, 277−284.

(29) *ISO 6978-1:2003, Natural Gas Determination of Mercury. Part 1: Sampling of Mercury by Chemisorption on Iodine*, **2019**. https:// www.iso.org/standard/38600.html.

(30) Zhenquan, T.; Quiju, W.; Bin, H. Determination of Mercury Content in Natural Gas by Chemisorption on Iodine-Impregnated Silica Gel. *Chem. Eng. Oil Gas* **2009**, 2009-03. (http://en.cnki.com. cn/Article_en/CJFDTotal-STQG200903022.htm)

(31) *ISO 6978-2:2003, Natural Gas−Determination of Mercury. Part 2: Sampling of Mercury by Amalgmation on Gold/Platinum Alloy*, **2019**. https://www.iso.org/standard/38601.html

(32) Dumarey, R.; Dams, R.; Hoste, J. Comparison of the Collection and Desorption Efficiency of Activated Charcoal, Silver, and Gold for the Determination of Vapor-Phase Atmospheric Mercury. *Anal. Chem.* **1985**, *57*, 2638−2643.

(33) Frech, W.; Baxter, D. C.; Bakke, B.; Snell, J.; Thomassen, Y. Highlight. Determination and Speciation of Mercury in Natural Gases and Gas Condensates. *Anal. Commun.* **1996**, *33*, 7H−9H.

(34) Frech, W.; Baxter, D. C.; Dyvik, G.; Dybdahl, B. On the Determination of Total Mercury in Natural Gases Using the Amalgamation Technique and Cold Vapour Atomic Absorption Spectrometry. *J. Anal. At. Spectrom.* **1995**, *10*, 769−775.

(35) Enrico, M.; Mere, A.; Zhou, H.; Carrier, H.; Tessier, E.; Bouyssiere, B. Experimental Tests of Natural Gas Samplers Prior to Mercury Concentration Analysis. *Energy Fuels* **2020**, *34*, 5205−5212.

(36) SilcoTek. *Prevent Mercury Loss During Transport and Storage with Silconert;* SilcoTek Corp.: Bellefonte, PA, **2019**.

(37) Hirner, A. V.; Feldmann, J.; Krupp, E.; Grümping, R.; Goguel, R.; Cullen, W. R. Metal(Loid)Organic Compounds in Geothermal Gases and Waters. *Org. Geochem.* **1998**, *29*, 1765−1778.

(38) Maillefer, S.; Lehr, C. R.; Cullen, W. R. The Analysis of Volatile Trace Compounds in Landfill Gases, Compost Heaps and Forest Air. *Appl. Organomet. Chem.* **2003**, *17*, 154−160.

(39) Pandey, S. K.; Kim, K. H. Experimental Bias Involved in the Collection of Gaseous Elemental Mercury by the Gold Amalgam Method. *Environ. Eng. Sci.* **2008**, *25*, 255−264.

(40) Beauchamp, J.; Herbig, J.; Gutmann, R.; Hansel, A. On the Use of Tedlar® Bags for Breath-Gas Sampling and Analysis. *J. Breath Res.* **2008**, *2*, 046001.

(41) Cachia, M.; Bouyssiere, B.; Carrier, H.; Garraud, H.; Caumette,̀ G.; Le Hecho, I. Development of a High-Pressure Bubbling Sampleŕ for Trace Element Quantification in Natural Gas. *Energy Fuels* **2017**, *31*, 4294−4300.

(42) Sanchez-Rodas, D.; Corns, W. T.; Chen, B.; Stockwell, P. B.́ Atomic Fluorescence Spectrometry: A Suitable Detection Technique in Speciation Studies for Arsenic, Selenium, Antimony and Mercury. *J. Anal. At. Spectrom.* **2010**, *25*, 933−946.

(43) ASTM D5954-98. *Standard Test Method for Mercury Sampling and Measurement in Natural Gas by Atomic Absorption Spectroscopy;* ASTM International: West Conshohocken, PA, **2014**.

(44) ASTM D6350-14. *Standard Test Method for Mercury Sampling and Analysis in Natural Gas by Atomic Fluorescence Spectroscopy;* ASTM International: West Conshohocken, PA, **2014**.

(45) Liang, L.; Horvat, M.; Cernichiari, E.; Gelein, B.; Balogh, S. Simple Solvent Extraction Technique for Elimination of Matrix Interferences in the Determination of Methylmercury in Environmental and Biological Samples by Ethylation-Gas ChromatographyCold Vapor Atomic Fluorescence Spectrometry. *Talanta* **1996**, *43*, 1883−1888.

(46) Vicentino, P. O.; Brum, D. M.; Cassella, R. J. Development of a Method for Total Hg Determination in Oil Samples by Cold Vapor Atomic Absorption Spectrometry after its Extraction Induced by Emulsion Breaking. *Talanta* **2015**, *132*, 733−738.

(47) Pontes, F. V. M.; Carneiro, M. C.; Vaitsman, D. S.; Monteiro, M. I. C.; Neto, A. A.; Tristao, M. L. B.; Guerrante, M. F. Comparative Study of Sample Decomposition Methods for the Determination of Total Hg in Crude Oil and Related Products. *Fuel Process. Technol.* **2013**, *106*, 122−126.

(48) Pereira, L.; Maranhao, T. A.; Frescura, V. L. A.; Borges, D. L. G. Multivariate Assessment of Extraction Conditions for the Fractionation Analysis of Mercury in Oily Sludge Samples Using Cold Vapor Atomic Fluorescence Spectrometry. *J. Anal. At. Spectrom.* **2019**, *34*, 1932−1941.

(49) Munoz, R. A. A.; Correia, P. R. M.; Nascimento, A. N.; Silva, C. S.; Oliveira, P. V.; Angnes, L. Electroanalysis of Crude Oil and Petroleum-Based Fuel for Trace Metals: Evaluation of Different Microwave-Assisted Sample Decompositions and Stripping Techniques. *Energy Fuels* **2007**, *21*, 295−302.

(50) Knauer, H. E.; Milliman, G. E. Analysis of Petroleum for Trace Metals. Determination of Mercury in Petroleum and Petroleum Products. *Anal. Chem.* **1975**, *47*, 1263−1268.

(51) Liang, L.; Horvat, M.; Fajon, V.; Prosenc, N.; Li, H.; Pang, P. Comparison of Improved Combustion/Trap Technique to Wet Extraction Methods for Determination of Mercury in Crude Oil and Related Products by Atomic Fluorescence. *Energy Fuels* **2003**, *17*, 1175−1179.

(52) Kelly, W. R.; Long, S. E.; Mann, J. L. Determination of Mercury in SRM Crude Oils and Refined Products by Isotope Dilution Cold Vapor ICP-MS Using Closed-System Combustion. *Anal. Bioanal. Chem.* **2003**, *376*, 753−758.

(53) Schickling, C.; Broekaert, J. A. C. Determination of Mercury Species in Gas Condensates by on-Line Coupled High-Performance Liquid Chromatography and Cold-Vapor Atomic Absorption Spectrometry. *Appl. Organomet. Chem.* **1995**, *9*, 29−36.

(54) Brandao, G. P.; de Campos, R. C.; Luna, A. S. Determination of Mercury in Gasoline by Cold Vapor Atomic Absorption Spectrometry with Direct Reduction in Microemulsion Media. *Spectrochim. Acta, Part B* **2005**, *60*, 625−631.

(55) Conaway, C. H.; Mason, R. P.; Steding, D. J.; Russell Flegal, A. Estimate of mercury emission from gasoline and diesel fuel consumption, San Francisco Bay area, California. *Atmos. Environ.* **2005**, *39*, 101−105.

(56) Uddin, R.; Al-Fahad, M. A.; Al-Rashwan, A. K.; Al-Qarni, M. A. A Simple Extraction Procedure for Determination of Total Mercury in Crude Oil. *Environ. Monit. Assess.* **2013**, *185*, 3681−3685.

(57) Yun, Z.; He, B.; Wang, Z.; Wang, T.; Jiang, G. Evaluation of Different Extraction Procedures for Determination of Organic Mercury Species in Petroleum by High Performance Liquid Chromatography Coupled with Cold Vapor Atomic Fluorescence Spectrometry. *Talanta* **2013**, *106*, 60−65.

(58) Osborne, S. P. Quantitation of Mercury in Petroleum by ETV-ICP-MS. *Appl. Spectrosc.* **1990**, *44*, 1044−1046.

(59) Tao, H.; Murakami, T.; Tominaga, M.; Miyazaki, A. Mercury Speciation in Natural Gas Condensate by Gas Chromatography-Inductively Coupled Plasma Mass Spectrometry. *J. Anal. At. Spectrom.* **1998**, *13*, 1085−1093.

(60) Shafawi, A.; Ebdon, L.; Foulkes, M.; Stockwell, P.; Corns, W. Determination of Total Mercury in Hydrocarbons and Natural Gas Condensate by Atomic Fluorescence Spectrometry. *Analyst* **1999**, *124*, 185−189.

(61) Ceccarelli, C.; Picon, A. R.; Mariangel, P. P.; Greaves, E. D.́ Total Mercury Determination in naphthas by Either Atomic Fluorescence or Absorption Spectroscopy. *Pet. Sci. Technol.* **2000**, *18*, 1055−1075.

(62) Liang, L.; Lazoff, S.; Horvat, M.; Swain, E.; Gilkeson, J. Determination of Mercury in Crude Oil by In-Situ Thermal Decomposition Using a Simple Lab Built System. Fresenius' *J. Anal. Chem.* **2000**, *367*, 8−11.

(63) Bouyssiere, B.; Ordóñez, Y. N.; Lienemann, C. P.; Schaumlöffel, D.; Łobinski, R. Determination of Mercury in Organić Solvents and Gas Condensates by μflow-Injection-Inductively Coupled Plasma Mass Spectrometry Using a Modified Total Consumption Micronebulizer Fitted with Single Pass Spray Chamber. *Spectrochim. Acta, Part B* **2006**, *61*, 1063−1068.

(64) Torres, D. P.; Dittert, I. M.; Höhn, H.; Frescura, V. L. A.; Curtius, A. J. Determination of Mercury in Gasoline Diluted in Ethanol by GF AAS after Cold Vapor Generation, Pre-Concentration in Gold Column and Trapping on Graphite Tube. *Microchem. J.* **2010**, *96*, 32−36.

(65) Olsen, S. D.; Westerlund, S.; Visser, R. G. Analysis of Metals in Condensates and naphtha by Inductively Coupled Plasma Mass Spectrometry. *Analyst* **1997**, 122, 1229−1234.

(66) Kumar, S. J.; Gangadharan, S. Determination of Trace Elements in naphtha by Inductively Coupled Plasma Mass Spectrometry Using Water-in-Oil Emulsions. *J. Anal. At. Spectrom.* **1999**, *14*, 967−971.

(67) Bouyssiere, B.; Szpunar, J.; Lobinski, R. Gas Chromatography with Inductively Coupled Plasma Mass Spectrometric Detection in Speciation Analysis. *Spectrochim. Acta, Part B* **2002**, *57*, 805−828.

(68) Vorapalawut, N.; Pohl, P.; Bouyssiere, B.; Shiowatana, J.; Lobinski, R. Multielement Analysis of Petroleum Samples by Laser Ablation Double Focusing Sector Field Inductively Coupled Plasma Mass Spectrometry (LA-ICP MS). *J. Anal. At. Spectrom.* **2011**, 26, 618−622.

(69) da Silva, C. S.; Oreste, E. Q.; Nunes, A. M.; Vieira, M. A.; Ribeiro, A. S. Determination of Mercury in Ethanol Biofuel by Photochemical Vapor Generation. *J. Anal. At. Spectrom.* **2012**, *27*, 689−694.

(70) de Jesus, A.; Zmozinski, A. V.; Vieira, M. A.; Ribeiro, A. S.; da Silva, M. M. Determination of Mercury in naphtha and Petroleum Condensate by Photochemical Vapor Generation Atomic Absorption Spectrometry. *Microchem. J.* **2013**, *110*, 227−232.

(71) Bouyssiere, B.; Baco, F.; Savary, L.; Lobinski, R. Analytical Methods for Speciation of Mercury in Gas Condensates: Critical Assessment and Recommendations. *Oil Gas Sci. Technol.* **2000**, *55*, 639−648.

(72) Gajdosechova, Z.; Pagliano, E.; Zborowski, A.; Mester, Z. Headspace in-Tube Microextraction and GC-ICP-MS Determination of Mercury Species in Petroleum Hydrocarbons. *Energy Fuels* **2018**, *32*, 10493−10501.

(73) Kawasaki, M.; Otsuka, M.; Yamada, J.; Kobayashi, A. Identification of Mercury Species in Liquid Hydrocarbons. *J. Jpn. Pet. Inst.* **2016**, *59*, 235−240.

(74) Pontes, F. V. M.; Carneiro, M. C.; Vaitsman, D. S.; Monteiro, M. I. C.; Neto, A. A.; Tristao, M. L. B. Investigation of the Grignard˜ Reaction and Experimental Conditions for the Determination of Inorganic Mercury and Methylmercury in Crude Oils by GC−ICP−MS. *Fuel* **2014**, *116*, 421−426.

(75) Snell, J. P.; Frech, W.; Thomassen, Y. Performance Improvements in the Determination of Mercury Species in Natural Gas Condensate Using an on-Line Amalgamation Trap or Solid-Phase Micro-Extraction with Capillary Gas Chromatography−Microwave−Induced Plasma Atomic Emission Spectrometry. *Analyst* **1996**, 121, 1055−1060.

(76) Rahman, G. M. M.; et al. Speciation of Mercury in Crude Oil Using Speciated Isotope Dilution Mass Spectrometry. *Spectroscopy* **2010**, 25.

(77) Filby, R. H. Origin and nature of trace element species in crude oils, bitumens and kerogens: implications for correlation and other geochemical studies. *Geol. Soc. Spec. Publ.* **1994**, *78*, 203−219.

(78) Lamborg, C. H.; Hammerschmidt, C. R.; Gill, G. A.; Mason, R. P.; Gichuki, S. An intercomparison of procedures for the determination of total mercury in seawater and recomandations regarding mercury speciation during GEOTRACES cruises. *Limnol. Oceanogr.: Methods* **2012**, *10* (2), 90−100

Partie 2: Arsenic analysis in the petroleum industry: a review

ACS Omega **2022, 7, 43, 38150–38157** - https://doi.org/10.1021/acsomega.2c03708
Received: June 14, 2022; Accepted: August 26, 2022; **Publication Date: October 18, 2022**

Aurore Mere[1,2,3], Maxime Enrico[1,2], Honggang Zhou[3], Emmanuel Tessier[1,2], Brice Bouyssiere[1,2*]

[1]Institut des Sciences Analytiques et de Physico-Chimie Pour L'environnement et les Materiaux, CNRS/ UNIV PAU & PAYS ADOUR/ E2S UPPA, UMR5254, 64000, Pau, France
[2]Joint Laboratory C2MC: Complex Matrices Molecular Characterization, Total Research & Technology, Gonfreville, BP 27, F-76700 Harfleur, France
[3]TOTALEnergies, CSTJF, Av. Larribau, 64018 Pau, France
*Corresponding Author: Brice Bouyssiere – brice.bouyssiere@univ-pau.fr

Abstract

The presence of arsenic in natural gas and liquid hydrocarbons is of great concern for oil companies. In addition to health risks due to its toxicity as well as environmental issues, arsenic is responsible for irreversible poisoning of catalysts and clogging of pipes via the accumulation of As-containing precipitates. To address these problems and to better design treatment units, robust methods for the analysis of arsenic and its compounds in oil streams are required. In addition, the use of feedstocks as a novel source of energy is becoming increasingly important. Most biomasses used as feedstocks are contaminated with arsenic. To avoid problems related to the presence of this element, it is therefore also necessary to have reliable methods for the analysis of arsenic and its compounds in these new fluids. This review outlines the sampling techniques, sample preparation methods and arsenic analysis techniques developed during recent decades and commonly used in the oil industry and in the new feedstocks energy domain.

1. Introduction

Arsenic (As) is the 20th most abundant element in the Earth's crust and is generally found in its inorganic form in soils, rocks and water[1] at concentrations of several mg/kg.[2] As is also present in biota, especially marine organisms, and in crude oil.[3] Marine organisms have the ability to bioaccumulate arsenic, with concentrations reaching up to 2 g kg^{-1} dry weight.[4] Long-term decomposition of marine organisms gives rise to oil with the persistence of As in the oil matrix,[2] with a suspected role of alkylation/dealkylation reactions in the solubilization of As.[2,5]

The presence of arsenic in petroleum fluids is the source of various problems in oil companies. First, As represents a health and safety risk for personnel in contact with these fluids. Arsenic might be responsible for skin lesions, respiratory diseases, and cardiovascular diseases and can cause several long-term cancer developments.[6-8] Another issue relates to the environmental impact of arsenic released to the atmosphere by natural gas burning.[9] From an industrial point of view, there are two major problems related to the occurrence of As. First, the precipitation of As-containing particles leads to the clogging of pipes and valves. This phenomenon was first observed in 1987 after the blockage of pipes in a US gas distribution company. Delgado-Morales et al.[5] suggested that the formation of these solid deposits occurred in the presence of a metallic substrate and were formed from arsenic and H_2S. Irgolic et al.[2] identified volatile alkylarsines as the source of these residues. The second major concern relates to catalyst poisoning during steam cracking and natural gas processing. Small amounts of As might cause severe and irreversible damage to catalysts, representing high financial costs.[9,10]

The total concentration range of arsenic in natural gas was determined to be 0.01 to 63 $\mu g.dm^{-3}$.[2] It was later demonstrated that different organic and inorganic forms of As are present,[11,12] with a dominance of trimethylarsine (TMA, $(CH_3)_3As$), triethylarsine ($(C_2H_5)_3As$), triphenylarsine ($(C_6H_5)_3As$) and arsine (AsH_3).[4,9,13,14] TMA is the most abundant volatile As species in natural gas (55 to 80% of the total As in natural gas).[5] The dominance of TMA is thought to be related to its higher stability over time compared than that of other As compounds.[4]

Few articles mention the total amount of As in crude oil; only Olsen et al.[15] and Stigter et al.[16] were able to identify a concentration range from < 10 to 26.2 $\mu g.kg^{-1}$ As in real crude oil samples. The main forms of arsenic in these matrices are TMA, which is predominant, dimethylated arsenic ($(CH_3)_2As$) and monomethylated arsenic ($(CH_3)As$).[3]

Arsenic removal systems can be set up by oil companies. The development of these units is based on the total arsenic concentration and, if possible, on the speciation of arsenic in the oil fluids. Therefore, before they are set up, it is essential to determine the arsenic content of natural gas and liquid hydrocarbons. This methodology will also be of great importance in the field of new energy feedstocks because As can be present in biogas (and thus biomethane)[17] and in bio-oil during the hydroliquefaction (HTL) of biomass such as swine manure, which may contain high levels of arsenic.[18]

2. Sampling and Analysis of As in Natural Gas

2.1. Sampling

2.1.1. As-Selective Sorption

2.1.1.1. Bubbling systems

This sampling technique consists of bubbling natural gas in one bubbler[2] or several bubblers[4,9,14,19] connected in series containing a trapping solution. Several trapping solutions can be used for this technique, but they must be able to oxidize volatile arsenicals for their pentavalent oxidizing species, such as oxidizing organic arsenic to the arsenate ion (AsO_4^{3-}).[4]

Concentrated nitric acid (HNO_3) can be used as a trapping solution.[2,14,19] However, it has been shown that a 2% aqueous silver nitrate ($AgNO_3$) solution provides better TMA trapping efficiency than a concentrated nitric acid solution.[4,14] Despite this, it has been shown that the arsenic trapping efficiency in a 2% $AgNO_3$ solution is only 70%. These results were obtained by comparing the amount of TMA found in a natural gas sample after bubbling in this solution and analyzing it directly by cryotrapping/gas chromatography–inductively coupled plasma–mass spectrometry (Cryo/GC–ICP–MS). This loss of efficiency can be explained by the potential absorption of arsenic on the walls of the bubblers.[9]

Furthermore, if the natural gas contains a high concentration of H_2S, a black solid is formed in the 2% $AgNO_3$ solution, which inhibits the analysis of this solution.[14]

2.1.1.2. Traps

This sampling technique involves passing a natural gas stream through a tube containing a solid sorbent. This technique allows for large volumes of gas to be sampled.[20] The sorbent used is silica gel impregnated with 1%[21] or 2%[9] $AgNO_3$. When the gas stream is passed through the trap, the arsenic retained within it is desorbed with concentrated HNO_3. The eluate is then analyzed either by UV irradiation–hybride generation–atomic fluorescence spectrometry (UV–HG–AFS), by ICP–MS or by flame atomic absorption spectrometry (FAAS) (see Section 3.2.2 Analysis after sampling). Uroic et al.[21] obtained a TMA absorption efficiency of 99.8% with this type of trap. However, Krupp et al.[9] obtained a TMA absorption efficiency of only 70% with this type of trap. This absorption efficiency was obtained by comparing the amount of TMA found in a natural gas sample after trapping on a silver nitrate-impregnated silica gel trap and by direct analysis of the sample by Cryo/GC–ICP–MS. This result is considered to be due to incomplete absorption inside the trap due to the very low polarity of TMA or incomplete desorption of TMA during its extraction from the trap with nitric acid.[9]

2.1.2. Gas Samplers: Cylinders and Inert Plastic Bags (Tedlar Bags)

Natural gas sampling can be conducted using pressurized cylinders or Tedlar bags. Arsenic analysis in natural gas sampled with these two types of samplers can be determined directly by Cryo/GC–ICP–MS.[9] Arsenic can also be determined by releasing some or all of the sampled gas into a silicon trap impregnated with $AgNO_3$, where the eluate (see Section 3.1.1.2 Traps) from this tube is then analyzed by UV–HG–AFS (see Figure 4).[21]

Pressurized cylinders can be used to sample gases at high pressures directly on the production system or in the well under initial pressure.[2] Although natural gas sampling with pressurized cylinders is a fast and easy-to-handle method, arsenic depletion has been observed in natural gas samples stored in steel cylinders.[4,5] To overcome this problem, a special coating (Silcosteel® or Sulfinert®) has been designed to create an inert internal surface in these cylinders to limit the interactions between arsenic and the cylinder walls.

Inert plastic bags (Tedlar bags) can also be used to sample natural gas.[22] However, unlike cylinders, natural gas must be depressurized to be sampled in Tedlar bags. It has been shown that within 24 hours, there is no significant loss in the various volatile arsenic species contained in these bags. However, it has been shown that over time, there is adsorption of

arsenic compounds to the inner surface of the Tedlar bags, which suggests that arsenic analysis should be carried out no later than 24 hours after sampling.[20]

2.2. Analysis

2.2.1. Direct Analysis

Total arsenic and its species in natural gas can be analyzed directly without a sample preparation and preconcentration step. Freije-Carrelo et al.[23] developed a GC–ICP–MS method that allows for the simultaneous analysis of total arsenic and its speciation in natural gas. To perform this simultaneous analysis, two gas injection valves were interconnected. The first valve directs the gas sample into the analytical column (GC column) for arsenic speciation analysis. The second valve allows for the same gas sample to be directed into a transfer line directly connected to the GC–ICP–MS interface to analyze the total arsenic by continuous flow injection analysis (FIA). The detection limits obtained with this technique are very low, i.e., 2 ppt for total analysis and 12 ppt for speciation, and matrix effects are negligible.[23]

Arsenic species in natural gas can also be analyzed directly using the cryotrapping technique. This technique is widely used in the research laboratory, but there are no publications mentioning its direct use in the field. This technique does not require any sample preparation beforehand. This method consists of trapping gas samples in a capillary column[2] or a GC column[22] or in a glass tube filled with a chromatographic packing.[24] This trapping is carried out cryogenically using liquid hydrogen,[9] liquid nitrogen[20] or an acetone/liquid nitrogen mixture.[25] The arsenic species contained in the gas samples are then thermally desorbed from these columns/tubes using temperature ramps reaching a maximum temperature of 160°C to 290°C. The carrier gas used is helium.

Arsenic species can be analyzed using different techniques/detectors and can first be separated by GC. After separation, As species can be analyzed by MS. The detection limit obtained with this technique is 0.5 $ng.dm^{-3}$.[2] After this separation by GC, the As species can also be analyzed by ICP–MS. Detection limits are generally on the order of a few $ng.m^{-3}$ but can vary depending on the amount of gas analyzed.[9,20-22,24] Arsenic species in the analyzed gases can also be directly analyzed by ICP–MS without a GC separation phase.[25]

The cryotrapping technique coupled with ICP–MS is an extremely sensitive and reproducible method, and when coupled with GC–ICP–MS, the speciation of arsenic in natural

gas can be analyzed. Furthermore, the trapping efficiency of cryotrapping is 100% compared to that obtained with bubbling solutions and traps.[9] However, the technique is very expensive and cannot be used directly in the field.

Uroic et al.[21] developed the cryotrapping/UV–HG–AFS method, which is a promising technique for direct field use for the measurement of arsenic compounds in natural gas. The cryotrapping and coupling technique was equivalent to that used by Cryo/GC–ICP–MS described in this same publication. The only difference is that the detector used was an AFS and that a precursor hydride generation step was performed. A detection limit of 1 $\mu g.m^{-3}$ for 20 L of natural gas was obtained. Despite the lack of sensitivity and precision of this technique compared to Cryo/GC–ICP–MS, it is inexpensive and can be used to carry out preliminary measurements directly in the field before moving on to more precise analyses.

2.2.2. Analysis after preconcentration

The bubbling solutions (see Section 3.1.1.1. Bubbling systems) obtained after bubbling the gas sample can be analyzed by ICP–MS to obtain the total arsenic concentration .[4,14,19] ICP–MS is a very sensitive and selective analytical method for the analysis of total arsenic in bubbling/trapping solutions.[4] The detection limit found in the trapping solution and with this type of detector (analysis with reaction cell) is 0.09 ppb.[14] To analyze the total arsenic in the trapping solutions, As species can also be mineralized (addition of nitric acid and concentrated hydrogen peroxide) by microwave assistance to transform all arsenic compounds into arsenate and then analyzed by FAAS (see Figure 4). The detection limit obtained with this analytical method was 5.0 $\mu g.L^{-1}$.[9] Irgolic et al.[2] were able to determine the total arsenic in their trapping solutions by mineralizing these solutions with sulfuric acid. These authors were also able to perform speciation by directly analyzing these trapping solutions by GC–MS after hydride generation without going through the mineralization step.[2]

The eluate obtained after desorption of arsenic retained on the surface of silica traps can be analyzed by FAAS or ICP–MS with a collision cell (to eliminate $ArCl^-$ interference) for the determination of total arsenic.[9] Total arsenic can also be determined from the eluate by UV–HG–AFS. UV photooxidation converts organic arsenic compounds to inorganic arsenic, and the addition of sodium borohydride to the eluate reduces all inorganic arsenic compounds to arsine. The detection limit obtained with the UV–HG–AFS technique is 1 $\mu g.m^{-3}$ for 20 L of sampled gas.[21]

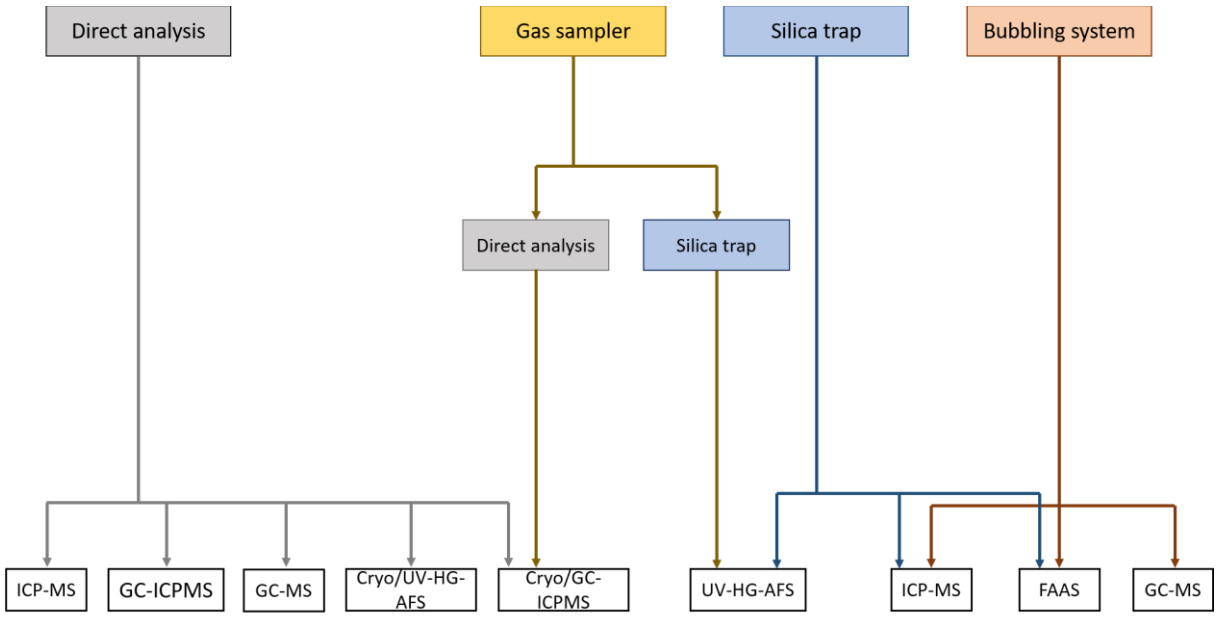

Figure 4. Diagram of Arsenic Analysis in Natural Gas

3. Sampling and Analysis of As in Hydrocarbon Liquids

3.1. Sample Preparation

3.1.1. Microemulsions

The microemulsion technique consists of stabilizing a liquid hydrocarbon sample in the form of a microemulsion before analysis. There are two types of microemulsions: those prepared with surfactants and those prepared without detergents.

Detergent-free microemulsions involve creating a homogeneous solution using three components. This solution is usually composed of the sample, propan-1-ol and HNO_3.[10,26] Water can also be added to this solution.[27] The volumetric ratios of these components vary depending on the sample analyzed. However, it was found that when the volume of the sample was greater than 10% of the final volume of the solution, the solution was not homogeneous.[27] It has been shown that there is no loss of arsenic from detergent-free microemulsions over time.[26] Despite this, arsenic recoveries in detergent-free microemulsions are 2.5% lower than those obtained in surfactant microemulsions.[27]

Surfactant microemulsions consist of mixing the sample with Triton X-100. The concentration and amount of surfactant added varies from author to author.[27-29] When the sample volume is greater than 20%, the solution obtained with Triton X-100 is biphasic even after immediate stirring after its addition.[27] Microemulsions prepared with Triton X-100 are stable for at least 2 h.[28] The recovery rates of arsenic in microemulsions are 86% with the addition of 2.5% Triton X-100[29] and close to 100% with the addition of 4% Triton X-100.[27] Both of these microemulsion techniques do not require any further sample pretreatment, are rapid techniques and allow for the accurate determination of arsenic in liquid hydrocarbons.[27,28] Finally, these preparations reduce background noise and make the signal more stable during analysis.[29]

3.1.2. Extraction, Mineralization and Digestion

Liquid hydrocarbons can be mineralized to analyze the arsenic contained in them. This step destroys the matrix and therefore limits interference with the matrix during the analysis. Sulfuric acid (H_2SO_4), HNO_3 or hydrogen chloride (HCl) can be used as well as water to carry out this mineralization.[3,30,31] Potassium permanganate ($KMnO_4$) solution can be added to facilitate mineralization.[31] Iodine can also be added to the solution to increase the water solubility of the arsenic compounds.[30]

The arsenic compounds can also be extracted from the matrix without destroying the matrix. In crude oil samples, a liquid–liquid extraction of arsenic compounds can be performed with HNO_3.[26] In naphthas, a liquid–liquid extraction of arsenic compounds can be performed with a solution of sodium hypochlorite (NaOCl), H_2SO_4 and water followed by digestion of the obtained aqueous solution (ASTM UOP946-96, n.d.). Arsenic in paraffin or petroleum can be extracted on a solid surface using a microcrystalline naphthalene or cetyltrimethylammonium bromide adsorbent. The detection limit obtained with this solid surface extraction is 0.016 ppm.[32] Arsenic can be extracted on a solid surface using a Chelex 100 column, but the sample must first be burnt in an oxygen bomb.[33]

Liquid hydrocarbons can also be digested to destroy the matrix and analyzed for arsenic. This digestion is usually an acid digestion where concentrated H_2SO_4, HNO_3 or HCl is added to the samples to achieve this digestion.[16,32-34] Hydrogen peroxide (H_2O_2) can be added to the acid solution to promote digestion of the matrix.[16]

Brandão et al.[26] determined the concentrations of As found in different liquid hydrocarbon samples by analyzing them with the microemulsion technique developed by them, the mineralization technique developed by Aneva and Iancheva,[30] the technique EPA SW-846 Test Method 3031[31] and the technique ASTM UOP946-96.[34] The arsenic concentrations found in these samples using these four sample preparation techniques are equivalent, showing their accuracy.[26] Despite this, arsenic remains one of the most volatile elements, which makes it difficult to analyze quantitatively, especially when it undergoes sample preparation or matrix destruction.[35]

3.1.3. Dilution and Direct Injection

Liquid hydrocarbons can be directly analyzed without sample preparation, which saves analysis time[36] and minimizes sample handling.[37]

Samples can either be diluted in xylene[15,36] or toluene[13] or injected directly into the analytical instrument.[37-39] It has been shown that dilution of liquid hydrocarbons in organic solvents increases sensitivity when these samples are analyzed by ICP–MS.[36] However, due to the high viscosity of liquid hydrocarbons, especially fuel oil,[3] the dilution factor must be relatively high, making it even more difficult to analyze arsenic, which is at trace levels in this type of sample.[15]

Direct injection of samples without a dilution step can significantly improve the sensitivity of the method if multiple injections are used.[39] If direct injections are carried out to analyze liquid hydrocarbons by graphite furnace atomic absorption spectrometry (GFAAS), a chemical modifier must be added to the sample (see Section 4.2.1 Analysis by GFAAS) to ensure that the pyrolysis temperature is sufficiently high to efficiently destroy the matrix in the furnace and, above all, that this high pyrolysis temperature does not result in arsenic losses.[26]

The dilution of liquid hydrocarbon samples followed by their analysis can make it possible to analyze the speciation of the arsenic contained in them, particularly by capillary GC–ICP–MS (see Section 4.2.2. Analysis by ICP–MS).[13]

3.2. Analytical Methods

3.2.1. Analysis by GFAAS

Liquid hydrocarbon samples that have undergone sample preparation, such as microemulsions, extraction or digestion (see Section 4.1. Sampling), can be analyzed by GFAAS, also known as electrothermal atomic adsorption (ETAAS). This analytical technique allows for direct analysis of these samples without the need for sample preparation.[10,37,39] Atomic absorption spectrometry is one of the most widely used techniques for analyzing liquid hydrocarbons, but arsenic remains a difficult element to analyze by this technique in complex matrices.[27] When coupled with a graphite furnace, this technique provides good sensitivity for arsenic analysis in complex matrices and is a relatively affordable technique compared to ICP–MS.[26,37] This technique consists of introducing the sample into a graphite furnace so that it is first pyrolyzed and then atomized. The arsenic is then analyzed by AAS. Temperatures and atomization times vary from 2100°C to 2600°C and 2 to 10 seconds, respectively; the carrier and purge gas used is usually argon.[10,26-28,30,31,37,39]

To apply such high pyrolysis and atomization temperatures without loss of arsenic, a chemical modifier must be injected into the furnace during the GFAAS analysis.[39] The most widely used chemical modifier, also known as the "conventional" or "universal" modifier, is $Pb/MgNO_3$.[26,27,31,37] Triton X-100 can be added to this chemical modifier to improve the analytical signal during analysis.[10,36] Other chemical modifiers can be used, such as $Ni(NO_3)$[226,30] or La_2O_3.[39] The latter provides a better detection limit for arsenic analysis in naphthas of 0.56 $\mu g.L^{-1}$ than the detection limit obtained with palladium, rhodium, tungsten, silver and mixed palladium and magnesium modifiers.[39] So-called "permanent" modifiers such as ruthenium[27] or iridium[28] can also be used. The iridium permanent modifier has been shown to improve the sensitivity of the analysis compared to the 'conventional' chemical modifier of $Pb/MgNO_3$.[28]

The detection limits obtained for arsenic analysis by GFAAS are between 0.5 $\mu g.L^{-1}$ and 5.6 $\mu g.L^{-1}$.[10,26-28,30,31,37-39] They are presented in Table 4.

3.2.2. Analysis by ICP-MS

Microemulsions and diluted liquid hydrocarbons (see Section 4.1 Sampling) can also be analyzed by ICP–MS. This technique is very sensitive and allows for the analysis of complex matrices with minimum sample preparation but remains very expensive.[26]

To introduce the sample into the instrument, Olsen et al.[15] used a Meinhardt-Scott chamber and obtained good analytical precision and a detection limit of 0.2 $ng.g^{-1}$ for arsenic. De Albuquerque et al.[36] used a concentric micronebulizer coupled to a refrigerated cyclonic spray chamber and obtained a detection limit of 0.04 $\mu g.kg^{-1}$. The carrier and nebulizer gas used is generally argon.[13,15,29,36] To avoid carbon deposition problems and to ensure plasma stability, O_2 should be used as an auxiliary gas in the analysis of liquid hydrocarbons by ICP–MS.[29,36]

Arsenic can also be analyzed by FI-HG-ICP–MS.[36] After acid digestion of the sample, HCl is added to the digestate to convert As(V) to As(III). The solution is then mixed with $NaBH_4$ and the hydrides are separated in a liquid–gas separator and introduced directly into the ICP–MS instrument. The detection limit obtained with this technique is very low, i.e., 0.002 $\mu g.kg^{-1}$, but the generation of hydrides lengthens the analysis time compared to analysis by ICP–MS alone.[36]

Speciation of arsenic in liquid hydrocarbons, especially in gas condensates, can be carried out using ICP–MS coupled with capillary GC.[13] The absolute detection limit obtained with this technique is 0.05 pg, but this technique makes it difficult to identify certain peaks of arsenical compounds that interfere with other peaks of other compounds present in the analyzed samples.[13]

3.2.3. Analysis by other methods

Arsenic in liquid hydrocarbon samples can be analyzed by atomic absorption spectrometry after hydride generation (HG–AAS). Generally, prior to hydride generation, reagents such as ammonia water and HCl,[33] ammonium oxalate ($(NH_4)_2C_2O_4$) (ASTM UOP946-96, n.d.) or a mixture of hydrochloric acid + hydroxylammonium chloride + potassium iodide as well as ascorbic acid[16] are added to the sample to adjust the pH. To generate the hydrides, $NaBH_4$[33] alone or a solution of NaBH4 and sodium hydroxide (NaOH)[16,34] are added to the sample as reducing agents. Generally, HCl is added throughout the analysis, and the

measured wavelength for arsenic is 193.7 nm.[33,34] The detection limit obtained for arsenic analysis by HG-AAS is approximately 10 ppb (see Table 1).

After extraction on a solid surface, arsenic in oil can be analyzed by differential pulse chromatography (DPP).[32] HCl-pyridine-NaCl is often used as the supporting electrolyte. This method is simple, fast and selective and has a detection limit of 0.016 ppm.[32]

After mineralization, arsenic compounds in crude oil can be analyzed by helium-DC plasma after hydride generation.[3] A buffer of oxalic acid was added to the ore to adjust the pH to identify and quantify the arsenic compounds in the samples. With this buffer, arsine, arsenate, methyl arsenate, dimethyl arsenate and trimethyl arsenate compounds were observed in the crude oil samples.[3]

Table 4. Summary of Sample Preparation Methods Used fo Arsenic Concentration Analysis with their Detection Limits (MDLs)

Reference	Sample type	Sample processing	Analysis	MDL
		Microemulsions		
Aucelio and Curtius[27]	Gasoline and kerosene	Detergent-free microemulsion (propan-1-ol + HNO_3 + water) Surfactant emulsion (Triton X-100 (in HNO_3))	ETAAS	2 µg.L^{-1}
Becker et al.[10]	Naphtha, gasoline and petroleum condensate	Detergent-free microemulsion (propan-1-ol + HNO_3)	GFAAS	1.9 µg.L^{-1}
Brandão et al.[26]	Diesel and naphtha	Detergent-free microemulsion (propan-1-ol + HNO_3)	GFAAS	Diesel = 1.8 µg.L^{-1} Naphtha = 1.5 µg.L^{-1}
Cassella et al.[40]	Naphtha	Surfactant emulsion (Triton X-100 (in HNO_3))	ETAAS	2.7 µg.L^{-1}
Kumar and Gangadharan[29]	Naphtha	Surfactant emulsion (Triton X-100 (in water))	ICP–MS	0.1 µg.L^{-1}
		Extraction, mineralization and digestion		
Aneva and Iancheva[30]	Gasoline	Iode/HNO_3 mineralization	ETAAS	5.6 µg.L^{-1}

ANSI Webstore[34]	Naphtha	Chemical extraction and $HNO_3/H_2SO_4/H_2O_2$ Digestion	HG–AAS	
Brandão et al.[26]	Gasoline	HNO_3 extraction	GFAAS	1.2 $\mu g.L^{-1}$
Dubey et al.[32]	Oil	Extraction in solid surface	DDP	0.016 ppm
EPA SW-846 Test Method 3031[31]	Diesel	Chemical mineralization	GFAAS	
Puri and Irgolic[3]	Refined hydrocarbons, Residual fuel oil and Crude oil	HNO_3/H_2SO_4 mineralization	HG + analysis helium-DC plasma	Absolute MDL = 1.0 to 0.1 ng
Narasaki[33]	Butter	Combustion in an oxygen bomb, extraction in solid surface and HCl digestion	HG–AAS	5 ppb
Stigter et al.[16]	Crude oil cargeos	HNO3/H2O2 digestion	HG–AAS	10 $\mu g.kg^{-1}$
Dilution and direct injection				
Bouyssiere et al.[13]	Gas condensate	Direct injection	GC–ICP–MS	Absolute MDL = 0.05 pg
de Albuquerque et al.[36]	Crude oil	Dilution in xylene	ICP–MS	0.04 $\mu g.kg^{-1}$
			FI-HG-ICPMS	0.002 $\mu g.kg^{-1}$
de Jesus et al.[38]	Crude oil	Direct injection	GFAAS	5.1 $\mu g.kg^{-1}$
Olsen et al.[15]	Condensate and Naphtha	Dilution in xylene	ICP–MS	0.2 $ng.g^{-1}$
Reboucas et al.[39]	Naphtha and Condensate	Direct injection	ETAAS	Naphtha = 0.56 $\mu g.L^{-1}$ Condensate = 1.33 $\mu g.L^{-1}$

4. Sampling and Analysis of As in the New Energy Feedstocks Domain

Arsenic is present in many biomasses, including plants,[41-43] paper,[44] pig manure,[18] sludge[45] and wood.[46] The byproducts resulting from this biomass are bio-oils as well as biogas and can be obtained notably by pyrolysis[41-43,45,46] or by coliquefaction.[18] These byproducts formed from these As-contaminated biomasses thus remain contaminated with this element.

To determine the total As concentration in bio-oils, they must first undergo digestion. This digestion process is usually performed by adding HNO_3 and HCl to the bio-oil samples.[18,42-44,46] Digestion can also be performed by adding HNO_3 and H_2O_2[41] or by adding HNO_3, HF and $HClO_4$.[45] Digestion of bio-oil samples can be promoted by performing microwave-assisted digestion after the addition of reagents.[18,42,43,46] Arsenic in these digestates is usually analyzed by ICP–MS.[41-45] Arsenic can also be analyzed in digestate by ICP–emission spectroscopy(ES)[46] or by ICP–optical emission spectroscopy (OES), with a detection limit of 25 mg/kg.[18] The total As concentrations found in bio-oils are in the $mg.kg^{-1}$ range.[41,43-45]

To analyze total As as well as its speciation in biogas, there are different sampling and analytical methods. Biogas can bubble in HNO_3 and H_2O_2 solutions contained in 3 bubblers in series. The total arsenic trapped in these bubbler solutions was then analyzed by ICP–MS.[47,48] Arsenic in biogas can also be trapped by passing a biogas stream through a silica trap impregnated with 1% $AgNO_3$.[49] The arsenic retained within the trap is desorbed with boiling concentrated HNO_3. The eluate was then analyzed by UV–HG–AFS to determine total arsenic. Arsenic speciation can be performed from the eluate of this tube by adding concentrated H_2O_2 and analyzing this solution by HPLC–IPC–MS.[49] With this analytical technique, Mestrot et al.[50] was able to quantify TMA, dimethylarsine and arsine in biogas samples. Finally, biogas can be sampled in Tedlar bags, and the speciation of arsenic contained in it can be directly determined by Cryo/GC–ICP–MS after transferring the biogas contained in the Tedlar bag to the Cryo-Catcher column.[17]

5. Conclusion

Various sampling techniques, sample preparation methods, pretreatment methods, and analytical methods for As concentration determination in the petroleum industry have been

described in this review. However, most articles focus on laboratory methods, but potential artifacts related to on-site sampling/analysis are not comprehensively discussed. Determining arsenic compounds in gaseous and petroleum effluents is difficult due to the possibility of contamination, loss by adsorption, or the occurrence of chemical reactions related to changes in temperature, pressure, and redox conditions. In the petroleum industry, the difficulty is not in obtaining samples, performing analyses or even detecting arsenic with a sufficiently low detection limit but in preparing the sampling campaign while anticipating the validation of the results by identifying and eliminating all possible artifacts related to the on-site environment. With the increasing development of new energy feedstocks, most of which contain arsenic, the determination of arsenic in biogas and bio-oil has become important. The proper consideration of potential artifacts related to the sampling and analysis of these fluids should be predominant to validate the concentration of arsenic found in these new fluids. Therefore, additional work is still needed to identify artifacts and avoid them by using appropriate sampling/analysis methods.

References

(1) Zheng, L.; Liu, G.; Chou, C.; Gao, L.; Peng, Z. Arsenic in Chinese Coals: Its Abundance, Distribution, Modes of Occurrence, Enrichment Processes, and Environmental Significance. *Acta Geoscientica Sinica* **2006**, *27*, 355–366.

(2) Irgolic, K. J.; Llger, D.; Zingaro, R. A.; Spall, D.; Puri, B. K. Determination of Arsenic and Arsenic Compounds in Natural Gas Samples. *Appl. Organomet. Chem.* **1991**, *5*, 117–124.

(3) Puri, B. K.; Irgolic, K. J. Determination of Arsenic in Crude Petroleum and Liquid Hydrocarbons. *Environ. Geochem. Health* **1989**, *11*, 95–99.

(4) Liu, Z. X.; Tang, D. Z.; Yan, Q. T.; Xu, H.; Wang, S. Y.; Xu, R.; Wu, S. Characteristic of the Volatile Arsenic in Natural Gas and its Novel Determination Method. *Appl. Mech. Mater.* **2014**, *522-524*, 1515–1521.

(5) Delgado-Morales, W.; Zingaro, R. A.; Mohan, M. S. Arsenic in Natural Gas: Analysis and Characterization of Pipeline Solids by 1H NMR and Other Methods. *Int. J. Environ. Anal. Chem.* **1994**, *57*, 313–328.

(6) Mazumder, D. G. Chronic Arsenic Toxicity & Human Health. *Indian J. Med. Res.* **2008**, *128*, 436–447.

(7) Rahman, M. M.; Ng, J. C.; Naidu, R. Chronic Exposure of Arsenic via Drinking Water and its Adverse Health Impacts on Humans. *Environ. Geochem. Health* **2009**, *31*, 189–200.

(8) Yeh, S.; How, S. W.; Lin, C. S. Arsenical Cancer of Skin: Histologic Study with Special Reference to Bowen's Disease. *Cancer* **1968**, *21*, 312–339.

(9) Krupp, E. M.; Johnson, C.; Rechsteiner, C.; Moir, M.; Leong, D.; Feldmann, J. Investigation into the Determination of Trimethylarsine in Natural Gas and its Partitioning into Gas and Condensate Phases Using (Cryotrapping)/Gas Chromatography Coupled to Inductively Coupled Plasma Mass Spectrometry and Liquid/Solid Sorption Techniques. *Spectrochim. Acta, Part B* **2007**, *62*, 970–977.

(10) Becker, E.; Rampazzo, R. T.; Dessuy, M. B.; Vale, M. G. R.; da Silva, M. M.; Welz, B.; Katskov, D. A. Direct Determination of Arsenic in Petroleum Derivatives by Graphite Furnace Atomic Absorption Spectrometry: A Comparison Between Filter and Platform Atomizers. *Spectrochim. Acta, Part B* **2011**, *66*, 345–351.

(11) Caumette, G.; Lienemann, C.-P.; Merdrignac, I.; Bouyssiere, B.; Lobinski, R. Element Speciation Analysis of Petroleum and Related Materials. *J. Anal. At. Spectrom.* **2009**, *24*, 263–276.

(12) Fish, R. H.; Brinckman, F. E.; Jewett, K. L. Fingerprinting Inorganic Arsenic and Organoarsenic Compounds in In Situ Oil Shale Retort and Process Waters Using a Liquid Chromatograph Coupled with an Atomic Absorption Spectrometer as a Detector. *Environ. Sci. Technol.* **1982**, *16*, 174–179.

(13) Bouyssiere, B.; Baco, F.; Savary, L.; Garraud, H.; Gallup, D. L.; Lobinski, R. Investigation of Speciation of Arsenic in Gas Condensates by Capillary Gas Chromatography with ICP-MS Detection. *J. Anal. At. Spectrom.* **2001**, *16*, 1329–1332.

(14) Xu, R.; Tang, D. Z.; Yan, Q. T.; Xu, H.; Wang, S. Y.; Tao, S.; Han, Z. X. Exploration of Detection Technology About Arsenic Content in Natural Gas and Application. *Energy Fuels* **2015**, *29*, 3863–3869.

(15) Olsen, S. D.; Westerlund, S.; Visser, R. G. Analysis of Metals in Condensates and Naphtha by Inductively Coupled Plasma Mass Spectrometry. *Analyst* **1997**, *122*, 1229–1234.

(16) Stigter, J. B.; de Haan, H. P. M.; Guicherit, R.; Dekkers, C. P. A.; Daane, M. L. Determination of Cadmium, Zinc, Copper, Chromium and Arsenic in Crude Oil Cargoes. *Environ. Pollut.* **2000**, *107*, 451–464.

(17) Pinel-Raffaitin, P.; Le Hecho, I.; Amouroux, D.; Potin-Gautier, M. Distribution and Fate of Inorganic and Organic Arsenic Species in Landfill Leachates and Biogases. *Environ. Sci. Technol.* **2007**, *41*, 4536–4541.

(18) Xiu, S.; Shahbazi, A.; Shirley, V. B.; Wang, L. Swine Manure/Crude Glycerol Co-Liquefaction: Physical Properties and Chemical Analysis of Bio-Oil Product. *Bioresour. Technol.* **2011**, *102*, 1928–1932.

(19) Cachia, M.; Bouyssière, B.; Carrier, H.; Garraud, H.; Caumette, G.; Le Hécho, I. Development of a High-Pressure Bubbling Sampler for Trace Element Quantification in Natural Gas. *Energy Fuels* **2017**, *31*, 4294–4300.

(20) Haas, K.; Feldmann, J. Sampling of Trace Volatile Metal(loid) Compounds in Ambient Air Using Polymer Bags: A Convenient Method. *Anal. Chem.* **2000**, *72*, 4205–4211.

(21) Uroic, M. K.; Krupp, E. M.; Johnson, C.; Feldmann, J. Chemotrapping-Atomic Fluorescence Spectrometric Method as a Field Method for Volatile Arsenic in Natural Gas. *J. Environ. Monit.* **2009**, *11*, 2222–2230.

(22) Hirner, A. V.; Feldmann, J.; Krupp, E.; Grümping, R.; Goguel, R.; Cullen, W. R. Metal(loid)organic Compounds in Geothermal Gases and Waters. *Org. Geochem.* **1998**, *29*, 1765–1778.

(23) Freije-Carrelo, L.; Moldovan, M.; García Alonso, J. I.; Vo, T. D. T.; Encinar, J. R. Instrumental Setup for Simultaneous Total and Speciation Analysis of Volatile Arsenic Compounds in Gas and Liquefied Gas Samples. *Anal. Chem.* **2017**, *89*, 5719–5724.

(24) Feldmann, J.; Hirner, A. V. Occurrence of Volatile Metal and Metalloid Species in Landfill and Sewage Gases. *Int. J. Environ. Anal. Chem.* **1995**, *60*, 339–359.

(25) Hirner, A. V.; Feldmann, J.; Goguel, R.; Rapsomanikis, S.; Fischer, R.; Andreae, M. O. Volatile Metal and Metalloid Species in Gases from Municipal Waste Deposits. *Appl. Organomet. Chem.* **1994**, *8*, 65–69.

(26) Brandão, G. P.; de Campos, R. C.; Luna, A. S. Determination of Mercury in Gasoline by Cold Vapor Atomic Absorption Spectrometry with Direct Reduction in Microemulsion Media. *Spectrochim. Acta, Part B* **2005**, *60*, 625–631.

(27) Aucelio, R. Q.; Curtius, A. J. Evaluation of Electrothermal Atomic Absorption Spectrometry for Trace Determination of Sb, As and Se in Gasoline and Kerosene using Microemulsion Sample Introduction and Two Approaches for Chemical Modification. *J. Anal. At. Spectrom.* **2002**, *17*, 242–247.

(28) Cassella, R. J.; Barbosa, B. A. R. S.; Santelli, R. E.; Rangel, A. T. Direct Determination of Arsenic and Antimony in Naphtha by Electrothermal Atomic Absorption Spectrometry with Microemulsion Sample Introduction and Iridium Permanent Modifier. *Anal. Bioanal. Chem.* **2004**, *379*, 66–71.

(29) Kumar, S. J.; Gangadharan, S. Determination of Trace Elements in Naphtha by Inductively Coupled Plasma Mass Spectrometry using Water-in-Oil Emulsions. *J. Anal. At. Spectrom.* **1999**, *14*, 967–971.

(30) Aneva, Z.; Iancheva, M. Simultaneous Extraction and Determination of Traces of Lead and Arsenic in Petrol by Electrothermal Atomic Absorption Spectrometry. *Analytica Chimica Acta* **1985**, *167*, 371–374.

(31) US EPA Method 3031. *Acid Digestion of Oils for Metals Analysis by Atomic Absorption or inductively Coupled Plasma (ICP) Spectrometry*; EPA SW-846 Test Method 3031, **1996.**

(32) Dubey, R. K.; Puri, B. K.; Hussain, M. F. Determination of Arsenic in Various Environmental and Oil Samples by Differential Pulse Polarography After Adsorption of its Morpholine-4-Carbodithioate on to Microcrystalline Naphthalene or Morpholine-4-Dithio-Carbamate-CTMAB-Naphthalene Adsorbent. *Anal. Lett.* **1997**, *30*, 163–172.

(33) Narasaki, H. Determination of Arsenic and Selenium in Fat Materials and Petroleum Products by Oxygen Bomb Combustion and Automated Atomic Absorption Spectrometry with Hydride Generation. *Anal. Chem.* **1985**, *57*, 2481–2486.

(34) ANSI Webstore. *ASTM UOP946-96. Arsenic in Petroleum Naphthas by HG-AAS*. n.d. https://webstore.ansi.org/standards/astm/astmuop94696?gclid=CjwKCAjwxOCRBhA8EiwA0X8hiwIWrPB2v9pkspCcezK2qfIAEL0bsxF2YXU06sQsN5gvkdraTEGCCBoCycoQAvD_BwE (accessed 2022–3–21).

(35) Hofstader, R. A.; Milner, O. I.; Runnels, J. H. Arsenic. In *Analysis of Petroleum for Trace Metals, Advances in Chemistry*, Hofstader, R. A., Milner, O. I., Runnels, J. H. Eds.; American Chemical Society: Washington, D. C., 1976; pp 55–67.

(36) de Albuquerque, F. I.; Duyck, C. B.; Fonseca, T. C. O.; Saint'Pierre, T. D. Determination of As and Se in Crude Oil Diluted in Xylene by Inductively Coupled Plasma Mass Spectrometry Using a Dynamic Reaction Cell for Interference Correction on 80Se. *Spectrochim. Acta, Part B* **2012**, *71-72*, 112–116.

(37) Reboucas, M. V.; Ferreira, S. L. C.; Neto, B. D. B. Arsenic Determination in Naphtha by Electrothermal Atomic Absorption Spectrometry After Preconcentration Using Multiple Injections. *J. Anal. At. Spectrom.* **2003**, *18*, 1267–1273.

(38) de Jesus, A.; Zmozinski, A. V.; Damin, I. C. F.; Silva, M. M.; Vale, M. G. R. Determination of Arsenic and Cadmium in Crude Oil by Direct Sampling Graphite Furnace Atomic Absorption Spectrometry. *Spectrochim. Acta, Part B* **2012**, *71-72*, 86–91.

(39) Reboucas, M.; Ferreira, S.; Debarrosneto, B. Behaviour of Chemical Modifiers in the Determination of Arsenic by Electrothermal Atomic Absorption Spectrometry in Petroleum Products. *Talanta* **2005**, *67*, 195–204.

(40) Cassella, R. J.; de Sant'Ana, O. D.; Santelli, R. E. Determination of Arsenic in Petroleum Refinery Streams by Electrothermal Atomic Absorption Spectrometry After Multivariate Optimization Based on Doehlert Design. *Spectrochim. Acta, Part B* **2002**, *57*, 1967–1978.

(41) Arnold, S.; Rodriguez-Uribe, A.; Misra, M.; Mohanty, A. K. Slow Pyrolysis of Bio-Oil and Studies on Chemical and Physical Properties of the Resulting New Bio-Carbon. *J. Cleaner Prod.* **2018**, *172*, 2748–2758.

(42) He, J.; Strezov, V.; Zhou, X.; Kumar, R.; Kan, T. Pyrolysis of Heavy Metal Contaminated Biomass Pre-Treated with Ferric Salts: Product Characterisation and Heavy Metal Deportment. *Bioresour. Technol.* **2020**, *313*, 123641.

(43) He, J.; Strezov, V.; Kan, T.; Weldekidan, H.; Asumadu-Sarkodie, S.; Kumar, R. Effect of Temperature on Heavy Metal(loid) Deportment During Pyrolysis of *Avicennia marina* Biomass Obtained from Phytoremediation. *Bioresour. Technol.* **2019**, *278*, 214–222.

(44) Zhang, Z.; Macquarrie, D. J.; De Bruyn, M.; Budarin, V. L.; Hunt, A. J.; Gronnow, M. J.; Fan, J.; Shuttleworth, P. S.; Clark, J. H.; Matharu, A. S. Low-Temperature Microwave-Assisted Pyrolysis of Waste Office Paper and the Application of Bio-oil as an Al Adhesive. *Green Chem.* **2015**, *17*, 260–270.

(45) Chiang, H.-L.; Lin, K.-H.; Lai, N.; Shieh, Z.-X. Element and PAH Constituents in the Residues and Liquid Oil from Biosludge Pyrolysis in an Electrical Thermal Furnace. *Sci. Total Environ.* **2014**, *481*, 533–541.

(46) Kim, J.-Y.; Kim, T.-S.; Eom, I.-Y.; Kang, S. M.; Cho, T.-S.; Choi, I. G.; Choi, J. W. Characterization of Pyrolytic Products Obtained from Fast Pyrolysis of Chromated Copper Arsenate (CCA)- and Alkaline Copper Quaternary Compounds (ACQ)-Treated Wood Biomasses. *J. Hazard. Mater.* **2012**, *227-228*, 445–452.

(47) Cachia, M.; Bouyssiere, B.; Carrier, H.; Garraud, H.; Caumette, G.; Le Hécho, I. Characterization and Comparison of Trace Metal Compositions in Natural Gas, Biogas, and Biomethane. *Energy Fuels* **2018**, *32*, 6397–6400.

(48) Chin, K. F.; Wan, C.; Li, Y.; Alaimo, C. P.; Green, P. G.; Young, T. M.; Kleeman, M. J. Statistical Analysis of Trace Contaminants Measured in Biogas. *Sci. Total Environ.* **2020**, *729*, 138702.

(49) Mestrot, A.; Uroic, M. K.; Plantevin, T.; Islam, M. R.; Krupp, E. M.; Feldmann, J.; Meharg, A. A. Quantitative and Qualitative Trapping of Arsines Deployed to Assess Loss of Volatile Arsenic from Paddy Soil. *Environ. Sci. Technol.* **2009**, *43*, 8270–8275.

(50) Mestrot, A.; Xie, W.-Y.; Xue, X.; Zhu, Y.-G. Arsenic Volatilization in Model Anaerobic Biogas Digesters. *Appl. Geochem.* **2013**, *33*, 294–297.

CHAPITRE II : FIABILITE DE L'ECHANTILLONNAGE ET DE L'ANALYSE DU MERCURE DANS LE GAZ NATUREL

Il existe différentes méthodologies pour la détermination de la concentration de mercure dans le gaz naturel (cf 3.1.Sampling method, p 27). L'une d'entre elles, repose sur l'échantillonnage du gaz naturel à pression atmosphérique à l'aide de sacs Tedlar ainsi qu'à haute pression à l'aide de cylindres en acier inoxydable avant de mesurer le Hg hors site (cf 3.1.4.Gas Samplers: Cylinders and Tedlar Bags, p 32).

Un revêtement interne est présumé empêcher l'adsorption du Hg à l'intérieur de ces cylindres ainsi que des sacs Tedlar, rendant vraisemblablement l'analyse du Hg fiable. Grâce à différentes expérimentations développées dans la partie 1 de ce chapitre, cette notion de fiabilité d'échantillonnage de gaz naturel pour l'analyse du mercure dans des cylindres est remise en question, en montrant que même les cylindres revêtus de silicium sont inefficaces pour empêcher l'adsorption du Hg sur les parois internes. Ces expérimentations décrites dans la partie 1, ont été réalisées avec un gaz propre et non sur un échantillon réel de gaz naturel contenant des concentrations substantielles de soufre par rapport au Hg.

Afin de déterminer si le soufre ainsi que l'oxygène ont un rôle dans le mécanisme d'adsorption du mercure sur les échantillonneurs, un sac Tedlar a été rempli avec ¼ d'air ambiant et de ¾ de gaz pétrolier auxquels du mercure gazeux y a été ajouté. La stabilité de celui-ci à l'intérieur du sac Tedlar a été suivi au cours du temps. Les résultats sont décrits dans la partie 2 de ce chapitre.

Les résultats de stabilité du mercure dans ces échantillonneurs au cours du temps, décrits dans les parties 1 et 2 de ce chapitre, ont permis, par la suite, d'élaborer des recommandations sur l'échantillonnage et l'analyse du mercure dans le gaz naturel au cours d'un essai de puits. Ces recommandations sont décrites dans la partie 3 de ce chapitre.

Partie 1 : Experimental Tests of Natural Gas Samplers Prior to Mercury Concentration Analysis

***Energy Fuels* 2020, 34, 5, 5205 – 5212 - https://doi.org/10.1021/acs.energyfuels.9b03540**
Received: October 14, 2019; Revised: December 26, 2019; **Publication Date: December 26, 2019**

Maxime Enrico[1,2], Aurore Mere[1,2,3], Honggang Zhou[3], Hervé Carrier[2,4], Emmanuel Tessier[1,2], Brice Bouyssiere[1,2*]

[1]Institut des Sciences Analytiques et de Physico-Chimie Pour L'environnement et les Materiaux, CNRS/ UNIV PAU & PAYS ADOUR/ E2S UPPA, UMR5254, 64000, Pau, France
[2]Joint Laboratory C2MC: Complex Matrices Molecular Characterization, Total Research & Technology, Gonfreville, BP 27, F-76700 Harfleur, France
[3]TOTAL E&P, CSTJF, Av. Larribau, 64018 Pau, France
[4]CNRS/TOTAL/ UNIV PAU & PAYS ADOUR / E2S UPPA, LFCR-IPRA UMR 5150, 64000, Pau, France
*Corresponding Author: Brice Bouyssiere – brice.bouyssiere@univ-pau.fr

Abstract

Mercury (Hg) is a natural, trace component of natural gas. Corrosion of aluminum heat exchangers by liquid metallic Hg can lead to dramatic issues. The quantification of the gaseous Hg concentration in natural gas streams is therefore crucial prior to the implementation of Hg removal units for preventing the formation of liquid Hg. Different methodologies exist for the determination of the Hg concentration in natural gas, one of which relies on the sampling of natural gas at high pressure using stainless-steel cylinders prior to off-site Hg measurement. An inert internal coating is supposed to hamper Hg adsorption, presumably making the Hg analysis reliable. Here, we challenge this statement by showing that even silicon-coated cylinders are inefficient for preventing Hg adsorption on internal walls. Different cylinders were tested for gaseous Hg concentration stability over time in a clean argon matrix. We find that the gaseous Hg concentration sharply declines in almost all tested cylinders (uncoated, polytetrafluoroethylene-coated, and silicon-coated) to reach undetectable levels within a day or two as a result of adsorption, with the notable exception of a brand-new silicon-coated cylinder. Heating cylinders up to 190°C allowed for the recovery of most adsorbed Hg and revealed the

occurrence of two distinct Hg species with distinct release temperatures. Our results suggest that Hg^0 is first physically adsorbed and further oxidized, presumably in relation to sulfur compounds covering the internal walls of the cylinders. The newly purchased silicon-coated cylinder kept a constant gaseous Hg concentration over 6 months because it never interacted with any real natural gas sample containing substantial sulfur concentrations relative to Hg.

1. Introduction

The occurrence of mercury (Hg) in natural gas is of great concern for the petroleum industry. Hg occurs naturally in petroleum and natural gas, with reported concentrations covering several orders of magnitude (from ng Nm^{-3} to mg Nm^{-3} ranges in natural gas).[1] Hg in petroleum reservoirs undergoes reduction and is therefore mostly present as Hg^0,[2] a highly volatile species. In hydrocarbon extraction and processing, Hg therefore likely goes to the light natural gas phase, although variations toward lower temperatures might allow for some oxidation.[3]

In addition to health and environmental problematics, the petroleum industry adds another issue concerning Hg. Specifically, the large drop in temperature during liquefied natural gas (LNG) production tends to lower the gaseous Hg saturation value, potentially leading to the formation of liquid metallic Hg.[4] The action of metallic mercury as a corrosion catalyst for aluminum heat exchangers is well-illustrated by two accidents that occurred in 1973 and 2004 in Skikda (Algeria). The corrosion of aluminum heat exchangers as a result of liquid Hg formation led to a dramatic failure, causing numerous deaths. Hg-induced corrosion can occur via two pathways: amalgam corrosion and liquid-metal embrittlement.[5,6] Both pathways require a breach in the surface aluminum oxide layer to allow for direct contact between metallic aluminum and liquid Hg.

The implementation of Hg removal units upstream of sensitive operations avoids such failure. These Hg removal units are, however, efficient up to a maximum amount of Hg treated, after which they have to be either regenerated or replaced. The knowledge of the Hg concentration in the natural gas treated is therefore a prerequisite for establishing appropriate operation procedures. Different methodologies exist for the quantification of the Hg concentration in natural gas. The sampling step can be performed by preconcentrating Hg on solid sorbents or gold traps (amalgamation)[7] or bubbling in oxidizing solutions.[8] All of these

sampling techniques have disadvantages related to sampling conditions (flow rate and pressure)[8,9] that can lead to long sampling periods depending upon the Hg concentration.

As an alternative, natural gas sampling at a high pressure can be performed using cylinders. This efficiently reduces the sampling time, and large amounts of gas can be stored. Although a subsequent amalgamation step is required prior to Hg quantification, this step is more conveniently performed off-site in a laboratory. Hg adsorption issues on metallic surfaces are, however, well-known, including potential amalgamation with other metals,[10] precipitation of Hg sulfides,[11,12] or simply physical adsorption. The efficiency of cylinders as natural gas samplers prior to Hg quantification is therefore doubtful, with the possibility of adsorption issues. Cylinders internally coated with inert materials [silicon and polytetrafluoroethylene (PTFE)] were developed to overcome adsorption issues for sulfur and Hg. Stability tests from the manufacturer[13] as well as another independent test[11] showed the efficiency of a silicon coating in preventing Hg losses from the gas phase.

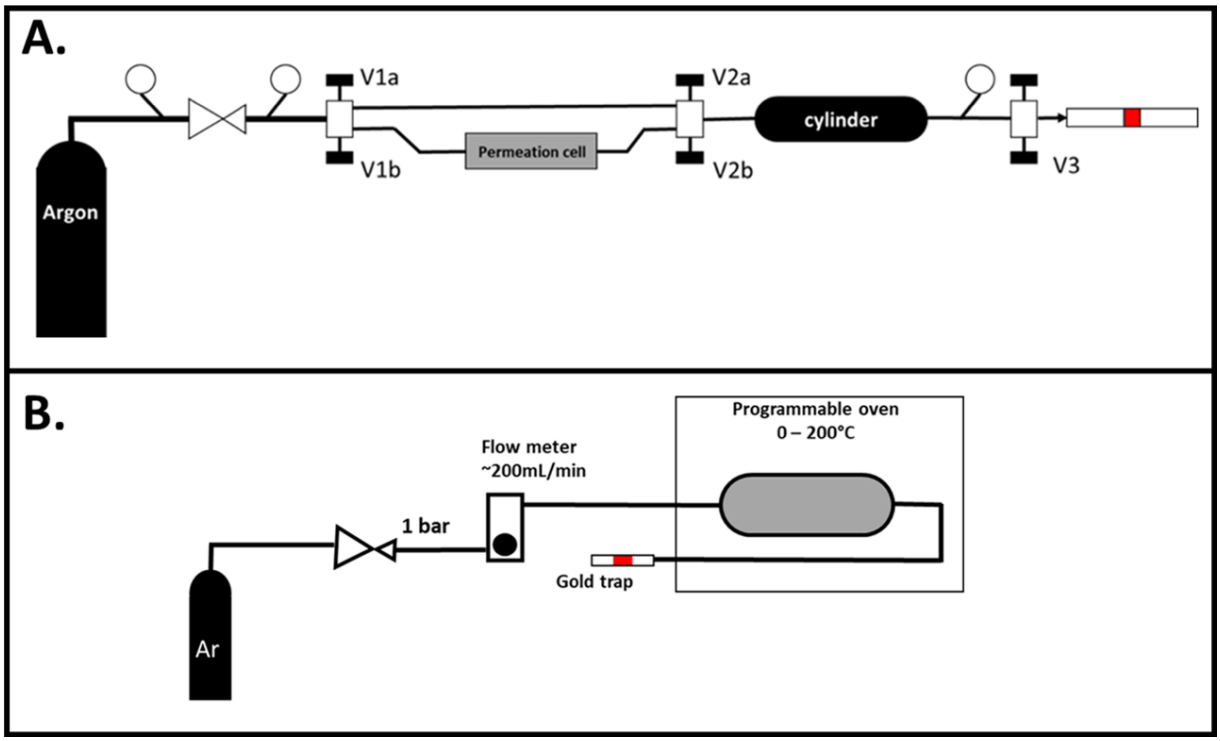

Figure 5. Schemes of the systems used for (A) loading of Hg-contaminated gas in the cylinders and (B) thermal desorption experiments.

To understand some positive and negative results that were highlighted in the laboratory during recent Hg sampling and measurement campaigns, we decided to perform our own experiments on different cylinders to confirm their efficiency prior to their use on the field. Moreover, none of the latter two studies investigated the efficiency of a silicon-coated cylinder that was previously used on the field (and might already contain adsorbed compounds or have been modified by the sampling or the transportation). The influence of a hydrocarbon gas with a complex matrix therefore remains poorly understood. Our tests thus focus on the comparison of new and used silicon-coated cylinders. We also included a PTFE-coated cylinder, an uncoated cylinder, and a Tedlar bag to obtain a full overview.

2. Experimental Section

2.1. Samplers

We purchased a new silicon-coated cylinder from Restek (Lisses, France). This cylinder had therefore never interacted with any hydrocarbon gas, and we could evaluate the initial inertness of the coating material.

Two other silicon-coated cylinders (hereafter referred to as silicon old A and B) purchased from Restek (Lisses, France) were used for our tests. These cylinders were both used approximately 10 times for sampling processed commercial natural gas. The major sulfur compound that was present in the sampled gas is tetrahydrothiophene (THT), an additive for detecting natural gas leaks (odorant).

We obtained one PTFE-coated and one uncoated cylinder from the Total Exploration Production Research Center (CSTJF, Pau, France). Both were used for natural gas sampling at production sites in the past, but the precise sampling history is unknown. However, the presence of gas components, such as H_2S or thiophenic compounds, is highly probable.

Another sampling option is the use of Tedlar bags (Lisses, France). These bags made of a fluoropolymer are supposed to be inert, and this material is commonly used in Hg research. Our tests therefore include experiments with a new Tedlar bag for comparison to cylinders.

2.2. Generation of Hg-Contaminated Gas

For loading, a cylinder was first connected to the previously developed system presented in Figure 5A.[8] Argon (5.0 from Linde) was delivered to the system at 70 bar, passing first through a permeation cell containing liquid Hg and then through the cylinder. Argon is contaminated in Hg when passing through the permeation cell. The Hg concentration depends upon the argon flow rate and system pressure. To generate reproducible Hg concentrations in cylinders, we adopted a procedure that used a 30 min flushing period with Hg-contaminated argon at 500 mL.min^{-1} prior to cylinder closure. All experiments, except when stated otherwise, were conducted using this procedure at a pressure of 70 bar.

A similar method was used for loading the Tedlar bag, except that the flow meter was installed upstream of the bag (no outlet on Tedlar bags). The Tedlar bag was connected after the 30 min flushing procedure and filled with 15 L of argon. The system with the permeation cell was further kept at 70 bar to ensure comparability of the cylinder results.

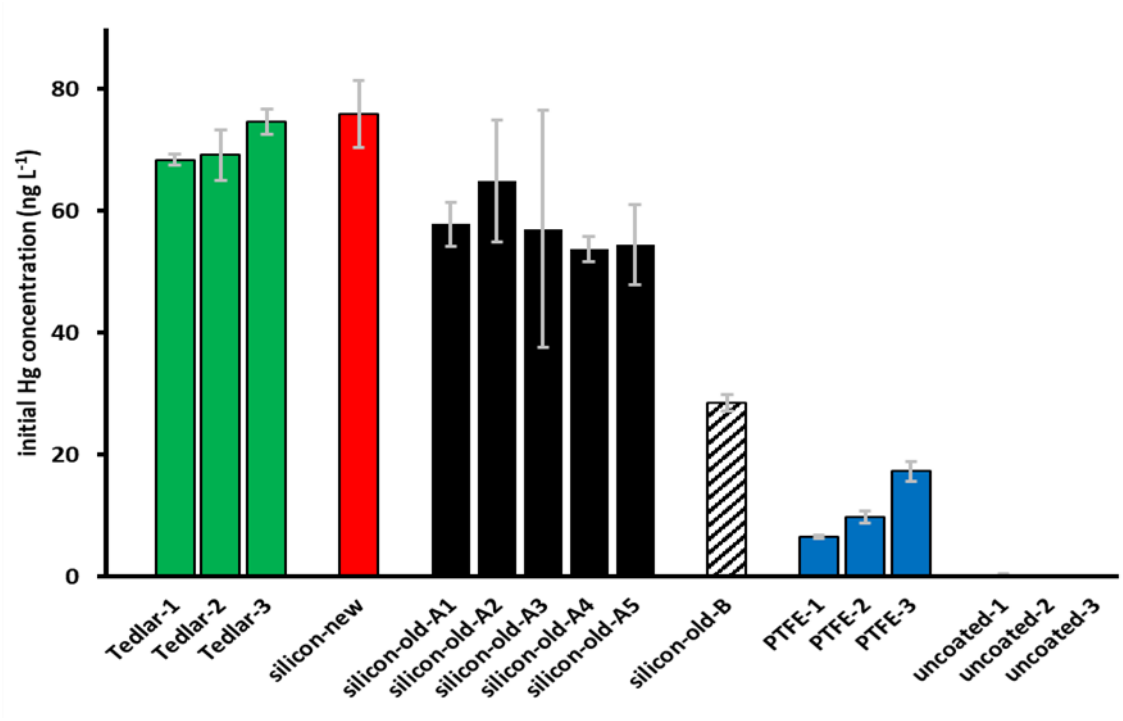

Figure 6. Initial Hg concentration measured after sampler loading with Hg-contaminated argon. Are shown only the initial Hg concentration for experiments including a 30 min preliminary flushing step during the loading experiment. The results for 6 different samplers are shown, as well as for the different tests conducted on each sampler.

For blank evaluation, argon was delivered directly to a gold trap using a bypass (Figure 5A). The system blank was relatively high (1 $ng.L^{-1}$), representing the repeated uses of this system for experimental work on Hg over the past decade.

2.3. Subsampling for the Hg Concentration Measurement

The gaseous Hg concentration was determined at several time steps for each test, including the evaluation of the initial Hg concentration. One valve of the cylinder was opened, and the stream out was adjusted to 150−200 $mL.min^{-1}$. A gold trap was then connected to sample the desired gas volume. The gas flow rate and sampled volume were controlled and measured by a gas counter (Mass-View MV-102, Bronkhorst).

Because the reliability of a single measurement is doubtful, every sampling used four distinct gold traps. The four subsampling replicates were performed successively by replacing gold traps. A volumetric gradient approach was adopted for reliable Hg quantification (see Figure 10 of the Supporting Information). The slope between the volume sampled and the amount of Hg recovered was used as the Hg concentration.

2.4. Thermal Desorption Experiments

Following the gaseous Hg stability experiments, thermal desorption was attempted on several cylinders. The cylinder was placed in a programmable oven under an argon flow of approximately 200 $L.min^{-1}$. Desorbed Hg was sampled using a gold trap installed downstream of the cylinder, outside the oven (Figure 5B).

The initial experimental temperature was 70°C. In addition to the control panel, the temperature was monitored using two independent sensors. The gold trap was left for 10 min (approximately 2 L of gas sampled) before being replaced. This was repeated 3 times to provide three different estimates for desorption rates at each temperature. The oven temperature was then increased by 10°C, and the procedure was repeated until 190°C. Because we used PTFE tape on screws to prevent gas leaks, we did not perform experiments at higher temperatures (PTFE melts at 205°C).

2.5. Hg Analysis

We used an automated double amalgamation system with atomic fluorescence spectrometry (Sir Galahad, PS Analytical, U.K.) for Hg analysis. Briefly, Hg from the gold traps was thermally desorbed by heating at 500°C for 50 s and carried to an analytical gold trap by an argon flow. The analytical gold trap is then heated at 500°C for 15 s, and an argon flow carries the released gaseous Hg to the atomic fluorescence detector. The instrumental detection limit is 10 pg. Considering that our system blank was 1 ng.L^{-1}, we had no issues related to the instrumental detection limit.

3. Results and Discussions

3.1. Initial Gaseous Hg Concentration and Temporal Stability

The loading procedure led to different initial Hg concentrations depending upon the cylinder that we tested. Three successive tests with the Tedlar bag gave consistent values of approximately 71 ± 3 ng.L^{-1} (n = 3; Figure 6), which compares well to a test performed on the new silicon-coated cylinder (76 ± 6 ng.L^{-1}). Two other tests were conducted on the silicon-coated cylinder, but we adopted a different peanut butter-based loading strategy. For these two tests (2 and 3), the 30 min flushing step was avoided, which led to initial gaseous Hg concentrations of 29 ± 1 and 33 ± 1 ng.L^{-1}, respectively. This lower concentration is related to the variable flow rates through the permeation cell during the loading, leading to different gas/liquid fractionation values.

The old silicon-coated cylinder A was successively tested 5 times with comparable initial Hg concentrations (average value of 58 ± 4 ng.L^{-1}; n = 5). This is slightly lower than the new silicon-coated cylinder and Tedlar bag. We acknowledge that small differences in the loading procedure (exact flushing flow rate in particular) might be responsible for small differences in the initial gaseous Hg concentration. The old silicon-coated cylinder B, however, gave a low initial Hg concentration of 29 ± 1 ng.L^{-1}. This low Hg concentration relative to the new silicon-coated cylinder is unlikely to be derived from the procedure itself and likely reveals adsorption already occurred during our loading procedure.

The three experiments conducted on the PTFE-coated cylinder gave three different initial Hg concentrations, with an increasing trend from 6.5 ± 0.3 to 17.3 ± 1.6 ng.L^{-1}. In comparison to the results obtained for the silicon-coated cylinders, these values are rather low and likely indicate that adsorption occurred. The results for the uncoated cylinder were even worse, with initial Hg concentrations evaluated to be an order of magnitude below the system blank (approximately 0.07 ng.L^{-1}, average of three tests). This clearly shows that uncoated cylinders efficiently adsorb Hg. In fact, even a test performed during the flushing procedure by sampling at the outlet of the uncoated cylinder reflected a negligible gaseous Hg concentration. Further stability tests were not conducted on uncoated cylinders, because all Hg seemed to be initially rapidly adsorbed. All other cylinders were tested for Hg concentration stability over time.

The newly purchased silicon-coated cylinder efficiently maintained a constant Hg concentration during short-term experiments (a few hours; see Figure 11 of the Supporting Information). A longer-term experiment showed that the gaseous Hg concentration is stable over at least 6 months, supporting previous tests performed by the manufacturer (Figure 7A). The old silicon-coated cylinders, however, behaved differently, with a clear decrease in the gaseous Hg concentration, visible after only a few hours (panels B and C of Figure 7). Despite the lower initial Hg concentration in the old silicon-coated cylinder B (Figure 6), the decline seems to be slower than that for cylinder A (panels B and C of Figure 7). The PTFE-coated cylinder showed a fast decline in the gaseous Hg concentration, reaching undetectable levels after only 3 h. Despite the differences in the initial Hg concentration among the three tests, we observe a surprisingly identical declining trend.

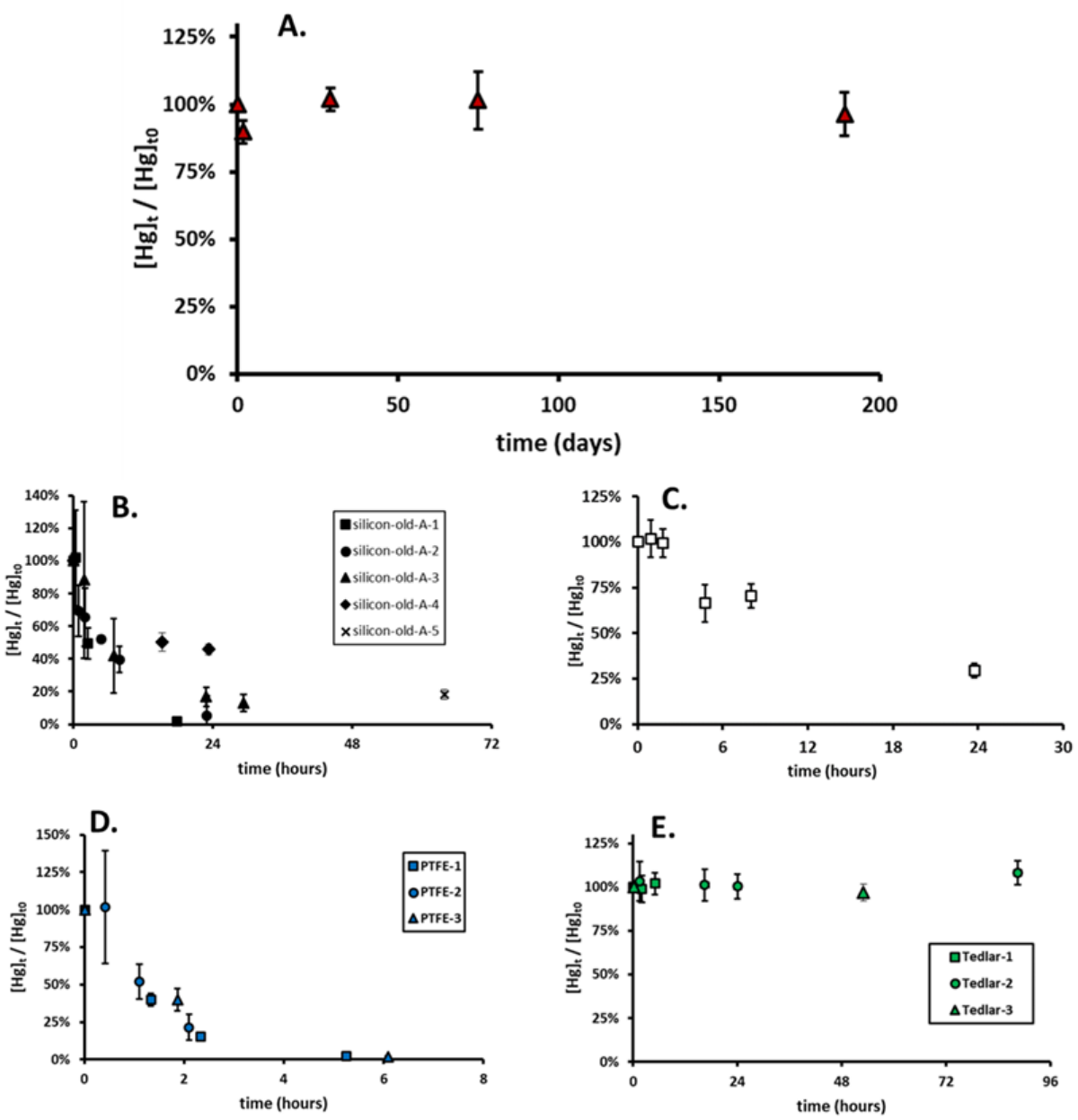

Figure 7. Gaseous Hg concentration variations over time during stability experiments conducted on (A) a new silicon-coated cylinder, (B) the old silicon-coated cylinders A and (C) B, (D) the PTFE-coated cylinder and (E) the Tedlar bag. Note the differences in the x-axis scale, especially for panel A (days unit compared to other panels in hours). Only the long-term test is shown for the new silicon-coated cylinder (panel A), and the results of short-term tests (1 and 2) can be found in supporting information Figure S2.

3.2. Adsorption of Gaseous Hg and Equilibrium

Only the new silicon-coated cylinder and the Tedlar bag were able to maintain a constant gaseous Hg concentration (panels A and E of Figure 7). From all of these observations, we

conclude that gaseous Hg is progressively adsorbed on the internal cylinder walls, at least in the old cylinders (silicon- and PTFE-coated). The five successive tests on the old silicon-coated cylinder A revealed different rates of decrease (Figure 7B), with a faster decline for the first tests (no Hg detected after 20 h) than the last (20% of Hg remaining after 60 h). Following these experiments, an empty cylinder was filled with uncontaminated argon (bypass shown in Figure 1) at 70 bar without flushing the system.

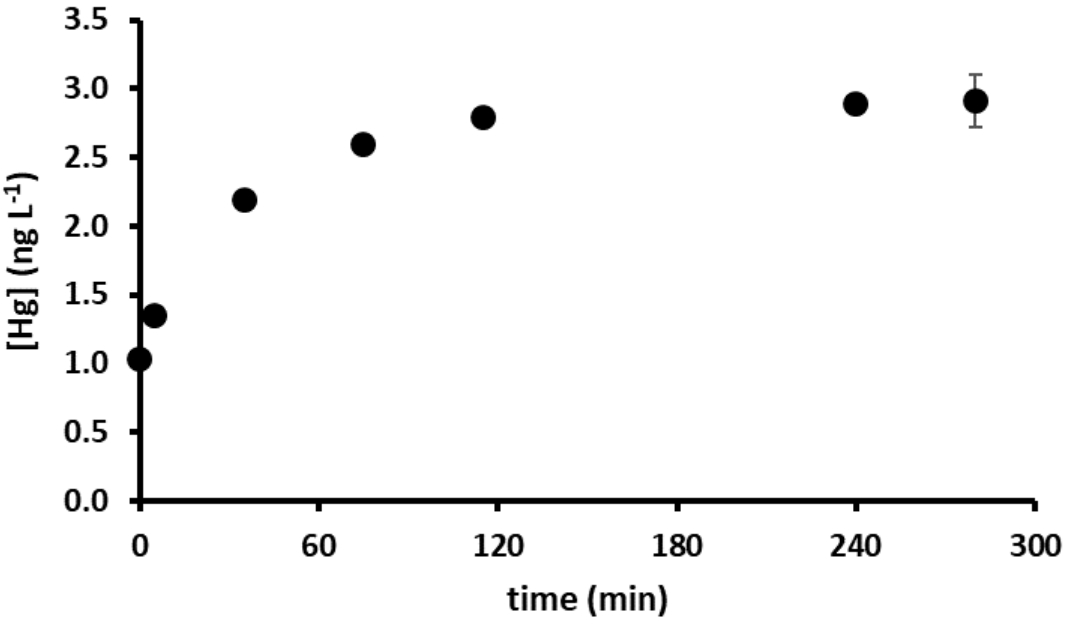

Figure 8. Evolution of gaseous Hg concentration in the old silicon-coated cylinder A after loading with uncontaminated argon. This test was conducted after the five tests with contaminated argon (Figure 7B). The initial gaseous Hg concentration of 1 ng.L^{-1} is consistent with the system blank value.

The gaseous Hg concentration was then monitored for 5 h. It increased from an initial Hg concentration of 1 ng.L^{-1} (similar to the system blank) to stabilize at approximately 2.9 ng.L^{-1} (Figure 8). This demonstrates that Hg adsorption is ruled at least partly by an equilibrium relationship with gaseous Hg.

All of our stability tests consisted of measurements performed on very small gas samples compared to the amount of gas stored in the cylinder, which is not informative regarding the behavior of Hg during cylinder purge. The old silicon-coated cylinder B was left filled with Hg-contaminated gas for 15 more days. The gas was then entirely flushed through gold traps at 150−200 mL.min^{-1}. Each gold trap was sampled and contained 1−3 L of gas. We determined

that the gaseous Hg concentration at the beginning of the procedure was approximately 0.5 $ng.L^{-1}$. It progressively decreased with pressure during the cylinder purge (Figure 9A). This finding shows that pressure influences the equilibrium relationship between adsorbed Hg and gaseous Hg.

3.3. Thermal Desorption Results

We tested the possibility of recovering adsorbed Hg by heating the cylinder. The cylinder was flushed with argon and heated from 70 to 190°C. A gold trap recovered desorbed Hg for 10 min before being replaced. We found that desorption rates generally increased with the temperature (Figure 9B). However, we also noted a double-peak shape, indicating two optimal desorption temperatures. The desorption rates first increased when the temperature was increased from 70 to 130°C. Desorption rates then stabilized or decreased, followed by a further increase.

The double-peak shape that we obtained during the thermal desorption experiment is likely indicative of the occurrence of two distinct forms of adsorbed Hg species, because the volatilization temperature indicates Hg species.[14,17,18] Adsorbed Hg^0 is classically released at low temperatures as a result of its volatility (from 70°C, peak around 80−150°C depending upon the procedure).[17] This is consistent with the first peak that we observe, with desorption starting around 80°C and increasing until 130°C. Other Hg forms, consisting of oxidized Hg (either as particulate, Hg salts, or Hg complexes), are released at higher temperatures that vary depending upon the species.

This is well-illustrated by a study showing that the gas chromatography (GC) injector temperature is critical for the evaluation of Hg^0 levels in liquid hydrocarbon samples. Thermal decomposition of Hg particles into Hg^0 might lead to overestimation of the Hg^0 concentration.[19] Our procedure does not allow for the identification of this species, but the double peak shape unambiguously suggests the presence of both physically adsorbed Hg^0 and an oxidized Hg form into the cylinder. The decomposition of Hg compounds to gaseous Hg^0 is also the principle of a Hg quantification method in liquid hydrocarbon samples consisting of heating at 200°C and measuring headspace gaseous Hg, in equilibrium with dissolved Hg^0.[20] Similarly, a Hg removal technique suggests heating liquid hydrocarbons at temperatures higher than 175°C to transform all Hg species to Hg^0, easier to remove from hydrocarbon streams.[3]

During our experiments, only Hg^0 and argon were delivered to the cylinder. Therefore, Hg oxidation obviously occurred in the cylinder. Sulfur species, especially H_2S, are known to indirectly cause depletion in gaseous Hg[12,15] by first reacting with metallic oxide surfaces. The sampling history of this cylinder (old silicon-coated cylinder B) indicated that its use was limited to the sampling of a natural gas containing very low amounts of Hg (on the $ng.Nm^{-3}$ level, measured independently by the amalgamation method). Sulfur species should have been present at very low levels as well, with the notable exception of THT, which is injected upstream for leak detection. As H_2S, THT contains reduced sulfur that might interact with Hg. The most likely explanation for our observations involves the adsorption of THT or other reduced sulfur compounds on internal cylinder walls, providing binding sites for Hg^0.

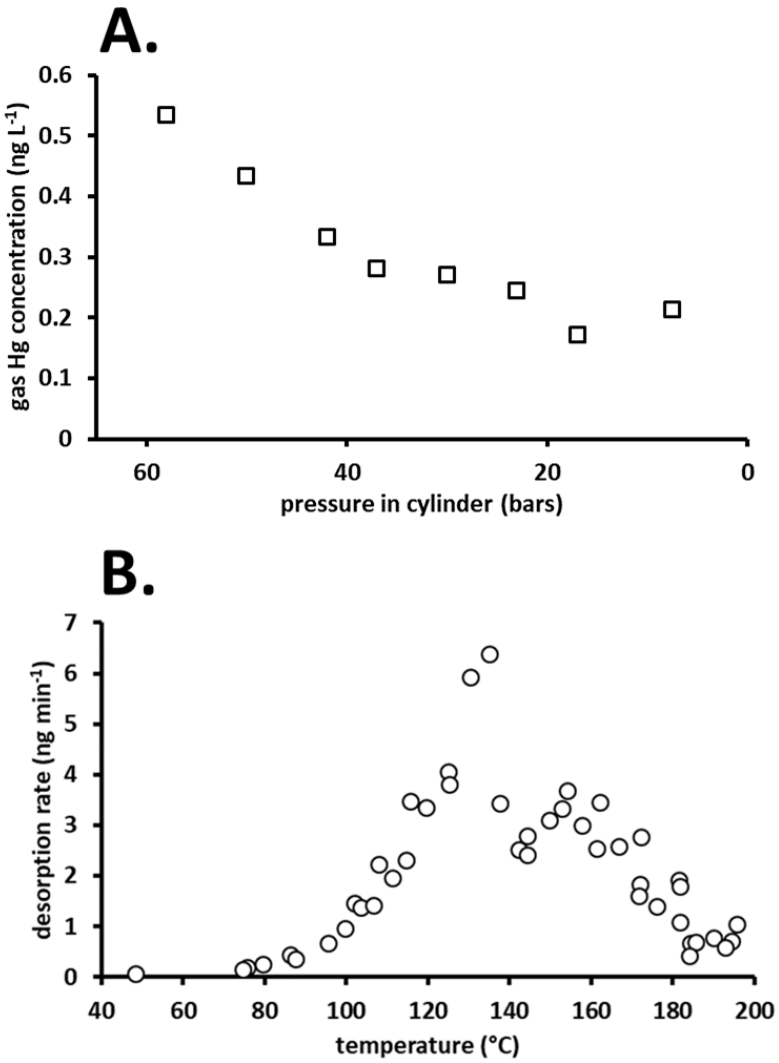

Figure 9. Hg recovery during (A) emptying and (B) heating the old silicon-coated cylinder B. Panel A shows the variations in gaseous Hg concentration during the emptying of the silicon-coated cylinder B, shown as a gaseous Hg concentration as a function of the pressure left in the cylinder. Panel B illustrates the temperature dependence of Hg desorption rates.

The oxidation of Hg from physically adsorbed Hg^0, followed by complexation with reduced sulfur, was already observed in solution.[16] We propose that a similar sorption and oxidation pathway also affects gaseous Hg.

We note that silicon coating is also expected to be inert to sulfur compounds. This is probably true to some extent, but the inertness is not perfect, as shown by tests from the manufacturer itself (from Restek Technical Resources). The main problem here is that typical sulfur and Hg concentrations differ by several orders of magnitude. In other words, although less than 1% sulfur adsorption is not problematic for sulfur measurement and speciation, it can affect Hg adsorption and lead to the complete depletion of Hg from the gas phase. The thermal desorption procedure was also applied to the uncoated cylinder and the PTFE-coated cylinder (see Figure 12 of the Supporting Information). In contrast to the silicon-coated cylinder B, however, the procedure was applied several months after the cylinder purge. Both revealed a very high content of adsorbed Hg, although exact quantification was not attempted. The results for the PTFE-coated cylinder also suggest two Hg species, although oxidized Hg seems to be very high compared to physically adsorbed Hg. This might derive from faster oxidation, which is supported by the fast depletion of the gaseous Hg concentration during our experiments (all Hg lost within 3 h). It could also be related to the lag between the gaseous Hg stability and thermal desorption experiments (2 months).

3.4. Mass Balance and Reaction Rates

The initial gaseous Hg concentration in the old silicon-coated cylinder B suggested that 600 ng of gaseous Hg was present inside the cylinder at the initial stage of the experiment. As already mentioned, this is quite different from the new silicon-coated cylinder, for which the same loading procedure led to an initial gaseous Hg amount of about 1500 ng. We already discussed this difference and attributed it to fast adsorption occurring during the loading procedure. The initial gaseous Hg amount in the silicon-coated cylinder B does not account for Hg adsorbed during the loading and, therefore, underestimates the initial Hg budget.

During the purge of silicon-coated cylinder B, we recovered a total of 5 ng of Hg (Figure 9A), which is somewhat negligible compared to the initial Hg budget. The thermal desorption procedure allowed us to recover 1100 ng of Hg (Figure 9B), almost twice the initial Hg budget. The 500 ng excess is unlikely to originate from the natural gas previously sampled using this

cylinder, because the Hg concentration was 4 orders of magnitude lower than that of the contaminated gas that we generated. It more likely derives from Hg that was adsorbed during the loading of the cylinder, prior to the evaluation of the initial gaseous Hg concentration. The total amount of Hg that we retrieve during the purge and thermal desorption is comparable to the 1500 ng that is present in the new silicon-coated cylinder when using the same loading procedure. The slight difference might be caused by minor differences during the loading procedure or the formation of another Hg species that is released at a higher temperature. Considering that we have two Hg species in the cylinder, fast adsorption might be related to the physical adsorption of Hg^0. Adsorption rates during the initial stage of the experiments (including during the loading procedure) are therefore controlled by sorption sites for Hg^0. The reaction scheme with subsequent oxidation, together with the slower adsorption rates observed during our experiments (Figure 7C), suggests that the oxidation step is the limiting factor when equilibrium is reached between physically adsorbed and gaseous Hg^0.

The reaction scheme that we inferred excludes the direct oxidation of gaseous Hg^0, because we speculated that Hg0 first requires physical adsorption. The observation of Larsson et al.[12] is, however, in good agreement with this hypothesis, because no Hg loss was observed at 75 and 100°C from a gas containing Hg^0 and H_2S. At such low temperatures, only the physical adsorption of Hg^0 should be inhibited; thus, direct oxidation of gaseous Hg^0 would induce losses of Hg even at 75−100°C. Additional indirect evidence is derived from a previous test of a silicon-coated cylinder. The authors showed no evolution of the gaseous Hg concentration in their cylinder upon heating at 100°C throughout the experiment,[11] although this study did not show any results for a similar cylinder kept at ambient temperature.

4. Conclusion and Recommendations

We provided experimental evidence showing the inefficiency of silicon coatings for natural gas sampling prior to Hg analysis (as well as PTFE coatings). The inertness of the coating regarding Hg adsorption is initially efficient but does not last in time. We suggest that the adsorption of sulfur species on the coated surfaces provides sorption sites for Hg and can ultimately lead to the transformation of Hg^0 into less volatile oxidized forms. Tedlar bags might be inert to Hg. However, our tests used only a new Tedlar bag, so that the fluoropolymer surfaces never experienced any contact with sulfur species. Further experiments are required

for evaluating Tedlar bags as a sampling alternative prior to Hg analysis in natural gas, but the fragility and size of this sampler system are also negative points that might be considered when the sample has to travel.

We acknowledge that appropriate sampling procedures using cylinders might be imagined (sampling at 100°C to avoid adsorption), but adsorption needs to be considered even in the case of silicon-coated cylinders. The repeated use of cylinders for sampling different natural gas samples might lead to both adsorption and desorption, because the partition is ruled by an equilibrium relation and depends upon the total Hg budget and pressure. Alternative standard methodologies involving Hg preconcentration by amalgamation or oxidation in acidic solutions ($KMnO_4/H_2SO_4$)[8] might be preferable, despite flow rate limitations.[9]

5. Complete information

5.1. Determination of Hg concentration

Every gaseous Hg concentration determination relied on 4 analyses during the stability tests, by adopting a volumetric gradient approach. Depending on the Hg concentration expected, sampled volumes were adapted in order to preconcentrated sufficient Hg to insure a precise analysis.

Figure 10 illustrates the volumetric gradient approach. The slope between sampled volumes and Hg sampled gives a good estimate of Hg concentration. On Figure 10 a negative intercept is observed. This is caused by a lag time between system connection and count volume count start.

The uncertainty on the determined concentration is given by the standard error on the slope. Uncertainties on yields over time (Figure 7 in the main text, Figure 11) is estimated by error propagation.

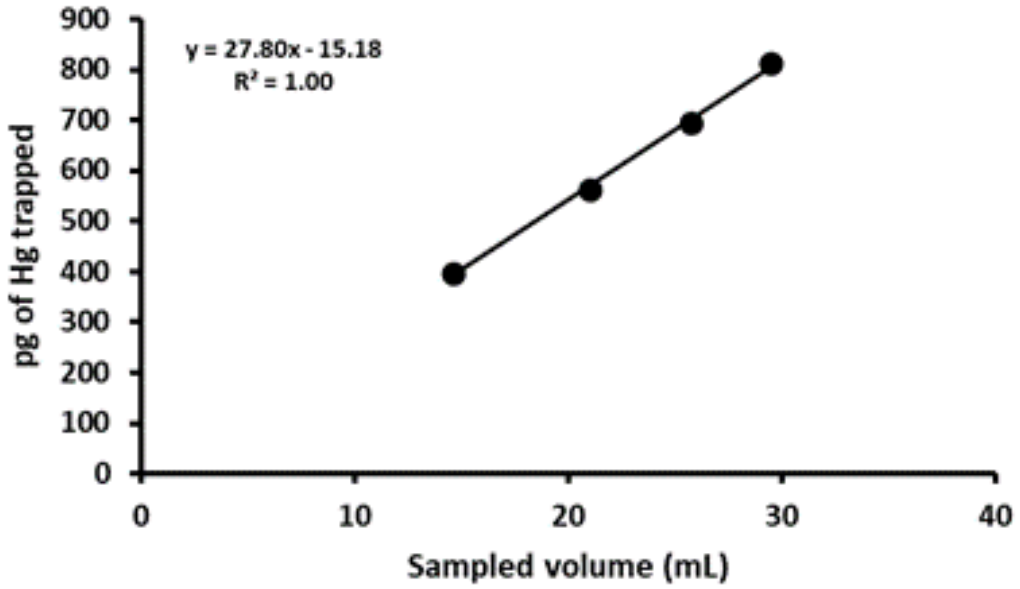

Figure 10. Example of a Hg concentration result given by the volumetric gradient approach

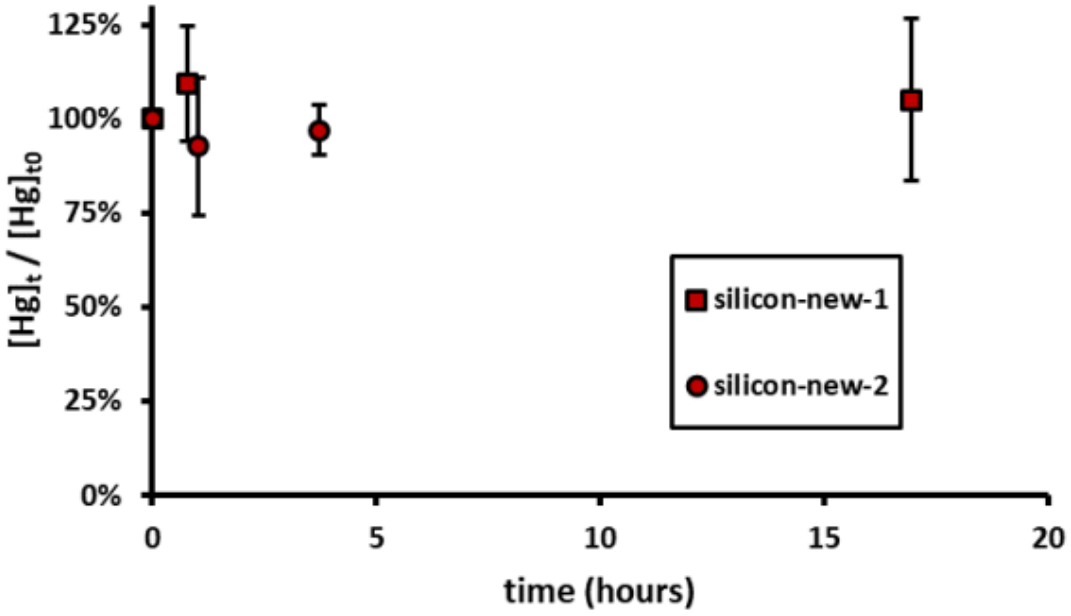

Figure 11. Stability of gaseous Hg concentration during tests performed on the new silicon-coated cylinder

5.2. Thermal desorption of PTFE-coated and uncoated cylinders

Thermal desorption was performed on the PTFE-coated cylinder and the uncoated cylinder up to 180°C (Figure 12 A and B). Results for the PTFE-coated cylinder suggest a

pattern similar to the one observed for the old silicon-coated cylinder, with an increase in desorption rate starting before 100°C and a second increase at higher temperatures. In contrast to the silicon-coated cylinder B, here the second increase is very high compared to the first peak. The total amount of Hg desorbed during the experiment was 7.7 µg. However, Hg desorption still occurred and we maintained a high temperature (190°C) during a few hours before we re-evaluate Hg desorption. We found a low desorption rate, suggesting the cylinder can be cleaned.

The uncoated cylinder however only revealed one peak, with a consistent increase in Hg desorption rate with temperature, possibly because physically-adsorbed Hg0 is absent or insignificant compared to oxidized Hg. At least 4.1 µg of Hg could be desorbed from the uncoated cylinder, and some is still adsorbed inside.

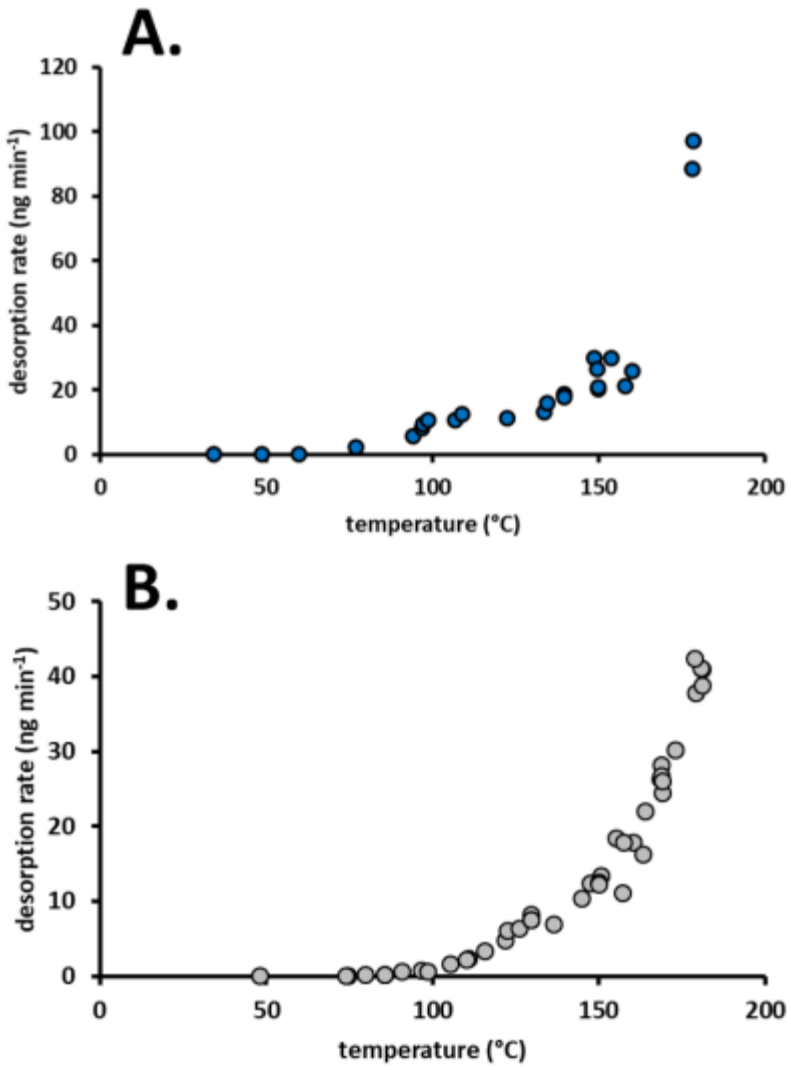

Figure 12. Thermal desorption results for (A) the PTFE-coated cylinder and (B) the uncoated cylinder

Acknowledgements

This work was supported by the Conseil Regional d´ 'Aquitaine (20071303002PFM) and the European Regional Development Fund (FEDER, 31486/08011464). Total is thanked for both funding this research study and providing cylinders.

References

(1) Wilhelm, S. M.; Bloom, N. Mercury in petroleum. *Fuel Process. Technol.* **2000**, *63* (1), 1−27.

(2) Lambertsson, L.; Lord, C. J.; Frech, W.; Bjorn, E. Rapid dissolution of cinnabar in crude oils at reservoir temperatures facilitated by reduced sulfur ligands. *ACS Earth Space Chem.* **2018**, *2* (10), 1022−1028.

(3) Lord, C. J.; Lambertsson, L. T.; Björn, E. L.; Frech, W.; Thomas, S. A. Removing Mercury from Crude Oil. WO Patent 2014143457 A1, Sept 18, **2014**.

(4) Huber, M. L.; Laesecke, A.; Friend, D. G. Correlation for the vapor pressure of mercury. *Ind. Eng. Chem. Res.* **2006**, *45* (21), 7351− 7361.

(5) Bingham, M. D. Field detection and implications of mercury in natural gas. *SPE Prod. Eng.* **1990**, *5* (02), 120−124.

(6) Wilhelm, S. M. Risk analysis for operation of aluminum heat exchangers contaminated by mercury. *Process Saf. Prog.* **2009**, *28* (3), 259−266.

(7) International Organization for Standardization (ISO). *ISO 6978- 1:2003, Natural Gas Determination of Mercury Part 1: Sampling of Mercury by Chemisorption on Iodine;* ISO: Geneva, Switzerland, **2003**; http://www.iso.org/cms/render/live/en/sites/isoorg/contents/data/standard/03/86/38600.html.

(8) Cachia, M.; Bouyssiere, B.; Carrier, H.; Garraud, H.; Caumette,` G.; Le Hecho, I. Development of a high-pressure bubbling sampler for trace element quantification in natural gas. *Energy Fuels* **2017**, *31* (4), 4294−4300.

(9) Frech, W.; Baxter, D. C.; Dyvik, G.; Dybdahl, B. On the determination of total mercury in natural gases using the amalgamation technique and cold vapour atomic absorption spectrometry. *J. Anal. At. Spectrom.* **1995**, *10* (10), 769−775.

(10) Leeper, J. Mercury−LNG's problem. *Hydrocarbon Process.* **1980**, *59* (11), 237−240.

(11) Harfoushian, J. H. Quantification of low levels of mercury in gas reservoirs using advanced sampling and analysis techniques. *Proceedings of the SPE Annual Technical Conference and Exhibition;* New Orleans, LA, Sept 30−Oct 2, **2013**; DOI: 10.2118/166220-MS.

(12) Larsson, T.; Frech, W.; Björn, E.; Dybdahl, B. Studies of transport and collection characteristics of gaseous mercury in natural gases using amalgamation and isotope dilution analysis. *Analyst* **2007**, *132* (6), 579−586.

(13) SilcoTek Corporation. Prevent Mercury *Loss during Transport and Storage with SilcoNert 2000;* SilcoTek Corporation: Bellefonte, PA, 2019; https://www.silcotek.com/prevent-mercury-loss.

(14) Rumayor, M.; Diaz-Somoano, M.; Lopez-Anton, M. A.; Martinez-Tarazona, M. R. Mercury compounds characterization by thermal desorption. *Talanta* **2013**, *114*, 318−322.

(15) Edmonds, B.; Moorwood, R.; Szczepanski, R. Mercury partitioning in natural gases and condensates. *Proceedings of the GPA European Chapter Meeting*, London, U.K., March 21, **1996**.

(16) Zheng, W.; Lin, H.; Mann, B. F.; Liang, L.; Gu, B. Oxidation of dissolved elemental mercury by thiol compounds under anoxic conditions. *Environ. Sci. Technol.* **2013**, *47* (22), 12827−12834.

(17) Coufalik, P.; Komarek, J. The use of thermal desorption in´ speciation analysis of mercury in soil, sediments and tailings. *J. Anal. Chem.* **2014**, *69*, 1123−1129.

(18) Biester, H.; Scholz, C. Determination of Mercury Binging Forms in Contaminated Soils: Mercury Pyrolysis versus Sequential Extractions. *Environ. Sci. Technol.* **1997**, *31* (1), 233−239.

(19) Gajdosechova, Z.; Boskamp, M. S.; Lopez-Linares, F.; Feldmann, J.; Krupp, E. M. Hg Speciation in Petroleum Hydrocarbons with Emphasis on the Reactivity of Hg Particles. *Energy Fuels* **2016**, *30* (1), 130−137.

(20) Lambertsson, L.; Lord, C. J.; Frech, W.; Björn, E. Rapid Dissolution of Cinnabar in Crude Oils at Reservoir Temperatures Facilitated by Reduced Sulfur Ligands. *ACS Earth Space Chem.* **2018**, *2* (10), 1022−1028

Partie 2 : Essai expérimental d'échantillonnage de gaz naturel contaminé en Hg^0 dans un sac Tedlar

Afin de déterminer si le phénomène d'adsorption du mercure est observé dans les échantillonneurs notamment les sacs Tedlar en contact avec des espèces soufrées et de l'oxygène, un échantillon de gaz pétrolier soufré réel a été introduit dans un sac Tedlar rempli, au préalable, avec de l'air ambiant. Le remplissage du sac Tedlar avec l'air ambiant et le gaz soufré a été effectué au sein du pôle PVT au CSTJF de TotalEnergies. Le gaz contenu dans le sac Tedlar a ensuite été enrichi en Hg^0 gazeux à l'IPREM et sa concentration a été analysée au cours du temps pendant une période d'environ 2 mois et demi.

1. Matériels et Méthodes

1.1. Préparation et échantillonnage.

Un sac Tedlar d'un volume de 3 L contenant un peu moins d'1L d'air a été complétement rempli avec un gaz pétrolier contenant 120 ppm d'H_2S. Ce « prétraitement » par l'air et l'H_2S a eu pour but de simuler le « vieillissement » des sacs Tedlar par des prélèvements de gaz contenant des composés soufrés. Le Hg^0 gazeux saturé a été prélevé dans l'espace de tête d'un récipient contenant du Hg^0 liquide, puis, a été introduit directement à l'aide d'une seringue étanche au gaz dans ce sac Tedlar rempli. La concentration en Hg^0 gazeux obtenu était de 5 $ng.L^{-1}$. Le suivi de la concentration du mercure en fonction du temps a été réalisé en échantillonnant directement 100 mL de gaz dans le sac Tedlar à l'aide d'une seringue étanche au gaz. Le Hg^0 gazeux a été analysé toutes les heures pendant les premières 12h, ensuite, chaque jour (hors week-end) pendant 1 semaine et 1 fois par semaine pendant 2 mois. Afin d'assurer la fiabilité de la mesure, l'échantillonnage ainsi que l'analyse ont été réalisée successivement trois fois pour chaque temps.

1.2. Analyse du Hg^0

Le Hg^0 gazeux a été analysé par spectrométrie de fluorescence atomique (Sir Galahad, PS Analytical, U.K.). Le gaz pétrolier, échantillonné dans la seringue, a été directement injecté dans un piège en or analytique à l'intérieur de l'appareil et le Hg a été piégé sur celui-ci. Le piège en or analytique a ensuite été chauffé à 500 °C pendant 15 s et un flux d'argon a transporté le Hg gazeux libéré, vers le détecteur de fluorescence atomique. La concentration en Hg^0 a été estimée en fonction de la pente obtenue par gradient volumétrique (cf 5.Complete information, p 91). La limite de détection instrumentale obtenue était de 10 pg.

2. Résultats et discussions

La concentration en Hg^0 gazeux contenue dans le sac Tedlar est restée constante pendant toute la durée du test, soit environ 2 mois et demi (Figure 13).

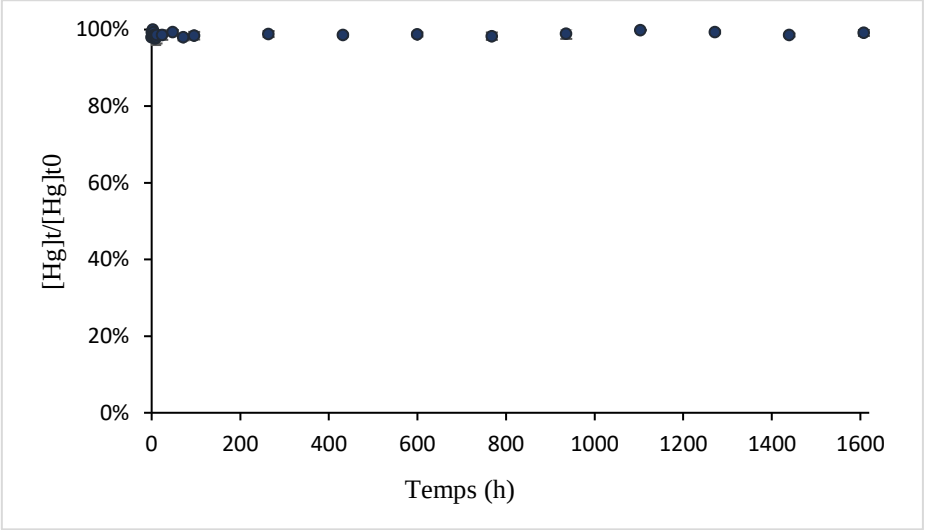

Figure 13. Variation de la concentration d'Hg0 gazeux au cours du temps pendant l'expérience de stabilité menée sur le sac Tedlar

Ce résultat montre que lorsque les surfaces en fluoropolymère du sac Tedlar sont en contact avec des espèces soufrées et de l'oxygène, on n'observe pas de perte significative d'Hg. Les sacs Tedlar ont donc une bonne fiabilité pour échantillonner le mercure, du moins quand la teneur de ce dernier est de l'ordre de quelques microgrammes par mètre cube.

3. Conclusion

La fiabilité des sacs Tedlar ne semble pas être altérée par leur contact avec les composés soufrés durant les campagnes d'échantillonnage précédentes : ce qui permet de valider leur utilisation. Toutefois, ce type d'échantillonneurs ne sont pas conçus pour échantillonner des gaz sous pression et une dépressurisation ainsi qu'une dérivation du flux principal du gaz naturel doivent être mise en place afin d'échantillonner celui-ci dans les sacs Tedlar. Ces interventions peuvent être la source de contamination et le changement brutal de conditions induira un point froid, ce qui pourrait fausser la concentration en Hg si toutes les précautions ne sont pas prises concernant la sélection, la préparation et la purge du point d'échantillonnage.

Partie 3 : Recommandations sur l'échantillonnage et de l'analyse du mercure dans le gaz naturel au cours d'un essai de puits

Lors d'un essai de puits, la mesure du mercure peut facilement être mal déterminée et conduire à la prise de décisions incorrectes. La principale incertitude ne provient pas de la mesure elle-même ou de l'étalonnage de l'appareil, mais de la méthode de collecte.

L'objectif lors d'un essai de puits est donc d'assurer la traçabilité et la réduction des artefacts qui peuvent survenir lors des opérations d'échantillonnage et d'assurer la représentativité des échantillons pendant un essai de puits.

Afin de répondre à ces objectifs, cette partie 3 qui est tirée d'un « General Specifiation » (Document confidentiel interne au sein de TotalEnergies), rédigée pendant cette période de thèse, documente les événements clés pendant l'opération d'échantillonnage.

L'échantillonnage et l'analyse du mercure dans le gaz naturel au cours d'un essai de puits, permet de prendre la décision concernant la nécessité de la mise en place d'une unité d'élimination du mercure (MRU) au sein des compagnies pétrolières.

1. Normes existantes et leurs insuffisances

Deux méthodes d'échantillonnage sont généralement recommandées par les normes : accumulation de mercure par amalgamation (ISO 6978.2-2003, 2003) et le barbotage de gaz dans une solution acide (ISO 6978.1-2003, 2003, p. 69; Norme NF EN 13211, 2001). La première méthode est recommandée uniquement car elle permet une plus grande sensibilité (ISO 6978.2-2003, 2003) et permet d'éviter ou de limiter la manipulation des produits chimiques sur site.

La spectrométrie en absorption atomique ou en fluorescence atomique est la méthode recommandée. Leur sensibilité est largement suffisante et après la préconcentration via des pièges d'amalgamation, toutes les interférences possibles sont éliminées, car les composants dans le gaz ayant une longueur d'onde de fluorescence proche de celle du mercure sont très largement éliminés et la détection par les spectromètres sont spécifiques aux longueurs d'onde

de mercure, ce qui rend les résultats très fiables (ASTM D5954-98, 2014; ASTM D6350-14, 2014).

Le respect strict de la norme ne permet pas cependant de garantir le succès d'une campagne d'échantillonnage. Les artefacts sont nombreux et dans un grand nombre de cas, les compagnies de services rendent des résultats ne permettant pas de les identifier : cela ne permettant pas de valider ou d'invalider les résultats obtenus.

L'objectif principal de ce travail est donc d'établir une procédure permettant, d'une part, d'éviter les erreurs et artefacts connus durant l'échantillonnage et d'autre part, de rendre traçables les problèmes et les artefacts rencontrés pendant la campagne d'échantillonnage.

2. Problèmes spécifiques sur les sites industriels ainsi que durant les tests de puits

Un analyste se contente parfois de déterminer correctement la teneur en mercure d'un échantillon que l'on lui donne. Quand il s'agit d'une campagne de prélèvements pendant un test de puits, la problématique est très différente. En dehors du fait qu'il faut garantir le dosage de la bonne quantité de mercure dans un échantillon, il est également nécessaire de garantir :

1. qu'il n'y ait ni perte, ni contamination depuis la prise d'échantillon.

2. que la teneur en mercure de l'échantillon est bien représentative de celle dans le fluide circulant dans la ligne pendant le test.

3. que la teneur en mercure du fluide circulant dans la ligne est bien représentative de celle dans le fluide de réservoir.

3. Relation entre la durée du test et le seuil de détection

Il a été souvent constaté que la teneur en mercure dans le fluide, au début d'un test de puits, n'est pas représentative de celle dans le fluide de réservoir. Plusieurs raisons peuvent expliquer ce phénomène :

- La boue utilisée par le forage peut affecter cette mesure soit parce qu'elle peut contenir des composés contenant du mercure, soit parce qu'elle peut contenir des composés pouvant capturer des espèces de mercure. Il est alors indispensable d'évacuer complètement cette boue avant de pouvoir obtenir des mesures non perturbées par celle-ci.

- L'équilibre adsorption/désorption de mercure sur la paroi interne des « pipes » et des équipements de test est fréquemment évoqué pour expliquer la « percée » souvent tardive du mercure.

Le temps de « percée du mercure » a été calculé sur trois tests de puits différents (Figure 14). Pour les trois tests de puits, le moment où on observe la percée du mercure est assez inégale. Dans deux cas (Puits de gaz A et C), la production d'au moins 1-2 millions de mètres cubes de gaz a été nécessaire pour observer une stabilisation de la teneur en mercure alors que pour les puits de gaz B, la production de plus de 5-6 millions de mètres cubes de gaz a été nécessaire avant d'observer une stabilité du Hg.

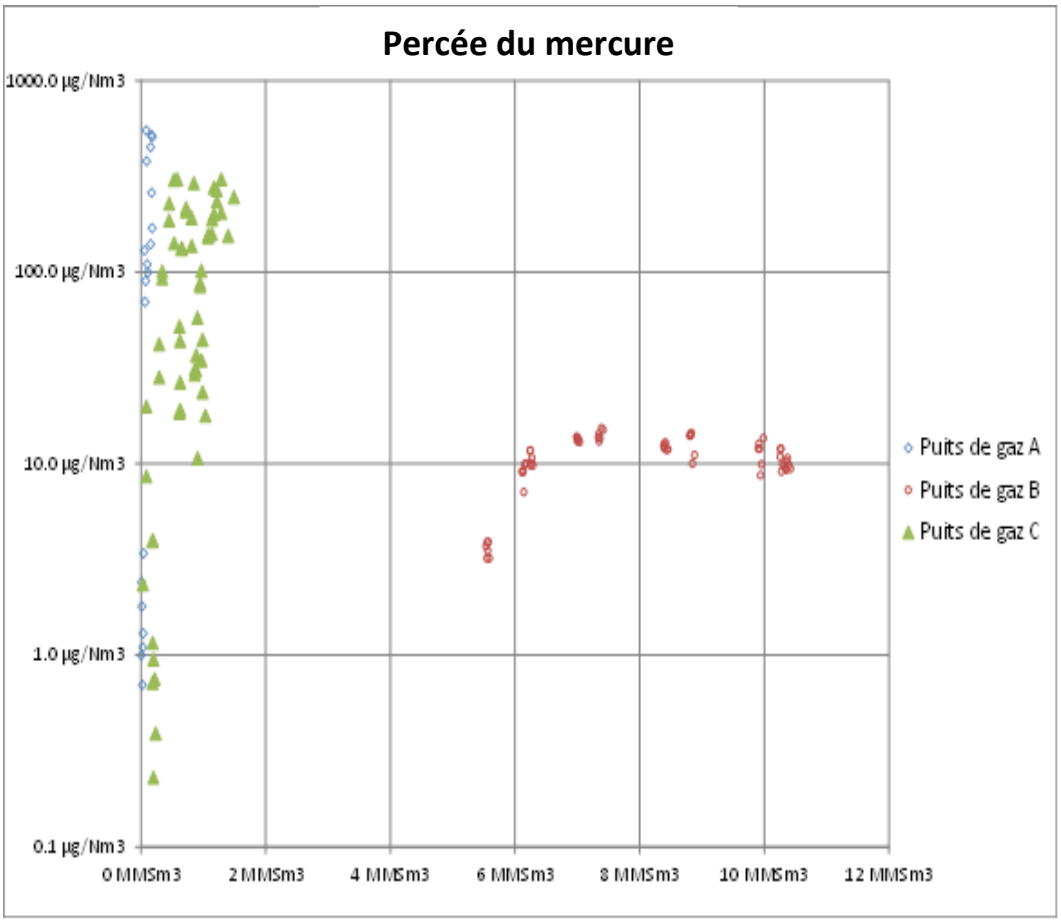

Figure 14. Temps de "percée du mercure" obtenu en fonction du volume de gaz produit lors de trois tests de puits

Cependant, la connaissance de la teneur en mercure du gaz, après stabilisation, permet de calculer l'ordre de grandeur de la quantité totale de mercure retenue par l'équipement de test avant la percée. En représentant la concentration en mercure du gaz mesurée pendant les tests, non pas en fonction du temps ou du cumul du volume de gaz produit, mais en fonction de la quantité totale de mercure censée être produite, il est observé cette fois-ci que la quantité de mercure retenue avant la percée est de l'ordre de quelques dizaines de grammes (Figure 15).

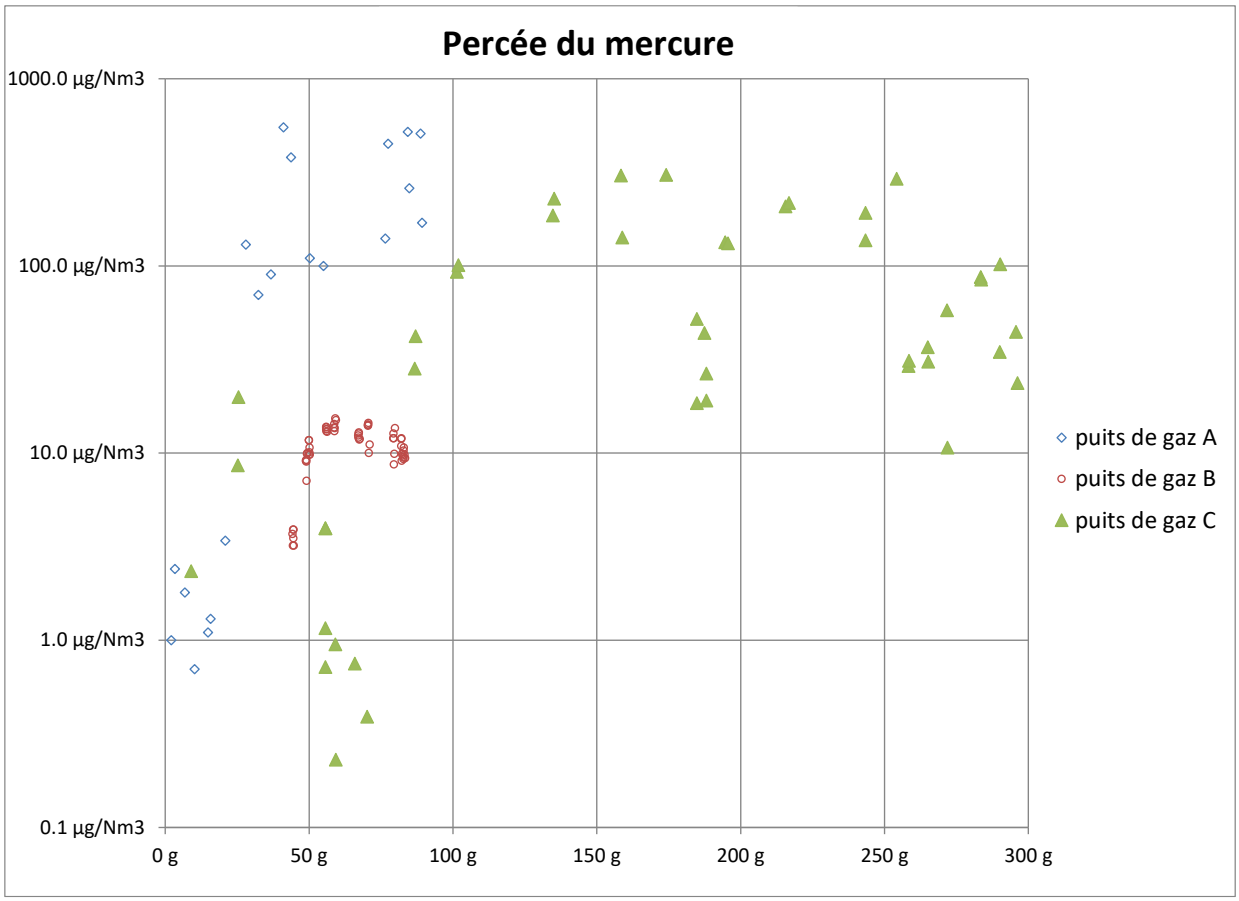

Figure 15. Temps de "percée du mercure" obtenu en fonction de la quantité totale produite estimée lors de trois tests de puits

Cette observation permet d'affirmer que la limite basse de détection du mercure dans le gaz, pendant un test de puits, dépend du volume total de gaz produit par le puits. Si un test est planifié pour produire 5 millions de mètres cubes de gaz, il ne serait pas raisonnable d'espérer déterminer une concentration précise de mercure dans le gaz si la teneur en mercure est de l'ordre 1 µg.Nm^{-3}, car, pour mesurer une telle valeur, il faudrait débiter 50 à 100 millions de mètres cubes de gaz au préalable. Si après production de 5 millions de mètres cubes de gaz, la teneur en mercure mesurée reste faible, la teneur en mercure du gaz dans le réservoir ne devrait pas dépasser 10-20 µg.Nm^{-3} car sinon, la percée devrait avoir déjà eu lieu.

L'adsorption d'une couche monoatomique très dense de mercure sur une surface est de l'ordre de 1 mg.m^{-2}. La surface macroscopique totale d'un équipement de test est typiquement de l'ordre de quelques centaines jusqu'à un millier de mètres carrés. Par conséquent, il est difficile d'expliquer la rétention de quelques dizaines de grammes de mercure par l'adsorption seule, à moins de prendre en compte la surface des produits de corrosion et des microparticules.

Une passivation de surface pourrait améliorer la vitesse de percée, mais sans prise en compte des microparticules naturellement présentes dans les pipelines et celles introduites par la boue de forage.

Il n'est donc pas judicieux lors d'un test de puits de mettre un point d'honneur à déterminer précisément la concentration en mercure dans le gaz car s'il est important de connaître la teneur en mercure du fluide pour prévoir les problèmes et dimensionner le traitement, le surcoût lié à l'augmentation de la durée de test empêche de descendre plus bas en sensibilité. Le but d'une campagne d'échantillonnage pendant un test de puits n'est donc pas de rechercher le mercure dans tous les ordres de grandeurs de concentration possible, mais de chercher à savoir si la teneur est en dessous de quelques microgrammes par mètre cube de gaz et quelle est la valeur de cette teneur si elle dépasse ce seuil.

4. Traque et élimination des artéfacts liés à la sélection et la préparation du point d'échantillonnage

Le mercure est un élément qui est fractionné entre la phase gazeuse et la phase liquide lorsque les deux phases sont présentes. Le coefficient de répartition entre les deux phases dépend de la pression et de la température, et plus modérément, des caractéristiques du gaz et du liquide. Pour cette raison, un entraînement de liquides ou de particules dans l'échantillon de gaz peut fausser notablement son analyse de la teneur en mercure. Il est donc important d'échantillonner un gaz propre, exempté de liquides et des particules.

De plus, une fois que le gaz et le liquide sont analysés, afin de remonter à la teneur en mercure du fluide global, il faut que les deux phases soient assez proches d'un état d'équilibre. Pour ces raisons, les points principaux d'échantillonnage pour la détermination de mercure doivent être les sortie gaz et sortie liquide du séparateur de test. Si le séparateur ou les connexions de celui-ci sont suspectés d'être contaminés par le mercure, un point d'échantillonnage alternatif peut être choisi pour vérifier cette suspicion. Dans ce cas, il faut veiller à ce que le volume mort entre la valve d'échantillonnage et la conduite principale soit inférieur à 0,5 L afin d'éviter que l'échantillon contienne un fluide de stagnation.

Lorsque l'échantillonnage de gaz naturel s'effectue par sacs Tedlar, le volume purgé doit être au moins 10 fois supérieur à la quantité de gaz stagnant dans le volume mort. Il est

recommandé que la valve de détente pour l'échantillonnage soit chauffée afin d'éviter la formation de liquide ou l'augmentation d'adsorption liée au froid créé par la détente.

Lorsque le mercure est échantillonné par amalgamation en connectant directement l'échantillonneur au point d'échantillonnage, celui-ci doit être placé au moins 10 minutes avec un débit de purge de l'ordre de 20 L (conditions atmosphériques) par minute à travers une ligne de by-pass. Cette purge doit être maintenue lors de la prise d'échantillon. Le débit recommandé, qui traverse les pièges, doit être compris entre 0,2 et 1 L par minute afin d'éviter un temps de résidence insuffisant du gaz dans les pièges.

5. Règles depuis l'échantillonnage jusqu'à l'analyse afin d'observer aucune perte et contamination de l'échantillon

Il est connu que les bouteilles d'échantillonnage sous pression préservent mal le mercure (cf Partie 1 : Experimental Tests of Natural Gas Samplers Prior to Mercury Concentration Analysis, p 77). Depuis, différents types d'inertage ont été inventés dans le but de préserver le mercure dans l'échantillon prélevé (SilcoTek Corporation, 2019). Ces bouteilles sont largement utilisées aujourd'hui par beaucoup de laboratoires de services. Cependant, il a été démontré que lorsque les bouteilles ne sont plus « neuves », il est non seulement possible de perdre à nouveau le mercure dans ces bouteilles, mais aussi, le mercure « stocké » dans ces vieilles bouteilles peut potentiellement contaminer un gaz qui n'en contenait pas ou peu (cf 3.4. Mass Balance and Reaction Rates, p 89).

Par conséquent, l'utilisation de ces bouteilles lors de l'échantillonnage de gaz naturel pour l'analyse du Hg est à éviter. L'utilisation des sacs Tedlar ou la prise d'échantillon par amalgamation doivent être privilégiées. L'analyse directe sur site, si elle est possible, reste la méthode la plus fiable pour de l'analyse du mercure lors d'un essai de puits.

En effet, lors des analyses sur site, de nombreux artefacts peuvent subvenir et ne sont pas toujours prévisibles. Il est donc important d'essayer de les déterminer immédiatement lors d'analyse directe sur site car dans le cas d'une analyse hors site, à posteriori, les dégâts occasionnés sur les résultats ne pourront pas être corrigés mais juste constatés.

La vérification croisée de la teneur en mercure dans le gaz et dans l'hydrocarbure liquide hors mercure particulaire pouvant être éliminées par filtration ou sédimentation, doit être effectuée. Ces valeurs doivent être compatibles à celle d'équilibre dans les conditions de

séparateur. La vérification de la teneur en mercure de fluide de forage et fluide de complétion est également utile afin d'identifier et éliminer certaines sources d'artefacts.

De plus, la contamination de l'équipement d'échantillonnage est aussi un souci réel. L'absence de mercure dans le système d'échantillonnage (vannes, tubes et connexions) utilisé en amont des pièges à mercure, ainsi que les bouteilles utilisées pour la prise d'échantillons de liquides doivent être vérifiées avant la campagne d'échantillonnage.

La valeur de blanc des pièges d'amalgamation est une question clé. La pratique la plus commune pour obtenir un blanc satisfaisant pour chaque piège est de les nettoyer par des cycles de chauffage répétés dans un four lié à un spectromètre, jusqu'à ce que la valeur résiduelle trouvée soit en dessous d'une limite qu'on considère comme satisfaisante. Il arrive cependant qu'en dessous de certaines valeurs, la teneur résiduelle en mercure d'un piège ne continue pas à diminuer malgré les cycles de chauffe, mais persiste à un niveau non satisfaisant ou devient erratique sans qu'on ne comprenne son origine. Face à cette difficulté, certains augmentent le volume d'échantillons qui accroît la quantité totale de mercure piégée, hissant celle-ci bien au-dessus de la zone de blanc. D'autres déduisent la quantité de mercure trouvée dans le piège de la valeur du dernier blanc trouvée.

Ces pratiques sont cependant problématiques car le mercure ne peut être généré spontanément dans le piège. Le fait de ne pas arriver à abaisser suffisamment les valeurs de blanc signifie simplement qu'il existe des sources de contamination non identifiées. L'augmentation du volume de gaz échantillonné peut avoir deux effets négatifs. La quantité en mercure passant dans le système d'échantillonnage accroît donc, augmentant de ce fait son degré de contamination. Cela a aussi pour effet, d'accumuler également plus de composés pouvant interférer avec l'efficacité de piégeage comme l'eau, les hydrocarbures lourds ou les composés soufrés.

Quant à la déduction de la dernière valeur de blanc, cela revient à supposer que la source de contamination contamine le piège de façon répétable, ce qui n'a pas de sens.

Dans le cas d'une opération d'échantillonnage, il est déjà arrivé que les bouchons des pièges de mercure ont été identifiés que la source de contamination. Cette contamination est arrivée probablement après que les bouchons aient touché une surface de travail contaminée. Dans ce cas, la contamination était d'une centaine de fois supérieure à la quantité de mercure capturée lors de la prise d'échantillon. La simple déduction de la valeur du dernier blanc ne permet nullement la prise en compte de ce problème.

Les pièges de mercure peuvent être aussi contaminés par les particules présentes dans ceux-ci. Le Tableau 5 présente les résultats de mesures à l'entrée et à la sortie d'une unité de démercurisation (MRU).

Tableau 5. Concentrations en mercure mesurées à l'entrée et à la sortie d'une MRU

		Concentration	volume	Hg per trap
Inlet MRU	12/03	31 ng/Nm3	49.0 L	1.5 ng
	12/03	56 ng/Nm3	30.3 L	1.7 ng
	13/03	34 ng/Nm3	27.8 L	0.9 ng
	15/03	17 ng/Nm3	50.0 L	0.9 ng
	15/03	30 ng/Nm3	39.0 L	1.2 ng
	18/03	49 ng/Nm3	33.3 L	1.6 ng
	19/03	18 ng/Nm3	77.0 L	1.4 ng
	20/03	49 ng/Nm3	30.0 L	1.5 ng
Outlet MRU	16/03	32 ng/Nm3	44.0 L	1.4 ng
	16/03	60 ng/Nm3	40.0 L	2.4 ng
	17/03	70 ng/Nm3	21.4 L	1.5 ng
	17/03	64 ng/Nm3	44.3 L	2.8 ng
	18/03	27 ng/Nm3	61.6 L	1.7 ng
	19/03	49 ng/Nm3	36.0 L	1.8 ng
	20/03	66 ng/Nm3	41.0 L	2.7 ng

L'ordre de grandeur de concentrations en Hg retrouvées en entrée et en sortie ne change pas en traversant l'unité de traitement et reste au-dessus de la spécification soit 10 ng.Nm^{-3} : ce qui pourrait signifier que l'MRU ne fonctionne plus correctement. Mais une analyse plus fine de ces résultats nous conduit à une conclusion radicalement différente : ces valeurs sont principalement dues aux valeurs de blanc des pièges utilisés. En effet, en oubliant la concentration affichée et en représentant la quantité de mercure trouvée dans chacun de ces pièges en fonction du volume de gaz les ayant traversés, la teneur en mercure des pièges ne varie quasiment pas avec le volume d'échantillon (Figure 16.

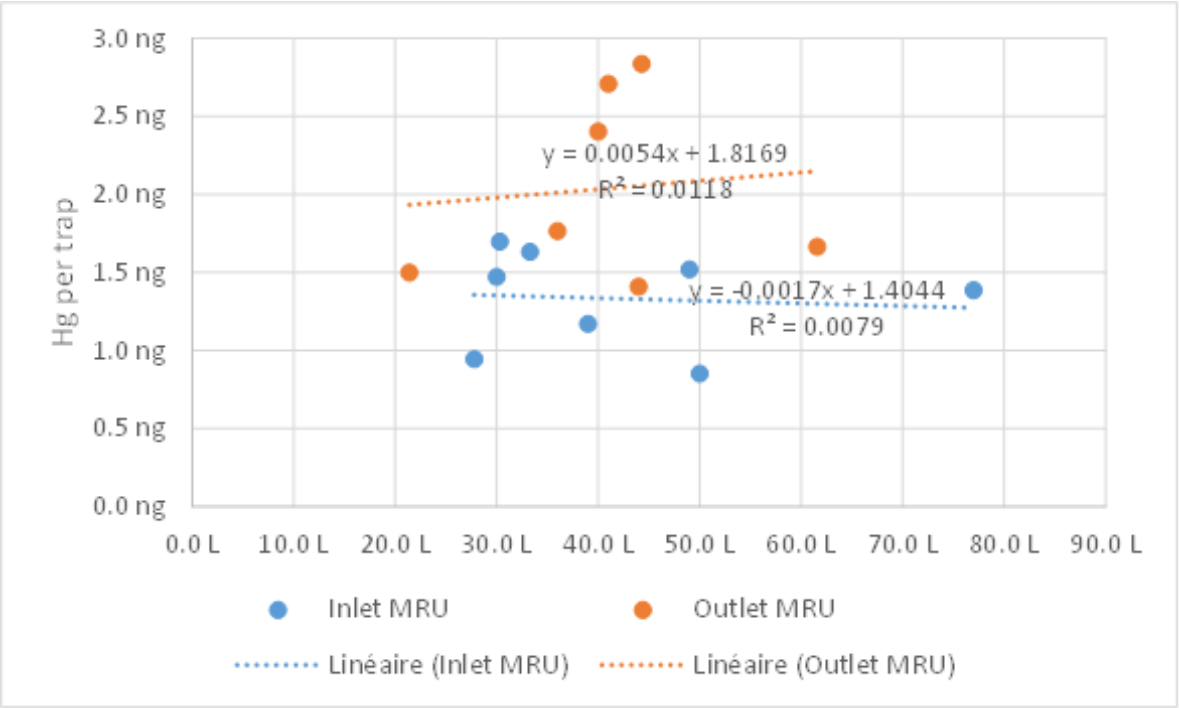

Figure 16. Concentrations en mercure analysées dans chaque piège en fonction du volume de gaz

La quantité de mercure trouvée dans les pièges reste dans la même zone de concentration soit de 0,9 à 1,7 ng pour les mesures à l'entrée de l'unité alors qu'en extrapolant la relation quantité de mercure par piège versus volume de gaz échantillonnée, on obtient des valeurs de 1,4 à 1,8 ng qui correspondent aux blancs statistiques.

Il a été démontré que le mercure n'est pas seulement piégé par la partie du piège contenant de l'or, mais une quantité importante peut être stockée dans le tube de quartz, probablement associée à des particules (Tableau 6. Le niveau de blanc d'un piège peut être abaissé au picogramme avec 2 cycles de chauffe. Mais le mercure a été éliminé lors d'un cycle de chauffe, seulement sur la partie centrale du piège. Le mercure retenu par les particules restant dans le tube de quartz loin de la partie centrale n'a quant à lui pas pu être éliminé. De ce fait, lorsqu'il y a un déplacement de la position du piège, ou lorsqu'un flux de gaz déplace ces particules, une quantité de mercure de l'ordre de 1000 fois de celle du dernier blanc pourrait être observée.

Tableau 6. Concentrations en Hg obtenues après analyses de blancs des pièges en changeant leurs positions lors du nettoyage

Follow-up of cartridge 2				
Date	Time	Nature (sample or blank)	Hg (pg / trap)	Comments
08/10/2003	14:55	blank	18	
08/10/2003	15:32	blank	2	
08/10/2003	18:31	sample	296	
08/10/2003	21:16	blank	14	
08/10/2003	21:42	blank	2	
09/10/2003	00:05	blank	16	heating inlet side of the cartridge
09/10/2003	00:08	blank	1	
09/10/2003	00:10	blank	3641	heating outlet side of the cartridge
09/10/2003	00:13	blank	3	
09/10/2003	07:50	blank	5	
09/10/2003	19:09	sample	11	
09/10/2003	21:33	blank	0	heating inlet side of the cartridge
09/10/2003	21:37	blank	5290	heating outlet side of the cartridge
09/10/2003	21:40	blank	6	
10/10/2003	07:45	blank	5	
10/10/2003	17:23	sample	64	

La difficulté de garantir des valeurs de blanc a été mise en évidence à travers ces exemples. La vérification des blancs avant la prise d'échantillons est nécessaire, mais ne garantit nullement l'absence de mercure dans les pièges. D'où la recommandation de ne pas se fier aux mesures effectuées sur des pièges isolés, mais faire des mesures par groupes contenant 3 à 6 pièges ayant vu de volume différent de gaz variant dans une proportion d'au moins 1 à 4.

CHAPITRE III : FIABILITE DE L'ECHANTILLONNAGE ET DE L'ANALYSE DE L'ARSENIC DANS LE GAZ NATUREL

Il existe différentes méthodologies pour la détermination de la concentration de l'arsenic dans le gaz naturel (cf 2.1.2.Gas Samplers: Cylinders and Inert Plastic Bags (Tedlar Bags), p 60). Comme pour le mercure, l'échantillonnage du gaz naturel à haute pression peut être effectué à l'aide de cylindres en acier inoxydable avant de mesurer l'As hors site.

Le revêtement intérieur de ces cylindres est supposé être inerte et donc empêcher l'adsorption de l'arsenic à l'intérieur de ceux-ci, rendant l'analyse de l'As fiable. Afin de déterminer si l'échantillonnage de gaz naturel pour l'analyse de l'arsenic dans ces cylindres est fiable, différentes expérimentations ont été développées.

Plusieurs échantillons de gaz naturel provenant de différents puits d'un même pays ont été prélevés dans des cylindres en acier inoxydable en 2009, 2010 et 2013. Ces campagnes d'échantillonnage de gaz naturel ont été réalisées afin de déterminer si les fluides provenant des puits étaient contaminés en As. Les échantillons de gaz naturel ont résidé dans ces cylindres jusqu'aux expérimentations réalisées en 2019. La concentration en arsenic contenue dans les échantillons de gaz naturel a été déterminée par HR-ICP-MS de solutions de barbotage obtenues après vidage complet des cylindres dans celles-ci. Une chauffe des cylindres a été réalisée afin de déterminer si de l'arsenic s'était absorbé sur leurs surfaces internes.

Deux cylindres contenaient du gaz naturel ainsi que du condensat de gaz : cette matrice organique a été aussi analysée afin de déterminer la concentration en arsenic total ainsi que sa spéciation.

1. Matériels et Méthodes

1.1. Echantillonnage

Six échantillons de gaz naturel ont été prélevés dans un même pays, sur différents puits et à des dates différentes (cf Tableau 7). Les échantillons de gaz naturel ont été prélevés dans des cylindres Swagelok® en acier inoxydable à doubles extrémités de 300 cc. Les cylindres remplis ont été stockés au sein du pôle PVT du Centre Scientifique et Technique de TotalEnergies jusqu'en 2019.

Tableau 7. Informations sur les échantillons de gaz naturel analysés

Code échantillon	Numéro du puits	Date de prélèvement	Volume échantillon (m^3)	Type d'échantillon
A – 1	1	2009	0,032	Gaz naturel
A – 2	1	2009	0,027	Gaz naturel + condensats de gaz
A – 3	2	2010	0,0315	Gaz naturel
A – 4	3	2013	0,0325	Gaz naturel
A – 5	3	2013	0	(Gaz naturel) + condensats de gaz
A – 6	3	2013	0,025	Gaz humide

L'échantillon A – 5 devait contenir du gaz naturel, après ouverture, il y avait uniquement présence de condensat de gaz. Il semble donc que le cylindre se soit vidé au cours du temps.
Les condensats de gaz des échantillons A – 2 et A – 5 ont été récupérés dans des flacons en verre, fermés hermétiquement avec des septums et ont été placés au noir à température ambiante avant leurs analyses.

1.2. Procédures d'analyse

1.2.1. Mesure de la concentration en arsenic total par système de barbotage

La concentration en arsenic totale de chaque échantillon de gaz naturel a été déterminée en faisant barboter la totalité des gaz contenus dans chaque cylindre dans un système de barbotage (Figure 17).

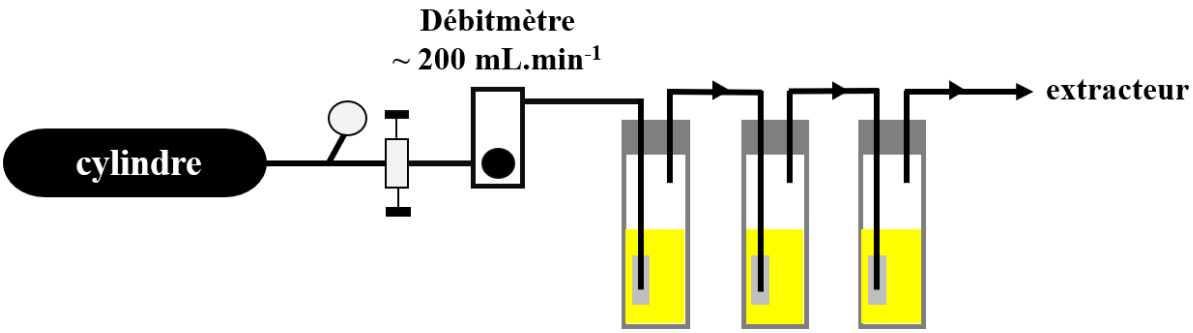

Figure 17. Schéma du système de barbotage utilisé pour la détermination de l'arsenic totale dans les échantillons de gaz naturel

Une valve du cylindre a été ouverte et le flux de gaz sortant a été ajusté à un débit de 200 $mL.min^{-1}$. Le gaz a barboté dans 3 barboteurs montés en série contenant chacun 10 mL d'acide nitrique à 10% (Cachia, 2017). Une fois les cylindres vidés, les solutions de barbotage ont été récupérées puis diluées avec un FD = 5 avec de l'eau MQ supra-pure et du germanium y a été ajouté comme étalon interne. Les solutions de barbotage ont ensuite été analysées par HR-ICP-MS selon les paramètres présentés Tableau 8.

Tableau 8. Paramètres d'analyse par HR-ICP-MS des solutions de barbotage obtenues après vidage complet des échantillons de gaz naturel contenus dans les cylindres ainsi que lors de la désorption thermique

ICP-MS Thermo Element XR	
Condition plasma	Humide
Puissance générateur	1145 W
Gaz plasma	Ar
Ar auxiliaire	1,00 $L.min^{-1}$
Résolution	Haute
Cônes	Nickel
Réplicats	20
Type scan	EScan
Temps échantillon	0,200 s
Mode détection	Triple
Eléments (isotopes)	^{72}Ge et ^{75}As

Afin d'assurer la fiabilité de la mesure, les solutions de barbotage ont été analysées en triplicat. La concentration en arsenic total a été déterminée en fonction de la pente obtenue à

partir d'une courbe d'étalonnage en As élémentaire. Les limites de détection et de quantification instrumentale obtenues étaient respectivement de 32 ppt et de 96 ppt.

1.2.2. Analyse des condensats de gaz contenus dans les cylindres

Les condensats de gaz provenant de l'échantillon A – 5 et A – 3 (Tableau 7) ont été dilués (FD = 2 et 10) dans du toluène et le xylène. Les échantillons ont été dilués en triplicatas dans chacun des deux solvants. Ceux-ci ont été analysés par GC-ICP-MS selon les paramètres optimisés par (Bouyssiere et al., 2001) (Tableau 9).

Tableau 9. Paramètres d'analyse par GC-ICP-MS des condensats de gaz selon Bouyssiere et al., 2001

***GC-MS Thermo* ISQ QD**	
Colonne chromatographique	HP – 5 (30 m × 0,32 mm × 0,25 µm)
Injection	Splitless, temps de purge : 1 min
Température d'injection	150°C
Volume d'injection	1 µL
Gaz porteur	Helium (2 mL/min)
Programme de température du four	60°C (1min) à 280°C de 50°C/min
Température ligne de transfert	250°C
ICP-MS Thermo X Series 2	
Gaz plasma	Argon
Ar auxiliaire	0.9 L.min-1
Cônes (Sampler et Skimmer)	Nickel
Réplicats	5
Eléments (Isotopes)	^{13}C,^{33}S,^{35}Cl, ^{75}As, ^{118}Sn, ^{121}Sb et $^{199,202}Hg$

En plus des condensats dilués, les condensats purs ont pu être injectés et analysés par cette même technique d'analyse. La concentration en As total a été semi-quantifiée en fonction de la pente obtenue à partir d'une courbe d'étalonnage en Ph_3As préparée dans le toluène et le xylène. La limite de détection et de quantification instrumentale était respectivement de 81 ppt et 243 ppt.

1.2.3. Expérience de désorption thermique

Après l'analyse de la concentration en As total des cylindres, une désorption thermique a été réalisée sur les cylindres A-3, A-6 et A-3 (Tableau 7). Les cylindres ont été placés dans un four programmable sous un flux d'argon à un débit d'environ 200 $mL.min^{-1}$ (**Figure 18**). La température expérimentale initiale était d'environ 20°C (T°C ambiante). La température du four a été augmentée de 10 °C toutes les 10 minutes et la procédure a été répétée jusqu'à 200°C. Puis les cylindres ont été laissés dans le four pendant 2h à 200°C.

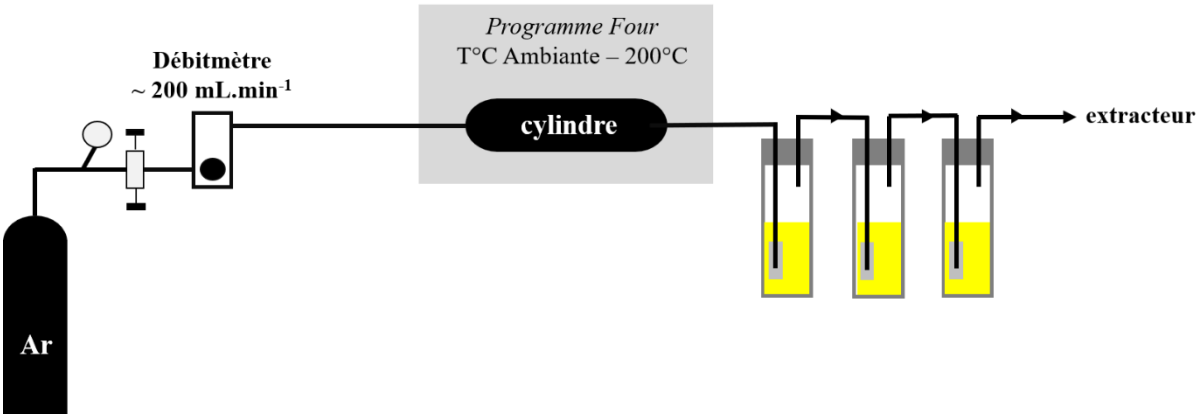

Figure 18. Schéma du système de désorption thermique pour la détermination de l'arsenic absorbé dans les cylindres.

L'arsenic désorbé a été piégé dans des solutions de 10% d'HNO_3 de la même façon que pour la « Partie 1.2.1, p 111 ». Les solutions une fois diluées (FD = 5) ont ensuite été analysées par HR-ICP-MS selon les paramètres présentés Tableau 8.

2. Résultats et discussions

2.1. Mesure de la concentration en arsenic total par système de barbotage

Suite au barbotage de la totalité des gaz contenus dans chaque cylindre dans le système de barbotage, la présence d'arsenic dans les solutions de barbotage n'a pas été mise en évidence après leurs analyses par HR-ICP-MS. La limite de détection instrumentale de l'appareil était de 32 ppt. Sachant que le volume de gaz qui a barboté dans ces solutions était compris entre 0,025

et 0,0325 m^3 (Tableau 7), la concentration en arsenic dans celles-ci était donc inférieure à la limite de détection expérimentale qui était de ~ 50 $ng.m^{-3}$ (Tableau 10).

Tableau 10. Limite de détection expérimentale obtenue pour chaque échantillon de gaz naturel en fonction du volume de gaz barboté

Code Echantillon	Limite de détection ($ng.m^{-3}$)
A – 1	50
A – 2	59
A – 3	51
A – 4	49
A – 6	64

La désorption thermique de ces cinq cylindres a donc été nécessaire afin de déterminer si l'arsenic potentiellement présent dans ces échantillons de gaz naturel s'était adsorbé à la surface interne de ces cylindres.

2.2. Analyse des condensats de gaz contenus dans les cylindres

Suite à l'analyse de la courbe d'étalonnage de Ph_3As réalisée dans le toluène et dans le xylène par GC-ICP-MS, le temps de rétention de cette espèce arséniée avec cette technique d'analyse était de 374 mS (Figure 19).

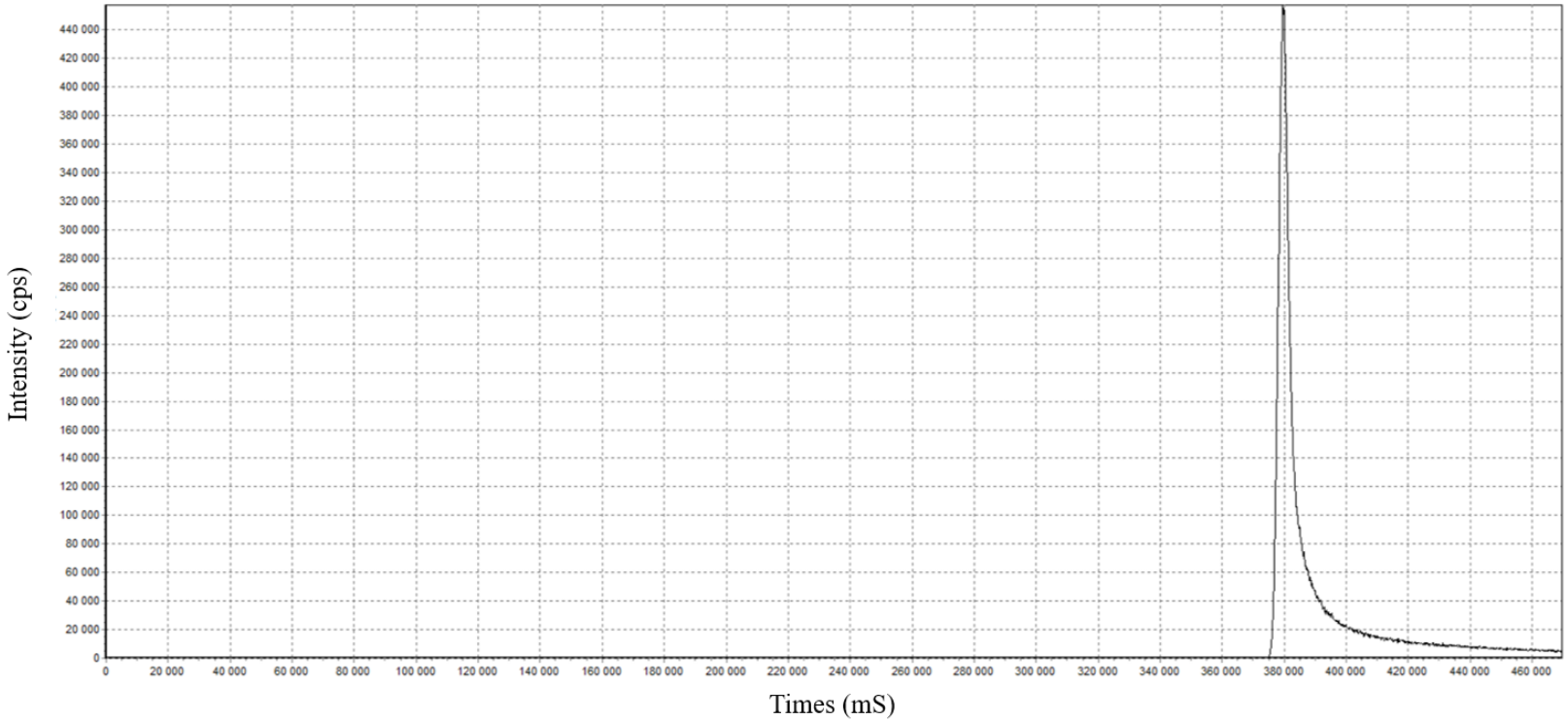

Figure 19. Chromatogramme du standard de Ph_3As à 25 ppb dans le toluène

L'analyse des condensats de gaz retrouvés dans les cylindres des échantillons A – 2 et A – 5 dilués et purs n'ont pas pu mettre en évidence la présence de Ph_3As et de d'autres composés arséniés (Figure 20).

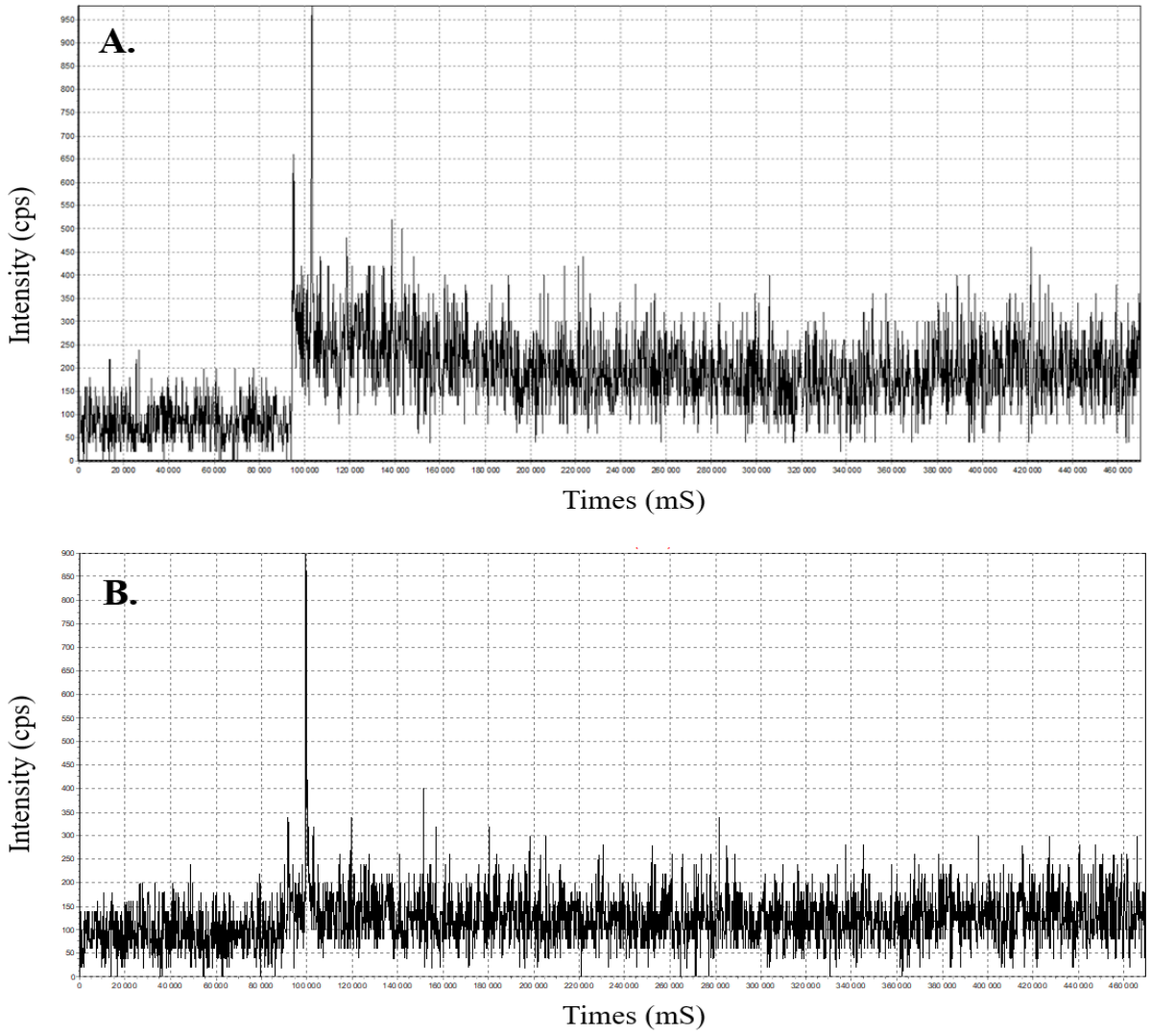

Figure 20. Chromatogramme de l'arsenic du condensat de gaz de (A.) l'échantillon A – 2 et de (B.) l'échantillon A – 5. Analyse des échantillons purs.

La désorption thermique du cylindre ayant contenu l'échantillon A – 5 semble tout de même nécessaire afin de déterminer si l'arsenic potentiellement présent dans le condensat de gaz ainsi que dans le gaz naturel initialement présent dans le cylindre, ne s'est pas adsorbé à la surface interne de ce cylindre.

2.3. Expérience de désorption thermique

Suite à la chauffe des cylindres à 200°C pendant 2 h, l'arsenic potentiellement désorbé de la surface interne de ceux-ci a été analysé dans les solutions de piégeage du système de barbotage Figure 18. De l'arsenic a été retrouvé dans les solutions de barbotage de trois cylindres désorbés thermiquement (Tableau 11).

Tableau 11. Concentration en As désorbé thermiquement des cylindres

Code Echantillon	Concentration ($\mu g.m^{-3}$)
A – 1	< LD
A – 2	< LD
A – 3	0,24
A – 4	0,74
A – 5	0,23
A – 6	< LD

La concentration en arsenic désorbé la plus importante était pour l'échantillon A – 4 où 0,74 $\mu g.m^{-3}$ d'As, a été retrouvée. Ces résultats montrent que l'arsenic contenu dans les échantillons de gaz naturel s'était effectivement adsorbé à la surface interne des cylindres.

De plus, l'échantillon de gaz naturel A – 4, A – 5 (présence uniquement de condensats de gaz) et A – 6 ont été échantillonnés dans le même puits , la même année (Tableau 7) : ce qui montre que le gaz naturel provenant de ce puits était effectivement contaminé en arsenic. Suite à ces résultats, la compagnie TotalEnergies a donc décidé de renouveler une campagne d'échantillonnage de gaz naturel en août 2019 sur ce puits, afin de pousser leur investigation quant à cette contamination du gaz naturel par l'As.

3. Conclusion

L’analyse des condensats de gaz et des solutions de piégeage obtenues suite au barbotage de la totalité des gaz contenus dans chaque cylindre, ainsi, n’ont pas permis de mettre en évidence la présence d’arsenic dans les échantillons de gaz naturel. La concentration en arsenic dans ceux-ci était inférieure à ~ 50 $ng.m^{-3}$. Malgré ces résultats, la désorption thermique des cylindres ayant contenu ces échantillons de gaz naturel a permis de mettre en évidence que l’arsenic contenu dans ceux-ci s’était adsorbé à la surface interne des cylindres.

Ces résultats expérimentaux ont donc montré que les cylindres en acier inoxydable n’étaient pas inertes à l’adsorption de l’arsenic et étaient donc inefficaces pour l’échantillonnage de gaz naturel avant l'analyse de l'As.

D’autres expérimentations sont nécessaires afin de déterminer si cette adsorption est liée à l'adsorption des espèces de soufre sur les surfaces internes des cylindres en acier inoxydable, devenant des sites d’adsorption pour l’arsenic comme pour le mercure (cf 4.Conclusion and Recommendations, p 90). De plus, l’évaluation de l’utilisation d’échantillonneurs alternatifs de gaz naturel comme les cylindres revêtus de silicium et les sacs Tedlar doit être effectuée afin de déterminer si ceux-ci sont inertes à l’adsorption de l’arsenic.

CHAPITRE IV : COMPREHENTION DU PHENOMENE D'ADSORPTION DE L'ARSENIC ET DU MERCURE SUR LA SURFACE INTERNE DES CYLINDRES

Afin d'essayer de mieux comprendre le phénomène d'adsorption de l'arsenic et du mercure sur la surface interne de cylindres de différents types lors de prélèvement de gaz naturel, du biogaz a été prélevé sur le site de Mendixka à Charrite-le-bas (site de valorisation de déchets verts et ménagers) à l'aide d'un réacteur contenant des plaques (en inox, recouvertes du revêtement Silconert® et Dursan®) représentant expérimentalement les cylindres d'échantillonnage. Ce biogaz est le produit résultant de la décomposition de déchets ménagers enfouis sur le site. Une analyse de surface des plaques a ensuite été réalisée par ablation laser couplée à un ICP-MS et par Scanning Electron Microscope (SEM) couplée à la spectroscopie de rayons X à dispersion d'énergie (EDX). Cette dernière analyse a été réalisée par le Bordeaux Imaging Center (BIC) afin de mieux observer et comprendre ce phénomène d'adsorption.

1. Matériels et méthodes

1.1. Détermination de la concentration en arsenic total dans le biogaz du site de Mendixka

La concentration en arsenic total contenue dans le biogaz a été déterminée en faisant barboter ce dernier dans un système de barbotage (Figure 21). Le système de barbotage à directement été connecté au flux primaire de biogaz. Le débit de ce flux était ~ 35 $ml.min^{-1}$. Le biogaz a barboté dans 3 barboteurs montés en série contenant chacun 10 mL d'acide nitrique à 10% (Cachia, 2017) pendant 120h. La quantité totale de biogaz qui a barboté dans ces solutions était ~ 252 L.

Figure 21. Système de barbotage mise en place sur le site de Mendixka pour la détermination de la concentration en As total dans le biogaz.

Les solutions de barbotage ont été récupérées puis diluées avec un FD = 5 avec de l'eau MQ supra-pure et du germanium y a été ajouté comme étalon interne. Les solutions de barbotage ont ensuite été analysées par ICP-MS avec utilisation de la cellule de collision selon les paramètres présentés Tableau 12. La cellule de collision a été utilisée afin de limiter les interférences $ArCl^-$. Un mélange d'argon et d'hélium a été utilisé comme gaz auxiliaire lors de l'utilisation de la cellule de collision.

Tableau 12. Paramètres d'analyse par ICP-MS des solutions de barbotage obtenues après barbotage du biogaz de Mendixka

ICP-MS Agilent 7700 s	
Puissance générateur	1500 W
Gaz plasma	Ar
Ar auxiliaire	1,06 $L.min^{-1}$
Cônes	Nickel
Réplicats	25
Cellule de collision	N_2 = 5.2 $mL.min^{-1}$
Eléments (Isotopes)	^{72}Ge et ^{75}As

Afin d'assurer la fiabilité de la mesure, les solutions de barbotage ont été analysées en triplicat. La concentration en arsenic total a été déterminée en fonction de la pente obtenue à partir d'une courbe d'étalonnage en As élémentaire. Les limites de détection et de quantification instrumentale obtenues étaient respectivement de 53 ppt et de 156 ppt.

1.2. Détermination de la concentration en mercure total dans le biogaz du site de Mendixka

La concentration en Hg total a été déterminée en échantillonnant le biogaz à l'aide de pièges Amasil®. Les pièges ont été directement connectés sur le flux de gaz primaire. Différents volumes de biogaz ont été prélevés : 5, 10, 20, 30 et 40 mL. Chaque prélèvement de gaz aux différents volumes a été effectué en duplicat.

Le mercure a ensuite été analysé par spectrométrie de fluorescence atomique (Sir Galahad, PS Analytical, U.K.). La procédure d'analyse était la même que pour la partie « 2.5. Hg Analysis, p 83 ». La concentration en Hg^0 a été estimée en fonction de la pente obtenue par gradient volumétrique (cf 5.Complete information, p 91). La limite de détection instrumentale obtenue était de 10 pg.

1.3. Analyse de surface des plaques représentant expérimentalement les cylindres d'échantillonnage

1.3.1. Prélèvement du biogaz dans le réacteur

Les plaques représentant expérimentalement les cylindres d'échantillonnage ont été obtenues auprès de Silcotek®. Elles mesuraient toutes 4 cm^2 et avaient une épaisseur de 0,1 cm. Il y avait trois catégories de plaques. La première catégorie était en acier inoxydable sans revêtement mais avec un traitement de surface. Le deuxième était en acier inoxydable recouverte par le revêtement Silconert®. La troisième était en acier inoxydable recouverte du revêtement Dursan®.

Le réacteur a été conçu au sein de UPPATech à l'université de Pau. Il a été fabriqué en téflon chargé de 20% de verre afin de limiter toute adsorption à l'intérieur de celui-ci. Il était composé d'une cavité centrale où deux portoirs à plaques ont été placés (cf Figure 22. Chaque portoir pouvait contenir 4 plaques.

Lors de l'échantillonnage, les 3 catégories de plaques ont été placées sur le portoir dans le réacteur soient 3 plaques recouvertes par le revêtement Silconert®, 3 plaques recouvertes du revêtement Dursan® et 2 en acier inoxydable sans revêtement.

Le réacteur a été connecté directement sur le flux primaire de biogaz du site de valorisation de déchets de Mendixka (Figure 22.). Le biogaz n'a pas été retenu dans le réacteur mais est passé à l'intérieur de celui-ci sous flux constant.

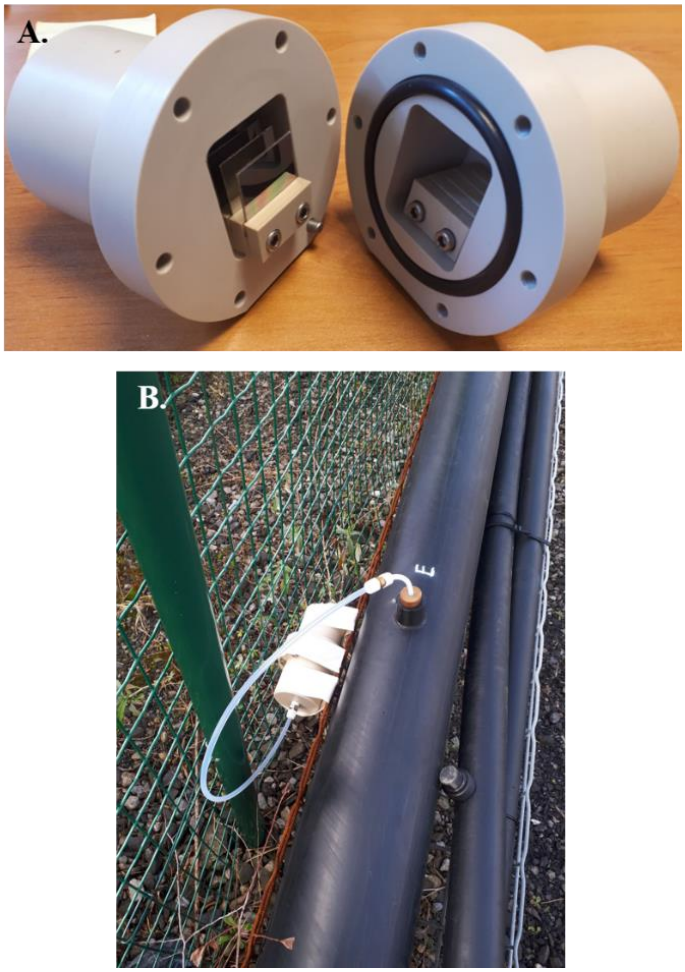

Figure 22. Vue intérieure du réacteur (A.) utilisé lors de l'échantillonnage du bio gaz de Mendixka (B.).

Le débit du flux primaire était ~ 5,5 mL.min^{-1}. Le biogaz a traversé le réacteur pendant 120h. Les plaques ont donc été en contact avec ~ 39,6 L de biogaz. Après l'échantillonnage, le réacteur a été fermé hermétiquement afin d'éliminer toute source de contamination avant l'analyse de surface des plaques.

1.3.2. Analyse de surface par LA-ICP-MS

Les plaques ont été récupérées des portoirs du réacteur et analysées par LA-ICP-MS selon les paramètres présentés dans le Tableau 13. La cellule de collision de l'ICP-MS a été utilisée lors de l'analyse de l'arsenic afin de limiter les interférences $ArCl^-$. L'hélium a été utilisé comme gaz auxiliaire lors de l'utilisation de la cellule de collision.

Tableau 13. Paramètres d'analyse par LA-ICP-MS des plaques utilisées lors de l'échantillonnage du biogaz sur le site de Mendixka

LA ESI NWR – 213	
Energie	30 %
Fluence	1,1 $J.cm^{-2}$
Fréquence	20 Hz
Diamètre faisceau laser	200 µm
Vitesse déplacement	500 $\mu m.s^{-1}$
Gaz vecteur	He = 800 $mL.min^{-1}$
ICP-MS Agilent 7700 s	
Puissance générateur	1500 W
Gaz plasma	Ar
Ar auxiliaire	1,08 $L.min^{-1}$
Gaz secondaire	0_2
Cônes	Platine
Réplicats	15
Cellule de collision	He = 9,6 $mL.min^{-1}$
Eléments (Isotopes)	^{32}S,^{75}As et ^{202}Hg

Une plaque de chaque catégorie, n'ayant pas été utilisée lors de l'échantillonnage du biogaz sur le terrain, a été analysée par LA-ICP-MS en tant que blanc. La quantification de l'arsenic, du mercure et du soufre n'a pas été réalisée lors de ces analyses. Les blancs ainsi que les plaques en inox non-revêtues et les plaques avec le revêtement Silconert® ont été scannées une seule fois. Les plaques avec le revêtement Dursan® ont été scannées 4 fois.

1.3.3. Analyse de surface par SEM-EDX

Suite à l'analyse par LA-ICP-MS, une analyse de surface de chaque plaque a été réalisée par SEM-EDX par Mme Svahn au Bordeaux Imaging Center (BIC). Les paramètres d'analyse sont présentés dans le Tableau 14.

Tableau 14. . Paramètres d'analyse par SEM-EDX des plaques utilisées lors de l'échantillonnage du biogaz sur le site de Mendixka

SEM Zeiss GeminiSEM300 – EDX Bruker XFlash 6/60	
Tension d'accélération	15 kV
WD	Dursan = 7,7 mm ; Silconert = 8,5 mm
Détecteur électrons secondaires – topographie	SE2
Détecteur électrons rétrodiffusés – contraste chimique	BSD1
Vacuum mode	Vide élevé

Ces analyses ont permis d'obtenir un spectre des éléments contenus sur la surface de chaque plaque, plus particulièrement sur les « taches » visualisées par microscope optique (Figure 26). Ces analyses ont aussi pu déterminer l'abondance de chaque élément en pourcentage sur ces mêmes taches.

2. Résultats et discussions

2.1. Détermination de la concentration en arsenic total dans le biogaz du site de Mendixka

Suite au barbotage du biogaz dans le système de barbotage, de l'arsenic a été retrouvé dans le barboteur n°1. La pente de la gamme étalon en arsenic dont l'équation était la suivante : y = 5555,2 x + 2789,1 ; a permis de déterminer que la concentration en As retrouvé dans le barboteur était de 74 ± 0,03 ppt. Sachant que le volume de biogaz qui a barboté dans les solutions de piégeage était de 252 L soit 0,252 m^3, la concentration en As retrouvée dans le biogaz de Mendixka était de **932,4 ng.m^{-3}**. Le réacteur a donc pu être mis en place sur le flux primaire de biogaz afin de mieux observer et comprendre l'adsorption de l'arsenic sur la surface des plaques.

2.2. Détermination de la concentration en mercure total dans le biogaz du site de Mendixka

La concentration en Hg total a été analysée dans chaque piège Amasil® ayant été utilisés pour échantillonner différents volumes en duplicat de biogaz. La pente obtenue par gradient volumétrique était de 7,4 et a permis d'estimer la concentration en Hg total contenu dans le biogaz produit sur le site de Mendixka (Tableau 15.

Tableau 15.Concentrations en Hg total déterminées dans le biogaz du site de Mendixka

Réplicats	Volume prélevé (L)	Aire	Quantité Hg dans piège Amasil (pg)	Concentration Hg Biogaz Mendixka ($ng.m^{-3}$)
1	0,005	187,6	25,5	5092,1
2	0,005	182,2	24,7	4945,5
1	0,01	359,7	48,8	4881,7
2	0,01	361,2	49,0	4902,1
1	0,02	728,1	98,8	4940,8
2	0,02	719,7	97,7	4883,8
1	0,03	1102,7	149,7	4988,5
2	0,03	1093,4	148,4	4946,4
1	0,04	1478,08	200,6	5015,0
2	0,04	1467,9	199,2	4980,5
1	0,05	1850,5	251,1	5022,9
2	0,05	1797,9	244,0	4880,1
		Concentration moyenne en Hg total ($ng.m^{-3}$)		**4956,6**
		Erreur ($ng.m^{-3}$)		**63**

La concentration en Hg total a d'abord été effectué en déterminant la quantité de celui-ci retenue dans les pièges Amasil®. La concentration a été estimée en fonction du volume de biogaz prélevé, ce qui a permis de déterminer que la concentration moyenne de Hg total contenu dans le biogaz produit à Mendixka est égale à 4956 ± 63 $ng.m^{-3}$. Le réacteur a donc pu être mis en place sur le flux primaire de biogaz afin de mieux observer et comprendre l'adsorption du mercure sur la surface des plaques.

2.3. Analyse de surface des plaques représentant expérimentalement les cylindres d'échantillonnage

2.3.1. Analyse de surface par LA-ICP-MS

Suite à l'analyse de surface par LA-ICP-MS de chaque catégorie de plaques ayant été utilisées lors de l'échantillonnage du biogaz de Mendixka, une adsorption du soufre, de l'arsenic ainsi que du mercure présents dans le biogaz a été observée sur chaque catégorie de plaques. Pour toutes les analyses, il n'y a pas eu de détection de ces trois éléments pendant les 20 premières secondes d'analyse. Ce résultat s'explique par le fait, que le laser chauffe pendant ces vingt premières secondes et ne scanne donc pas l'échantillon. Le signal obtenu est l'analyse de ces trois éléments dans le gaz vecteur.

Pour la plaque en acier inoxydable non-revêtue, la plaque en inox sans revêtement, avec le revêtement Silconert® ainsi que celle avec le revêtement Dursan®, non mises en contact avec des échantillons de gaz (blancs), contenaient toutes dans leur composition initiale une infime présence de soufre, une petite quantité d'arsenic (intensité ~ 1000 cps) ainsi que du mercure (intensité ~ 4000 cps pour la plaque non-revêtue ainsi que la plaque Silconert® et intensité ~ 1500 cps pour la plaque Dursan®). Ces résultats ont été obtenus après analyse d'une plaque neuve (blanc) de chaque catégorie plaque.

Lors de l'analyse de la plaque en inox non-revêtue ayant été utilisée lors de l'échantillonnage du biogaz du Mendixka, l'intensité pour le soufre était ~ 800 fois supérieure pour la plaque utilisée lors de l'échantillonnage que celle utilisée comme blanc (Figure 23 A.). Pour l'arsenic, l'intensité était ~ 22,5 fois supérieure pour la plaque utilisée lors de l'échantillonnage que celle utilisée comme blanc (Figure 23 B.). Enfin pour le mercure, cette augmentation d'intensité, qui était ~ 3 fois supérieure par rapport au blanc, a aussi été observée.

Ces augmentations d'intensité par rapport aux blancs ont aussi été observées sur la plaque ayant le revêtement Silconert® ainsi que sur celle ayant le revêtement Dursan®. Pour le soufre, l'intensité était ~ 1800 fois supérieure pour la plaque Silconert® (Figure 24 A.) et ~ 6000 fois supérieure pour la plaque Dursan® (Figure 25 A.). Pour l'arsenic, l'intensité était ~ 20 fois supérieure pour la plaque Silconert® (Figure 24 B.) ainsi que pour la plaque Dursan® (Figure 25 B.). Pour finir, pour le mercure, l'intensité était ~ 3,5 fois supérieure pour la plaque Silconert® (Figure 24 C.) et ~ 3,3 fois supérieure pour la plaque Dursan® (Figure 25 C.).

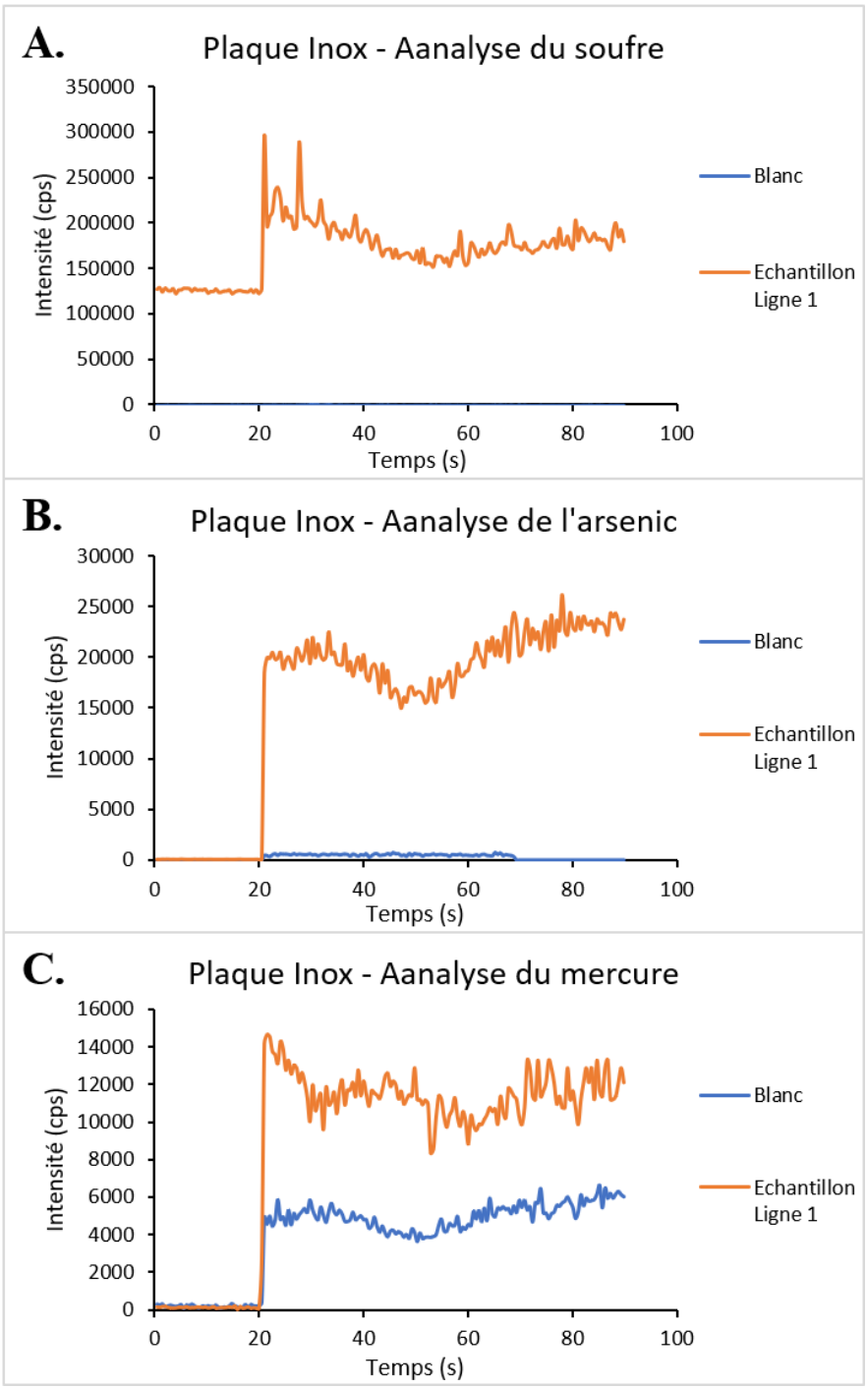

Figure 23. Analyse du soufre (A.), de l'arsenic (B.) et du mercure (C.) par LA-ICP-MS de la surface de la plaque en acier inoxidable non-revêtue neuve (blanc) ainsi que celle utilisée lors de l'échantillonnage du biogaz du site de Mendixka

Ces augmentations d'intensité entre le blanc et les échantillons ont montré que quelle que soit la catégorie de plaques, il y a une adsorption du soufre, de l'arsenic ainsi que du mercure à la surface de celles-ci. L'adsorption du mercure et de l'arsenic est un peu moins importante sur la

plaque ayant le revêtement Silconert® et ainsi que sur celle ayant le revêtement Dursan® par rapport à la plaque en inox n'ayant pas de revêtement mais un traitement de surface. Ces résultats montrent que ces revêtements spécialement conçus pour être inertes à l'adsorption d'éléments notamment le mercure et l'arsenic, permettent la diminution de ce phénomène mais ne permettent pas de l'éliminer.

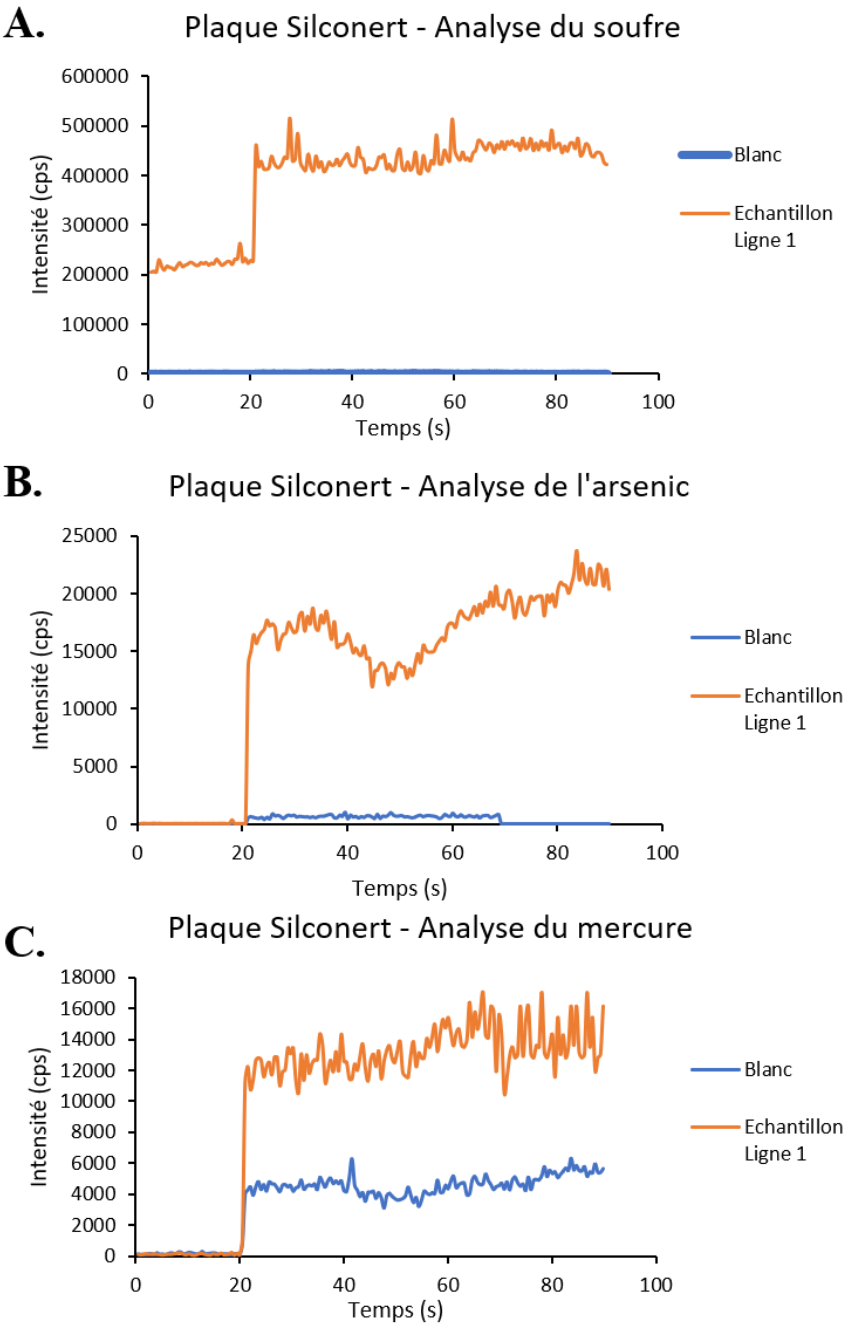

Figure 24. Analyse du soufre (A.), de l'arsenic (B.) et du mercure (C.) par LA-ICP-MS de la surface de la plaque ayant le revêtement Silconert® neuve (blanc) ainsi que celle utilisée lors de l'échantillonnage du biogaz du site de Mendixka

A l'inverse, l'adsorption du soufre était beaucoup plus importante sur les deux plaques revêtues que sur la plaque sans revêtement. La spéciation du soufre contenue dans le biogaz de Mendixka n'a pas été effectuée, ne permettant donc pas de déterminer quelle espèce de soufre s'est adsorbée à la surface de ces plaques. Ces expérimentations ne permettent pas de conclure sur l'utilisation de cylindres contenant ces revêtements ou non, lors de la recherche de la présence d'espèces soufrées dans le gaz naturel et le biogaz.

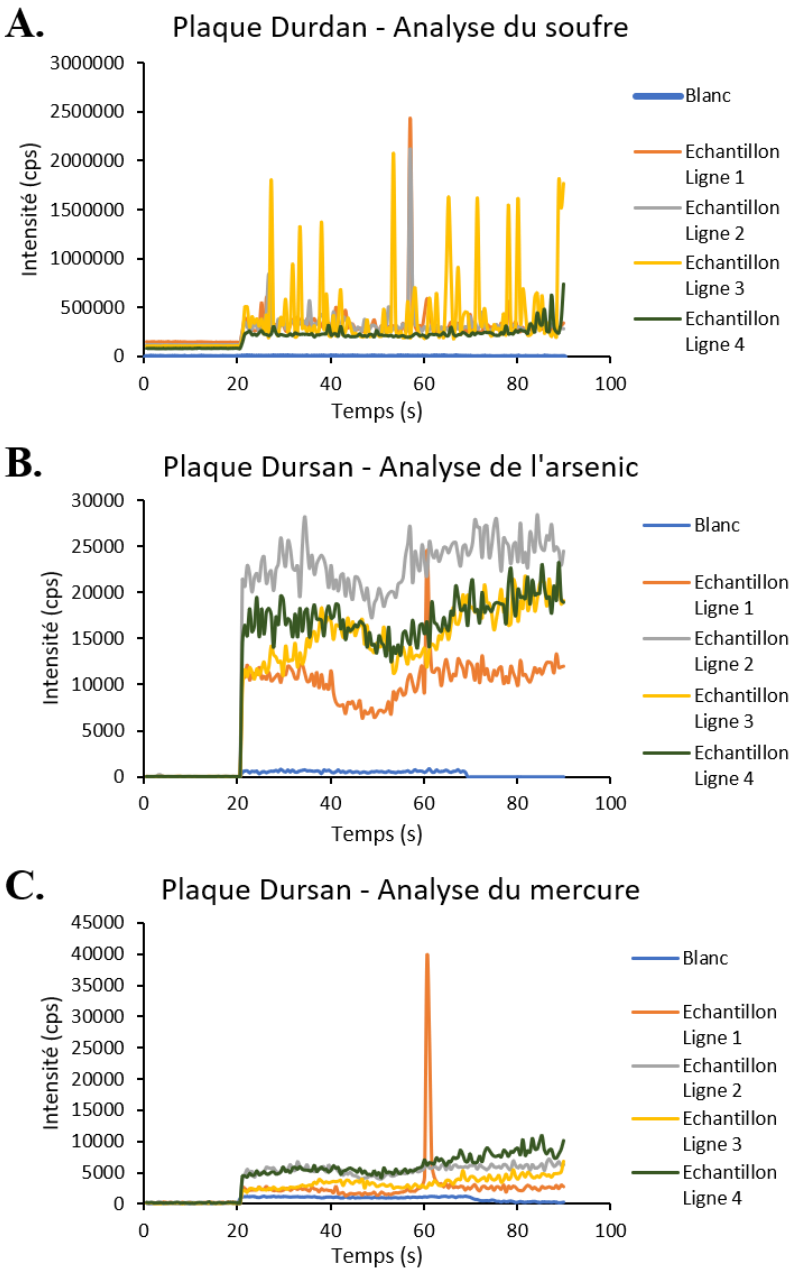

Figure 25. Analyse du soufre (A.), de l'arsenic (B.) et du mercure (C.) par LA-ICP-MS de la surface de la plaque ayant le revêtement Dursan® neuve (blanc) ainsi que celle utilisée lors de l'échantillonnage du biogaz du site de Mendixka

Ces résultats montrent donc que les cylindres en acier inoxydable ou ayant le revêtement Silcornert® et Dursan® ne sont pas inertes à l'absorption du soufre, de l'arsenic et du mercure. L'utilisation de ces échantillonneurs ne sont donc pas recommandés pour l'analyse de ces composés.

Pour finir, lors du premier scan de la plaque Dursan® pour les trois éléments (courbe en orange sur la Figure 25), un pic élevé d'intensité est observé à ~ 60 secondes. Pour cette même plaque, le troisième scan de la plaque montre une forte variation de l'intensité du soufre (courbe en jaune sur la Figure 25 A.).

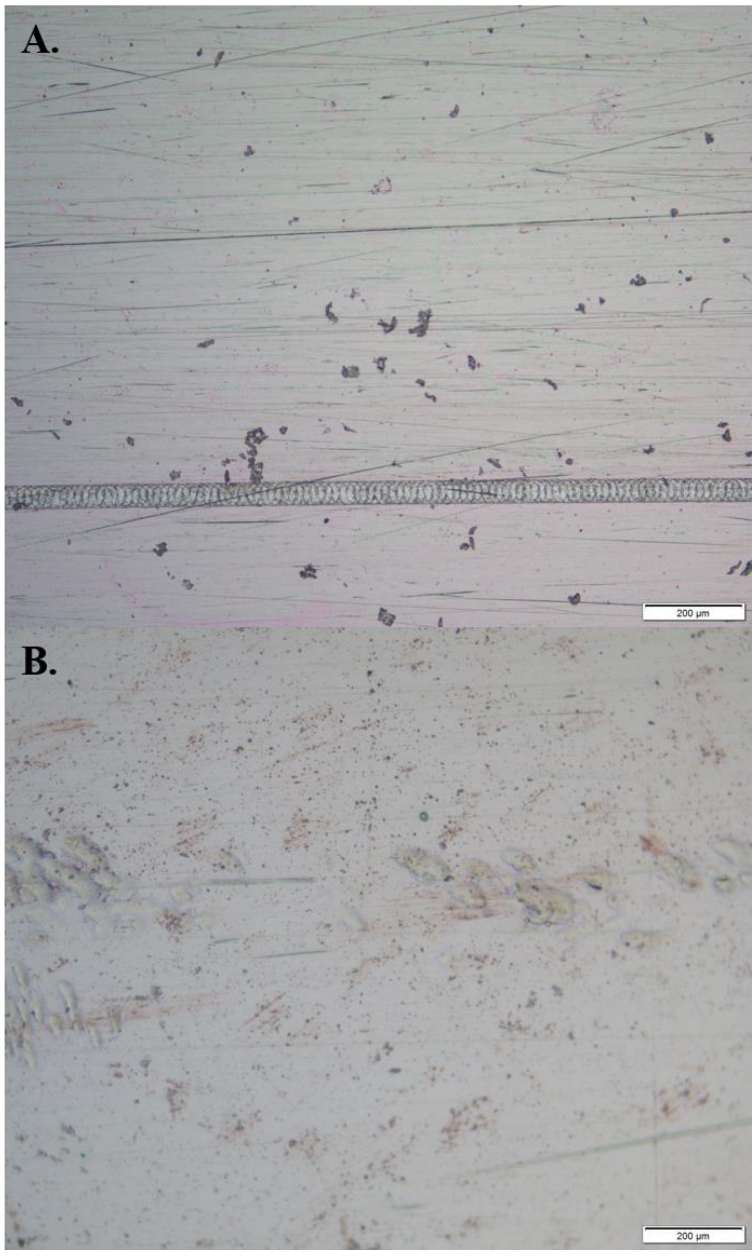

Figure 26. Photographie de la surface de la plaque ayant le revêtement Silconert® (A.) ainsi que celle ayant le revêtement Dursan® obtenue par microscope optique (Grossissement : 200 µm)(B.).

De manière générale, même si les variations d'intensité sont plus importantes pour la plaque Dursan®, lors du scan de la plaque non-revêtue ainsi que la plaque Silconert®, il y a tout au long de l'analyse de plaques, quel que soit l'élément analysé, des variations de l'intensité ont été observées. Ce phénomène peut être expliqué par la présence de petites « taches » noires (Figure 26 A.) ou rosées (Figure 26 B.), où les éléments, quelle que soit la catégorie de plaques semblent s'être davantage adsorbés que sur le reste de la plaque.

Ces petites « taches » observées par microscope optique semblent être des impuretés ou des microfissures (Figure 26) n'ayant donc pas de revêtement ou de traitement de surface expliquant la raison de l'adsorption plus importante sur celles-ci que sur le reste de la plaque. L'analyse par SEM-EDX va donc permettre de mieux comprendre la répartition de l'adsorption des 3 éléments sur ces plaques et sur ces taches.

2.3.2. Analyse de surface par SEM-EDX

L'analyse par SEM-EDX, réalisée par Mme Svahn au Bordeaux Imaging Center (BIC), de la plaque ayant le revêtement Silconert ainsi que la plaque ayant le revêtement Dursan utilisée lors de l'échantillonnage du biogaz du site de Mendixka, a permis de cartographier la répartition de l'adsorption du soufre, de l'arsenic et du mercure sur plusieurs sites d'analyses de ces deux plaques.

L'analyse de la plaque Silconert® (Figure 27, Annexe 1 p 142) et de la plaque Dursan® (Figure 28, Annexe 2 p 145) a permis de mettre en évidence la présence de soufre, d'arsenic et de mercure sur la surface des sites analysés de ces deux plaques. Ces résultats montrent bien qu'une adsorption de ces trois éléments s'est opérée à la surface de la plaque. De plus, il y a présence de soufre, d'arsenic et de mercure sur toute la surface des sites analysés. Ce résultat suggère donc que l'adsorption de ces trois éléments est diffuse sur la surface interne des cylindres.

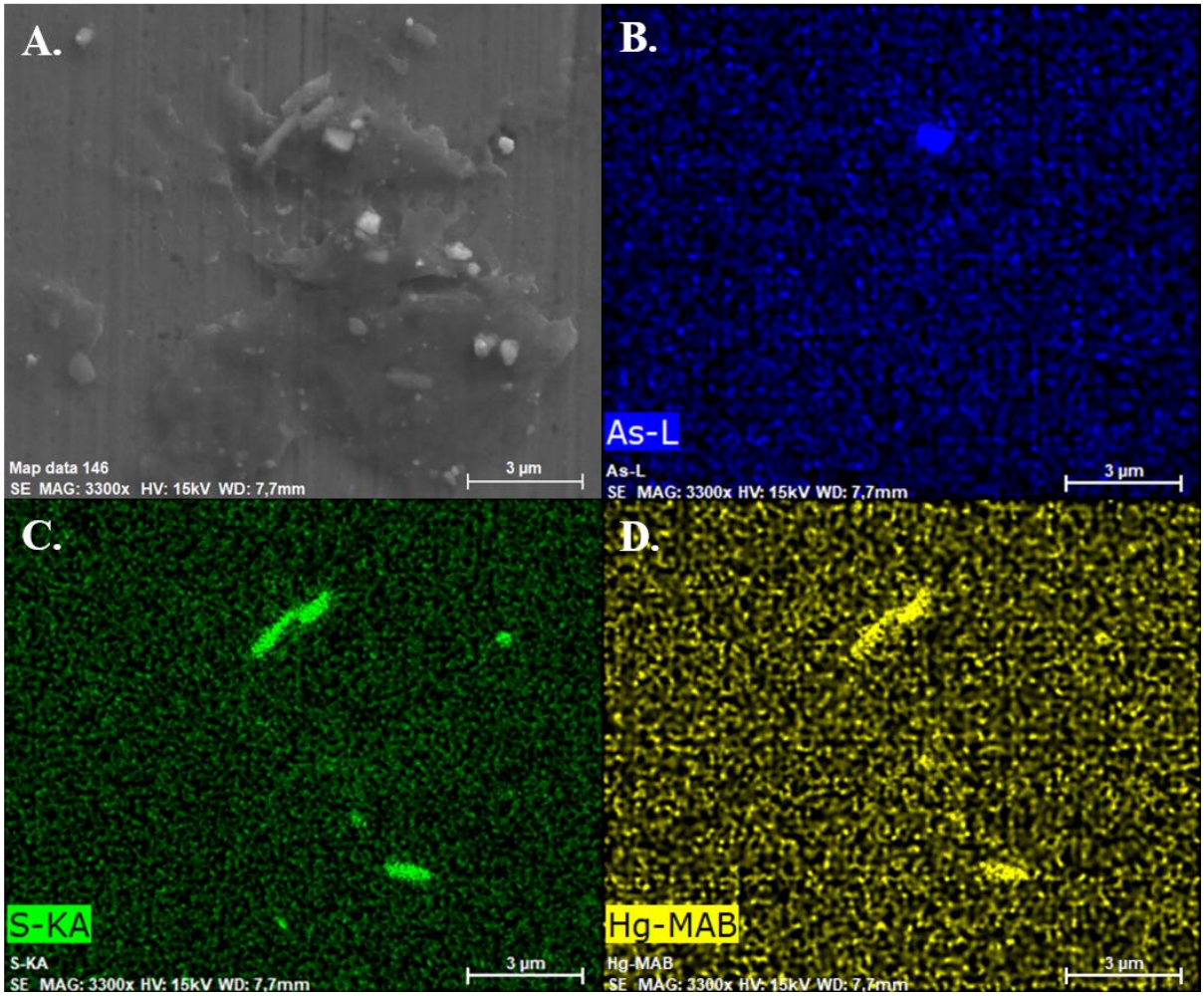

Figure 27. Analyse par SEM-EDX de l'arsenic (B.), du soufre (C.) et du mercure (D.) adsorbé sur la surface du site n°1 (A.) de la plaque Silconert®

Toutefois, l'intensité de l'arsenic analysé sur un des sites de la plaque Silconert® (Figure 27 A.) est plus importante sur un point précis de ce site analysé (Figure 27 B.). Cet endroit semble vraisemblablement être une tache similaire à celles observées par microscope optique (Figure 26 A.). L'analyse d'un des sites de la plaque Dursan® (Figure 28 A.) a été focalisée sur une de ces « taches ». L'intensité de l'arsenic est plus intense sur celle-ci (Figure 28 B.) que sur le reste du site analysé. Pour le reste des sites analysés, que ce soit pour la plaque Silconert® (Annexe) ou la plaque Dursan® (Annexe), ce même phénomène est observé.

Pour le mercure ainsi que le soufre, l'intensité de ceux-ci sont également plus importante sur ces « taches » que sur le reste de la surface des sites analysés que ce soit pour la plaque Silconert® (Figure 27 C. et D., Annexe) que pour la plaque Dursan® Figure 28 C. et D., Annexe).

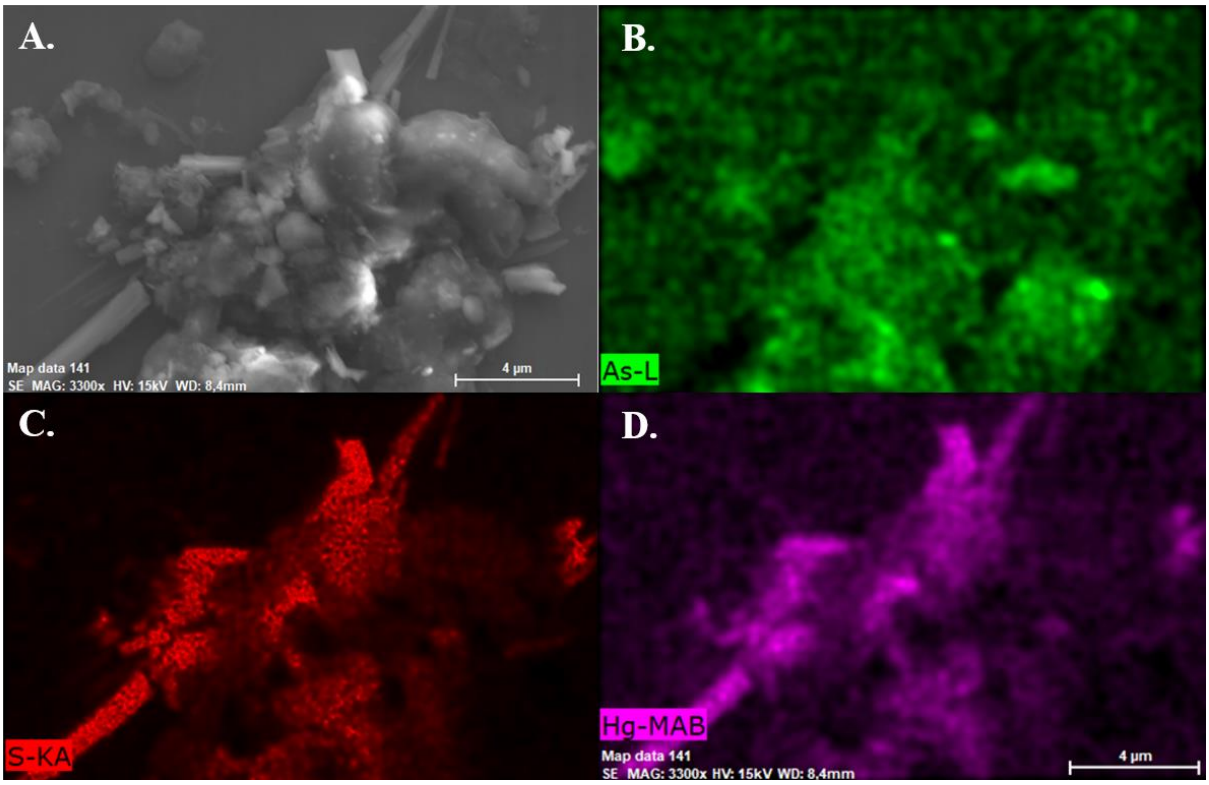

Figure 28. Analyse par SEM-EDX de l'arsenic (B.), du soufre (C.) et du mercure (D.) adsorbés sur la surface du site n°1 (A.) de la plaque Dursan®

Ces résultats montrent donc que même si ces trois éléments se sont adsorbés sur toute la surface des deux plaques, il y eu une adsorption plus importante à la surface des « taches » comme supposé lors de l'analyse de la surface des plaques par LA-ICP-MS (cf 2.3.1.Analyse de surface par LA-ICP-MS, p 128). L'adsorption du soufre, de l'arsenic et du mercure est donc plus importante lorsqu'il y a présence d'impuretés et/ou de microfissures à la surface interne de ces cylindres.

Pour finir, l'arsenic ne s'est pas adsorbé sur les mêmes impuretés/microfissures que le mercure et le soufre. A l'inverse, ces deux derniers éléments se sont tous les deux absorbés sur les mêmes impuretés/microfissures. Ces résultats valident donc l'hypothèse émise dans la partie « 4.Conclusion and Recommendations, p 90 » sur la capacité des espèces soufrées à s'adsorber sur la surface interne des cylindres et à devenir des sites d'adsorption pour le mercure.

3. Conclusion

L'analyse de la surface par LA-ICP-MS et par SEM-EDX des plaques non-revêtues, des plaques ayant le revêtement Siclonert® ainsi que des plaques ayant le revêtement Dursan® utilisées lors de l'échantillonnage de biogaz sur le site de valorisation des déchêts de Mendixka a permis de confirmer le phénomène d'adsorption du soufre, du mercure et de l'arsenic à leur surface et par conséquent à la surface interne des cylindres utilisés lors de l'échantillonnage de gaz naturel. Ces analyses ont permis de déterminer que l'adsorption de ces trois éléments était diffuse sur toute la surface des cylindres.

De plus, l'analyse des plaques par EDX-SEM a permis de confirmer que l'adsorption de ces élements était plus importante lorsqu'il y avait présence d'impuretés et/ou de microfissures sur la surface interne des plaques et donc des cylindres. Pour finir, il a été montré que le mercure ne s'adsorbe pas directement sur la surface mais c'est le soufre, qui, une fois adsorbé à la surface des cylindres, devient un site d'adsorption pour le mercure.

CONCLUSION GENERALE ET PERSPECTIVES

Le travail réalisé sur la fiabilité de l'échantillonnage et de l'analyse du mercure et de l'arsenic dans l'industrie pétrochimique et pétrolière a permis d'identifier que les cylindres haute pression, avec ou sans revêtement spécial, utilisés pour la prise d'échantillons de gaz naturel n'étaient pas fiables, la plupart du temps, pour l'analyse de mercure et d'arsenic en laboratoire, malgré leurs revêtements supposés diminuer l'adsorption de ces deux éléments. L'inertie des cylindres ayant un revêtement spécial (Silconert® ou Dursan®) était effectivement initialement efficace concernant l'adsorption du Hg et de l'As, mais cette efficacité est rapidement compromise après leur première utilisation rendant l'analyse de ces deux éléments non fiables, lorsque ceux-ci sont échantillonnés dans du gaz naturel à l'aide de ces échantillonneurs, notamment lors d'un test de puit.

L'adsorption de ces deux éléments à la surface internes des cylindres a été déterminée comme étant diffuse sur toute la surface de ceux-ci mais plus notablement importante lorsqu'il y a présence d'impuretés et/ou de microfissures à l'intérieur de ces cylindres. Il a été montré que le soufre après s'être adsorbé à la surface interne de ces cylindres devient un site d'adsorption pour le mercure.

L'utilisation de sacs Tedlar lors d'échantillonnages de gaz naturel avant l'analyse du mercure a été déterminée comme fiable et inerte à l'adsorption du Hg. Malgré cela, cette utilisation semble problématique lors d'échantillonnages de gaz naturel sur le terrain car ceux-ci ne sont pas conçus pour échantillonner des gaz sous pression. Une dépressurisation ainsi qu'une dérivation du flux principal du gaz naturel doit être mise en place, afin de pouvoir échantillonner du gaz naturel à l'aide de ceux-ci. Ces deux opérations peuvent être la source de pertes (points froids) ou de contamination et peuvent fausser la concentration en Hg. Les sacs Tedlar sont également très fragiles et très volumineux une fois remplis, rendant leur transport très difficile. L'analyse directe sur le terrain du mercure mais aussi de l'arsenic semble donc le plus recommandé pour limiter les artéfacts et évaluer avec fiabilité leur concentration dans les fluides pétroliers. L'analyse sur site est d'autant plus recommandée, qu'elle permet

l'identification immédiate des artéfacts alors qu'une analyse off-site ne permet pas de constater les dégâts, dans beaucoup de cas, si des artéfacts sont effectivement observés.

La recherche de nouveaux revêtements inertes de cylindres pour l'échantillonnage de gaz naturel sous pression lors d'analyses du mercure et de l'arsenic semble donc nécessaire si ces deux éléments traces ne peuvent pas être déterminés directement sur le terrain. De plus, l'évaluation de la fiabilité de l'échantillonnage de gaz naturel pour l'analyse de d'autres éléments, notamment l'oxygène et le soufre peut être aussi intéressante à réaliser.

Les travaux réalisés ont aussi permis de déterminer le lien entre la durée d'un test de puit, la quantité d'hydrocarbures à produire et le seuil de détection minimal des composés traces. La spécification concernant le mercure dans un gaz naturel est souvent de l'ordre de 0,01 $\mu g.Nm^{-3}$. Il a été démontré dans cette étude, l'impossibilité de déterminer la concentration en mercure dans un gaz naturel de l'ordre des $\mu g.m^{-3}$, sans un test de puit extrêmement long. En effet, la recherche de mercure à un niveau de quelques $\mu g.Nm^{-3}$ peut être réalisable au cours d'un test mais exigerait une production et donc le brûlage de plusieurs dizaines de millions de mètres cubes de gaz naturel : ce qui correspondrait au rejet de plus d'une dizaine de milliers de tonnes de CO_2, sans parler du coût financier correspondant au rallongement de la durée du test. La recherche de la présence de mercure dans le gaz naturel à un niveau plus bas que le $\mu g.Nm^{-3}$ est donc non nécessaire pendant les tests de puits

La recherche d'une teneur en mercure très basse dans un fluide de réservoir, sans passer par un test de puits très long, serait donc un grand progrès pour les compagnies pétrolières. Certains laboratoires et compagnies de services développent et testent des échantillonneurs de fond, à parois inerte, afin d'éviter l'étape de saturation de la surface des équipements, réduisant ainsi considérablement la durée d'un test de puit. Cependant, pour valider une telle méthode, il faut d'une part prouver que la rétention de mercure ou de d'autres composés en ultra-traces est due à l'adsorption sur des surfaces d'équipement seul et que la boue et les particules utilisées et générées par le forage, ont une capacité de rétention bien inférieures. D'autre part, il faut trouver une méthode de validation des résultats, ce qui n'est pas chose aisée comme il a pu être constaté à travers les travaux présentés dans cette thèse.

Pour finir, la production de bio-huiles et de biogaz à partir de biomasses, obtenues par exemple après pyrolyse ou coliquefaction de celles-ci, semble prendre de plus en plus d'ampleur afin de remplacer les énergies fossiles. Le mercure et l'arsenic sont présents dans la plupart des biomasses utilisées pour la production de leurs sous-produits. Ceux-ci restent donc contaminés en ces deux éléments après leur production. Au vu des problèmes liés à leur

présence dans les fluides pétroliers et à la difficulté de déterminer la teneur du Hg et de l'As dans ceux-ci, il ne paraît pas aberrant de penser que des problématiques similaires seront observés dans la production de ces nouvelles énergies. Il sera donc primordial d'évaluer la fiabilité de l'échantillonnage et de l'analyse du mercure et de l'arsenic dans le biogaz ainsi que dans les bio-huiles.

Références (hors publications)

ASTM D5954-98, 2014. Standard Test Method for Mercury Sampling and Measurement in Natural Gas by Atomic Absorption Spectroscopy, 2014. West Conshohocken, PA, United States.

ASTM D6350-14, 2014. ASTM International. Standard Test method for Mercury Sampling and Analysis in Natural Gas by Atomic Fluorescence Spectroscopy, 2014.West Conshohocken, PA, United States.

Boffetta, P., Merler, E., Vainio, H., 1993. Carcinogenicity of mercure and mercury compounds. Scand. J. Work. Environ. Health 1–7.

Bouyssiere, B., Baco, F., Savary, L., Garraud, H., Gallup, D.L., Lobinski, R., 2001. Investigation of speciation of arsenic in gas condensates by capillary gas chromatography with ICP-MS detection. J. Anal. At. Spectrom. 16, 1329–1332. https://doi.org/10.1039/b105765k

Cachia, M., 2017. Caractérisation des transferts d'éléments trace métalliques dans une matrice gaz/eau/roche représentative d'un stockage subsurface de gaz naturel. Université de Pau et des Pays de l'Adour.

Delgado-morales, W., Zingaro, R.A., Mohan, M.S., 1994. Arsenic in Natural Gas: Analysis and Characterization of Pipeline Solids by 1H NMR and Other Methods. Int. J. Environ. Anal. Chem. 57, 313–328. https://doi.org/10.1080/03067319408027463

Filby, R.H., 1994. Origin and nature of trace element species in crude oils, bitumens and kerogens: implications for correlation and other geochemical studies. Geol. Soc. Spec. Publ. 203–2019.

Irgolic, K.J., Llger, D., Zingaro, R.A., Spall, D., Puri, B.K., 1991. Determination of arsenic and arsenic compounds in natural gas samples. Appl. Organomet. Chem. 5, 117–124. https://doi.org/10.1002/aoc.590050209

ISO 6978.1-2003, 2003. International Standard Organisation (ISO). ISO 6978.1-2003, Natural gas - Determination of mercury - Part 1: Sampling of mercury by chemisorption on iodine. ISO: Geneva, Switzerland, 2003.

ISO 6978.2-2003, 2003. International Standard Organisation (ISO). ISO 6978.2-2003, Natural gas - Determination of mercury - Part 2: Sampling of mercury by amalgmation on gold/platinum alloy. ISO: Geneva, Switzerland, 2003.

Krupp, E.M., Johnson, C., Rechsteiner, C., Moir, M., Leong, D., Feldmann, J., 2007. Investigation into the determination of trimethylarsine in natural gas and its partitioning into gas and condensate phases using (cryotrapping)/gas chromatography coupled to inductively coupled plasma mass spectrometry and liquid/solid sorption techniques. Spectrochim. Acta Part B At. Spectrosc. 62, 970–977. https://doi.org/10.1016/j.sab.2007.07.009

Lambertsson, L., Lord, C.J., Frech, W., Björn, E., 2018. Rapid Dissolution of Cinnabar in Crude Oils at Reservoir Temperatures Facilitated by Reduced Sulfur Ligands. ACS Earth Space Chem. https://doi.org/10.1021/acsearthspacechem.8b00096

Leeper, J., 1980. Mercury-LNG's problem. Hydrocarb. Process 59, 237–240.

Liu, Z.X., Tang, D.Z., Yan, Q.T., Xu, H., Wang, S.Y., Xu, R., Wu, S., 2014. Characteristic of the Volatile Arsenic in Natural Gas and its Novel Determination Method. Appl. Mech.

Mater. 522–524, 1515–1521. https://doi.org/10.4028/www.scientific.net/AMM.522-524.1515
Norme NF EN 13211, 2001. Association Francaise de Normalisation (AFNOR). NF EN 13211, Qualité de l'Air - Émissions de Sources Fixes - Methode Manuelle de Determination de la Concentration en Mercure Total (Air Quality - Fixed Source Emissions - Manual Method for Total Mercury Determination). AFNOR: Paris, France, 2001.
Rumayor, M., Gallego, J.R., Rodríguez-Valdés, E., Díaz-Somoano, M., 2017. An assessment of the environmental fate of mercury species in highly polluted brownfields by means of thermal desorption. J. Hazard. Mater. 325, 1–7. https://doi.org/10.1016/j.jhazmat.2016.11.068
SilcoTek Corporation, 2019. SilcoTek Corporation. Prevent Mercury Loss during Transport and Storage with SilcoNert, 2000. SilcoTek Corporation: Bellefonte, PA, 2019.
Wilhelm, S.M., Bloom, N., 2000. Mercury in petroleum. Fuel Process. Technol. 63, 1–27. https://doi.org/10.1016/S0378-3820(99)00068-5
Yeh, S., How, S.W., Lin, C.S., 1968. Arsenical cancer of skin: Histologic study with special reference to Bowen's disease. Cancer 21, 312–339. https://doi.org/10.1002/1097-0142(196802)21:2<312::AID-CNCR2820210222>3.0.CO;2-K

Annexes

1. Annexe 1 : Analyse par SEM-EDX du site 2 à 4 de la plaque Silconert®

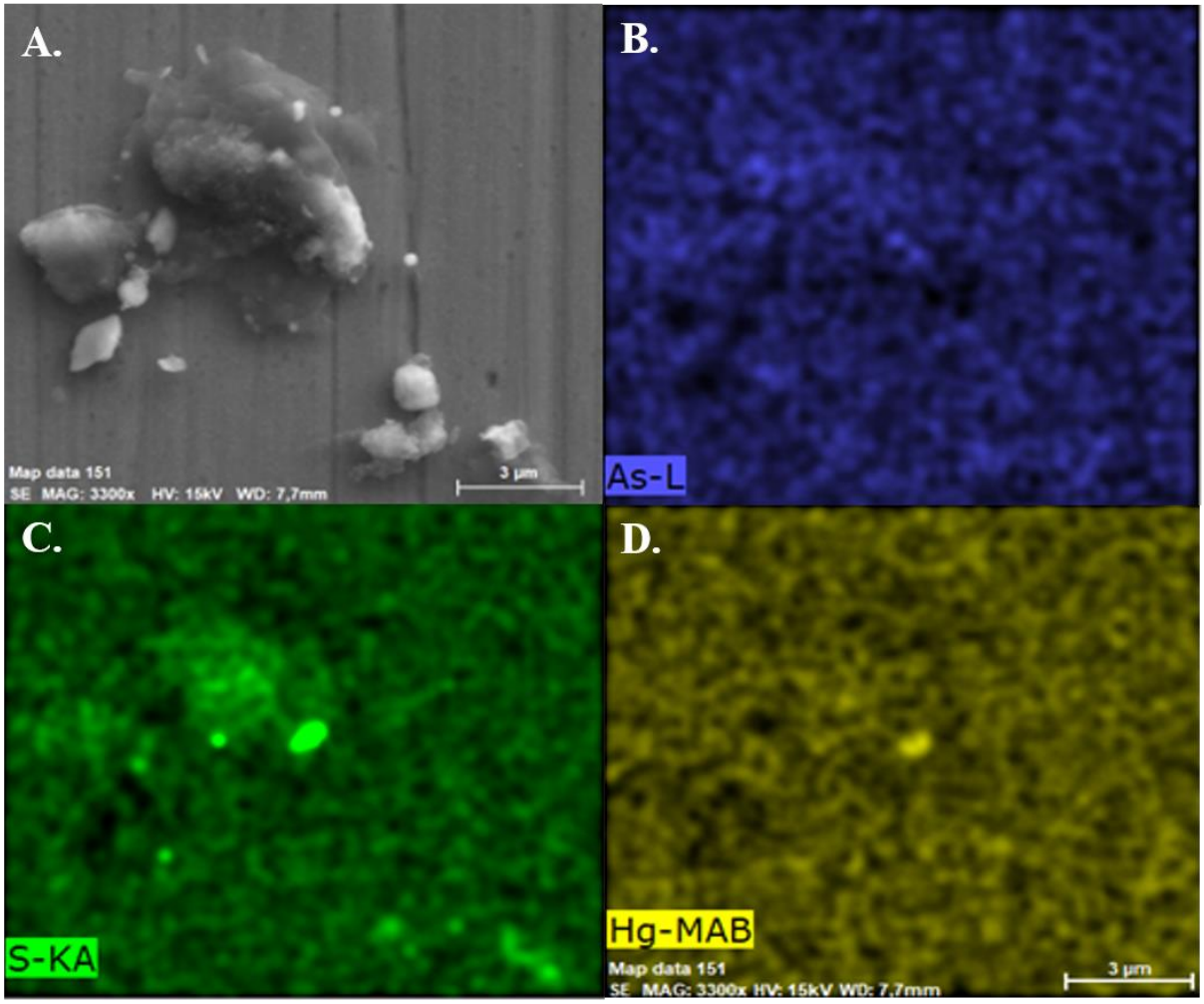

Figure 29. Analyse par SEM-EDX de l'arsenic (B.), du soufre (C.) et du mercure (D.) adsorbés sur la surface du site n°2 (A.) de la plaque Silconert®

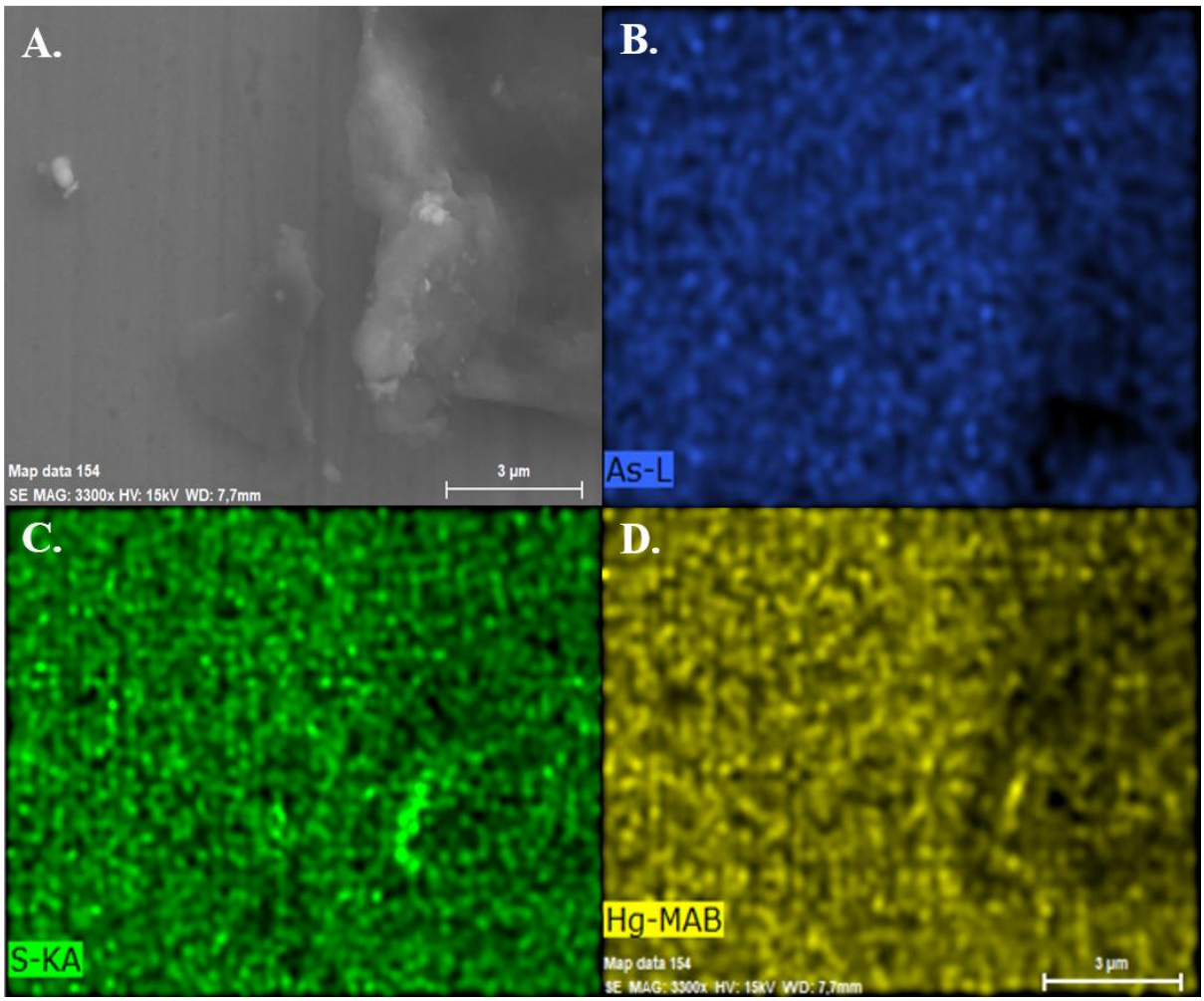

Figure 30. Analyse par SEM-EDX de l'arsenic (B.), du soufre (C.) et du mercure (D.) adsorbés sur la surface du site n°3 (A.) de la plaque Silconert®

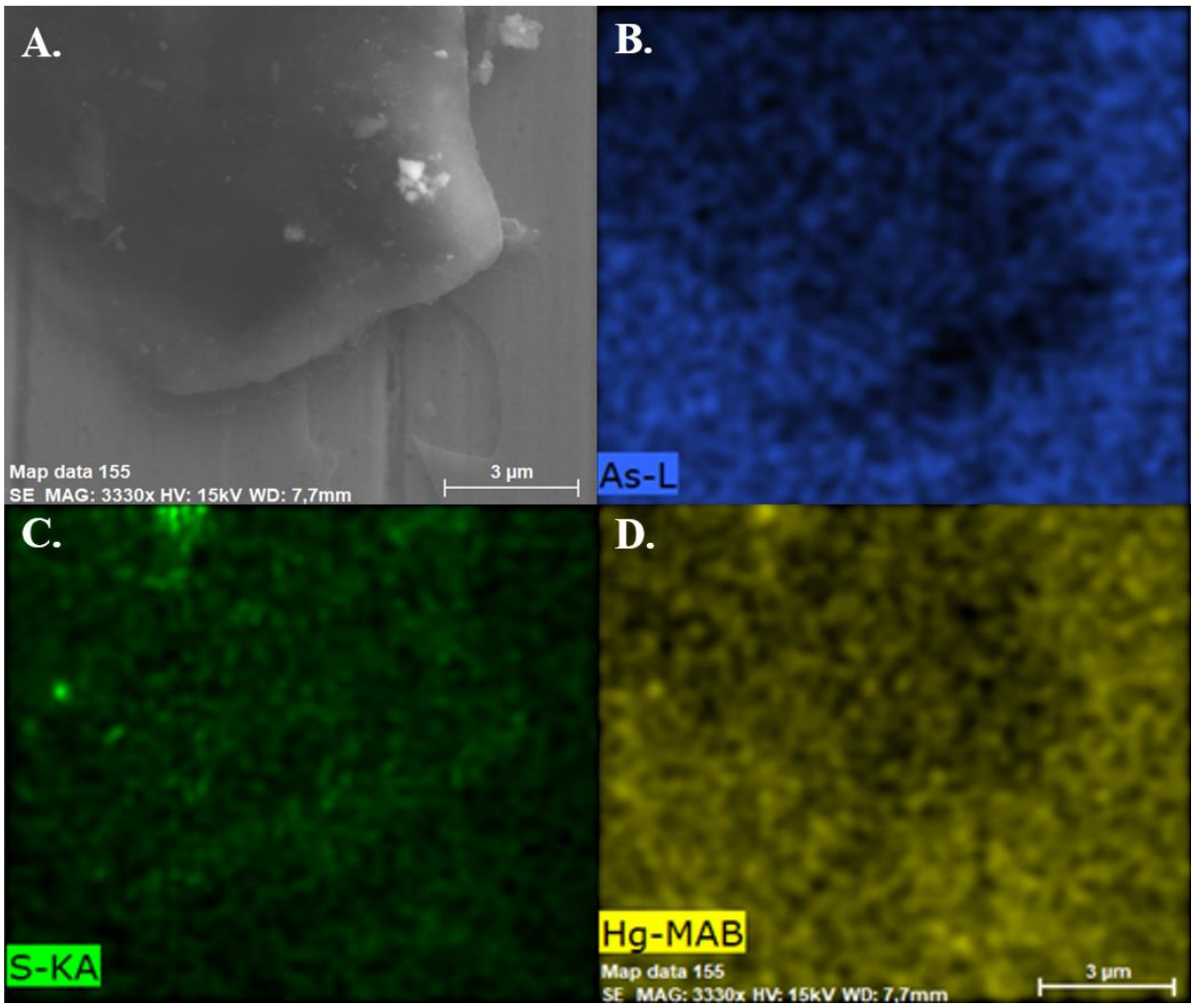

Figure 31. Analyse par SEM-EDX de l'arsenic (B.), du soufre (C.) et du mercure (D.) adsorbés sur la surface du site n°4 (A.) de la plaque Silconert®

2. Annexe 2 : Analyse par SEM-EDX du site 2 à 5 de la plaque Dursan®

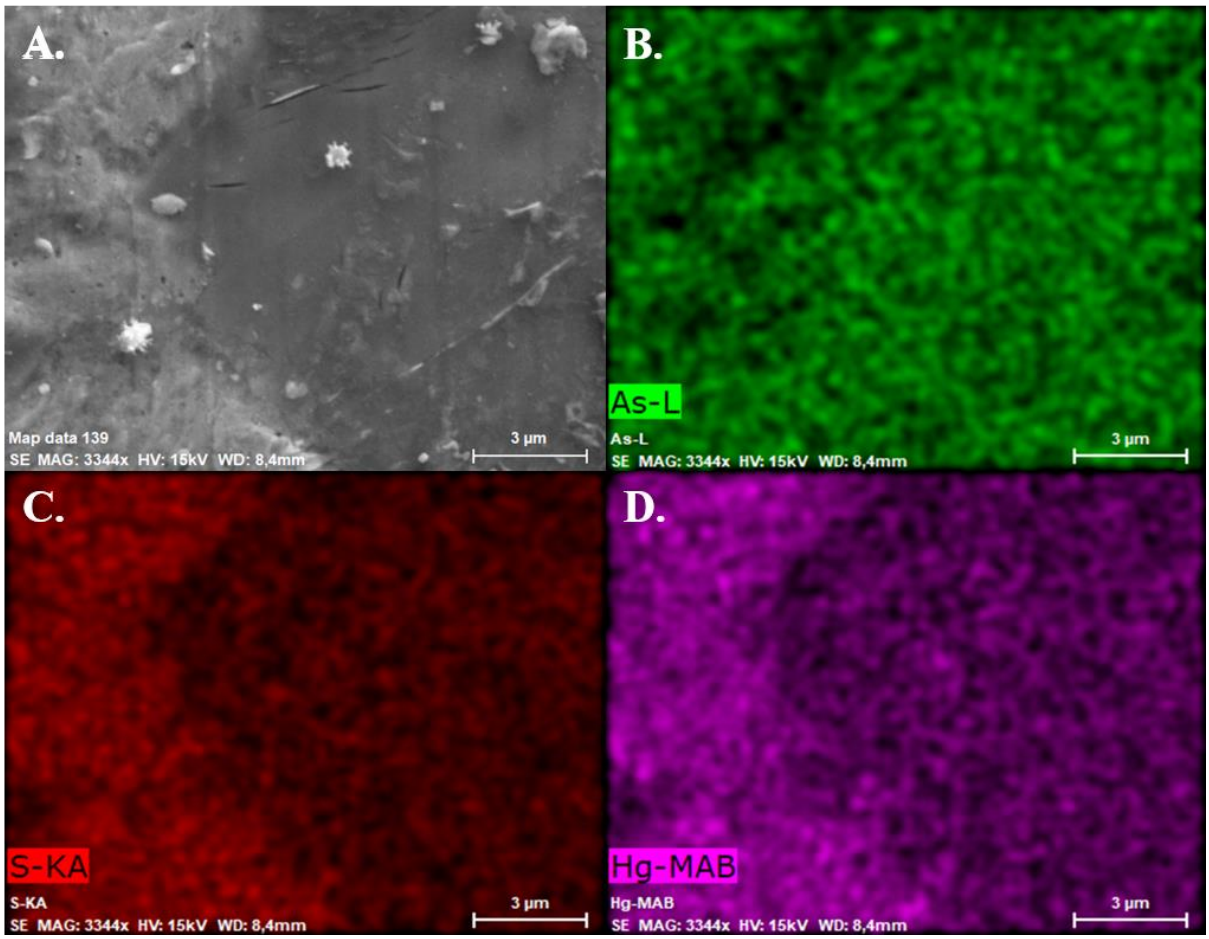

Figure 32. Analyse par SEM-EDX de l'arsenic (B.), du soufre (C.) et du mercure (D.) adsorbés sur la surface du site n°2 (A.) de la plaque Dursan®

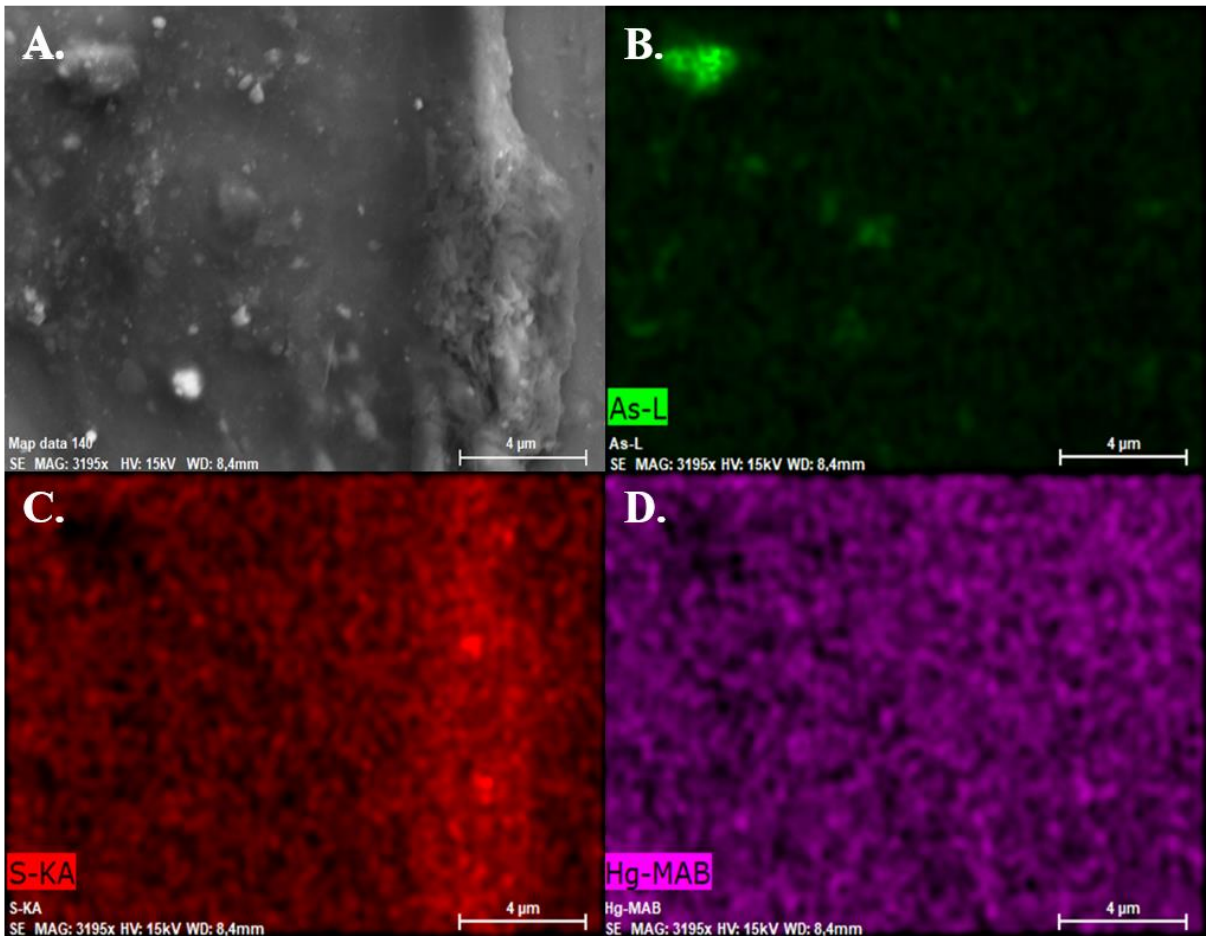

Figure 33. Analyse par SEM-EDX de l'arsenic (B.), du soufre (C.) et du mercure (D.) adsorbés sur la surface du site n°3 (A.) de la plaque Dursan®

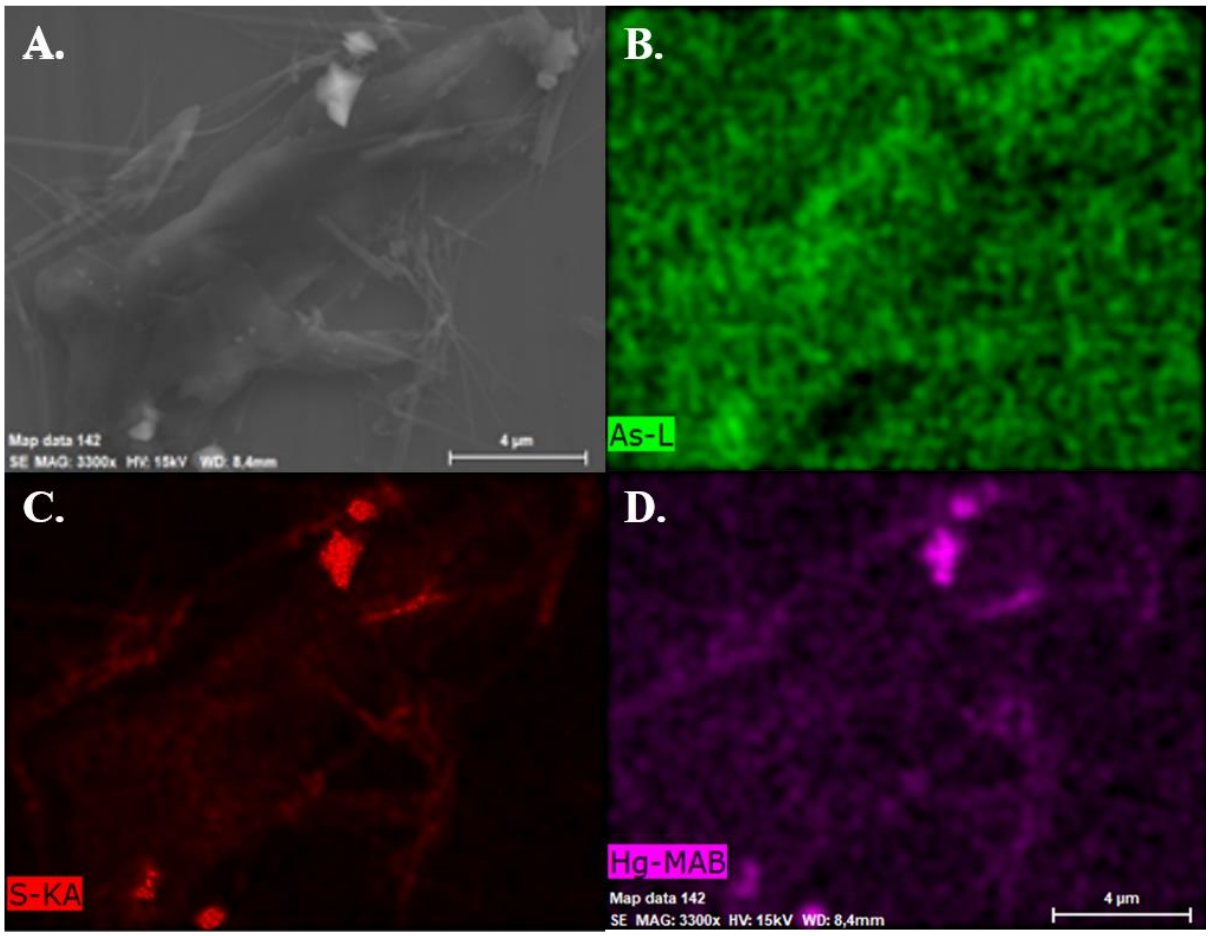

Figure 34. Analyse par SEM-EDX de l'arsenic (B.), du soufre (C.) et du mercure (D.) adsorbés sur la surface du site n°4 (A.) de la plaque Dursan®

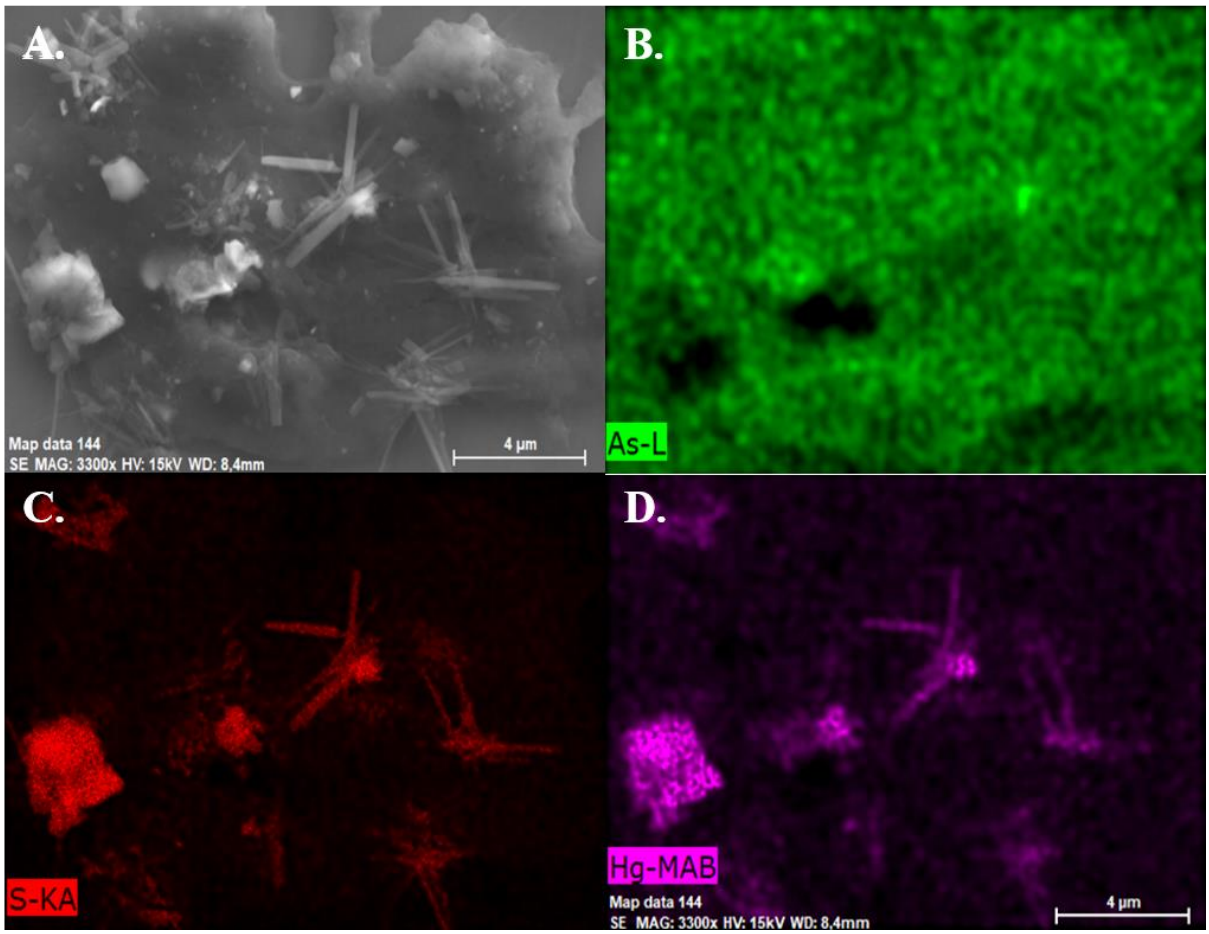

Figure 35. Analyse par SEM-EDX de l'arsenic (B.), du soufre (C.) et du mercure (D.) adsorbés sur la surface du site n°5 (A.) de la plaque Dursan®